JPTM

Journal of Pathology and Translational Medicine

July 2015
Vol. 49 / No. 4
jpatholtm.org
pISSN: 2383-7837
eISSN: 2383-7845

ISSN 2383-7837

A Review of Inflammatory Processes of the Breast with a Focus on Diagnosis in Core Biopsy Samples

The Utilization of Cytologic Fine-Needle Aspirates of Lung Cancer for Molecular Diagnostic Testing

Journal of Pathology and Translational Medicine

Volume 49 • Number 4 • July 2015 (bimonthly)
Published since 1967
Printed on 11 July 2015 Published on 15 July 2015

J Pathol Transl Med
pISSN: 2383-7837
eISSN: 2383-7845

Aims & Scope

The Journal of Pathology and Translational Medicine is an open venue for the rapid publication of major achievements in various fields of pathology, cytopathology, and biomedical and translational research. The Journal aims to share new insights into the molecular and cellular mechanisms of human diseases and to report major advances in both experimental and clinical medicine, with a particular emphasis on translational research. The investigations of human cells and tissues using high-dimensional biology techniques such as genomics and proteomics will be given a high priority. Articles on stem cell biology are also welcome. The categories of manuscript include original articles, review and perspective articles, case studies, brief case reports, and letters to the editor.

Subscription Information

To subscribe to this journal, please contact the Korean Society of Pathologists/the Korean Society for Cytopathology. Full text PDF files are also available at the official website (http://jpatholtm.org). *Journal of Pathology and Translational Medicine* is indexed by PubMed, PubMed Central, Scopus, KoreaMed, KoMCI, WRPIM and CrossRef. Circulation number per issue is 700.

Contact the Korean Society of Pathologists/the Korean Society for Cytopathology

Publishers: Changsuk Kang, M.D., So Young Jin, M.D.
Editors-in-Chief: Soon Won Hong, M.D., Chong Jai Kim, M.D.
Published by the Korean Society of Pathologists/the Korean Society for Cytopathology

Editorial Office
Room 1209 Gwanghwamun Officia, 92 Saemunan-ro, Jongno-gu,
Seoul 110-999, Korea/#406 Lilla Swami Bldg, 68 Dongsan-ro,
Seocho-gu, Seoul 137-899, Korea
Tel: +82-2-795-3094/+82-2-593-6943
Fax: +82-2-790-6635/+82-2-593-6944
E-mail: office@jpatholtm.org

Printed by ML communications Co., Ltd.
Jungang Bldg. 18-8 Wonhyo-ro 89-gil, Yongsan-gu, Seoul 140-846, Korea
Tel: +82-2-717-5511 Fax: +82-2-717-5515 E-mail: ml@smileml.com

Manuscript Editing by InfoLumi Co.
210-202, 421 Pangyo-ro, Bundang-gu, Seongnam 463-926, Korea
Tel: +82-70-8839-8800 E-mail: infolumi.chang@gmail.com

Front cover image: Fluorescence *in situ* hybridization (FISH) of anaplastic lymphoma kinase (*ALK*)-rearranged pulmonary adenocarcinoma. p311.

This journal was supported by the Korean Federation of Science and Technology Societies Grant funded by the Korean Government.

Journal of Pathology and Translational Medicine

J Pathol Transl Med
pISSN: 2383-7837
eISSN: 2383-7845

Volume 49, Number 4, July 2015

CONTENTS

REVIEWS

ORIGINAL ARTICLES

CASE REPORTS

CONTENTS CONTINUED

Instructions for Authors for *Journal of Pathology and Translational Medicine* are available at http://jpatholtm.org/authors/authors.php

Journal of Pathology and Translational Medicine 2015; 49: 279-287
http://dx.doi.org/10.4132/jptm.2015.06.11

REVIEW

A Review of Inflammatory Processes of the Breast with a Focus on Diagnosis in Core Biopsy Samples

Timothy M. D'Alfonso
Paula S. Ginter · Sandra J. Shin

Department of Pathology and Laboratory Medicine, Weill Cornell Medical College, New York, NY, USA

Received: June 2, 2015
Revised: June 10, 2015
Accepted: June 11, 2015

Corresponding Author
Timothy M. D'Alfonso, MD
New York-Presbyterian Hospital/Weill Cornell Medical College, 525 East 68th Street, Starr 1031E, New York, NY 10065, USA
Tel: +1-212-746-2700
Fax: +1-212-746-6484
E-mail: tid9007@med.cornell.edu

Inflammatory and reactive lesions of the breast are relatively uncommon among benign breast lesions and can be the source of an abnormality on imaging. Such lesions can simulate a malignant process, based on both clinical and radiographic findings, and core biopsy is often performed to rule out malignancy. Furthermore, some inflammatory processes can mimic carcinoma or other malignancy microscopically, and vice versa. Diagnostic difficulty may arise due to the small and fragmented sample of a core biopsy. This review will focus on the pertinent clinical, radiographic, and histopathologic features of the more commonly encountered inflammatory lesions of the breast that can be characterized in a core biopsy sample. These include fat necrosis, mammary duct ectasia, granulomatous lobular mastitis, diabetic mastopathy, and abscess. The microscopic differential diagnoses for these lesions when seen in a core biopsy sample will be discussed.

Key Words: Breast; Core biopsy; Inflammatory; Mammogram

Inflammatory and reactive conditions of the breast are relatively uncommon among benign breast lesions, and may present with clinical and radiologic abnormalities akin to malignant processes. As such, core biopsy may be performed to exclude the possibility of malignancy. In most cases, the diagnosis based on microscopy is clear, but in fragmented core biopsy samples, some conditions may mimic malignancy. Conversely, some malignancies can also simulate benign inflammatory or reactive conditions.

The clinical, radiographic, and histologic features of commonly encountered inflammatory and reactive breast lesions, namely, fat necrosis, mammary duct ectasia, granulomatous lobular mastitis, diabetic mastopathy, and abscess will be reviewed (Table 1). In addition, we will discuss the histologic features on core biopsy that distinguish the items on this differential.

FAT NECROSIS

Fat necrosis is most often seen in traumatized breast tissue, particularly in areas of prior surgery or biopsy. Radiation therapy can also lead to fat necrosis in breast[1-3] and has been seen in up to 50% of patients following balloon-based brachytherapy.[4] Clinically, fat necrosis can present as a palpable mass with or without skin retraction, or it can be asymptomatic.[5]

On mammography, oil or lipid cysts, which are often calcified, are characteristic of fat necrosis (Fig. 1A). Calcifications in fat necrosis may be clustered, pleomorphic, and linear, simulating ductal carcinoma *in situ* (DCIS).[6,7] Fat necrosis can also appear as a stellate mass with irregular margins on mammography and ultrasound.[8-10]

Microscopically, fat necrosis is characterized by infiltration of foamy histiocytes and foreign body type giant cells around necrotic fat cells and lipid vacuoles (Fig. 1B). Cysts lined by foamy histiocytes are often present (Fig. 1C). Lymphocytic infiltration, often accompanied by plasma cells, can be present to varying degrees. As fat necrosis evolves, fibrosis develops within the lesion, forming a scar and fibrous walled cysts that can calcify (Fig. 1D–F). Adjacent glandular structures in a biopsied sample may show changes indicative of radiation therapy, such as cytologic atypia, squamous metaplasia, and thickened basement membranes.

The differential diagnosis for fat necrosis includes less common types of invasive carcinoma, including the lipid-rich variant and carcinomas with "histiocytoid" morphology, such as apocrine carcinoma and invasive lobular carcinoma. A broad-spectrum cytokeratin can be used to exclude the presence of carcinoma.

pISSN 2383-7837
eISSN 2383-7845

Table 1. Pertinent features of inflammatory lesions of the breast

	Clinical	Etiology and associations	Imaging	Microscopic features	Differential diagnosis
Fat necrosis	Mass Nipple/skin retraction	Trauma Surgery/biopsy Radiation	MMG: oil cyst; calcifications; spiculated mass US: oil cyst; solid mass; complex cyst	Lipid vacuoles and necrotic adipocytes surrounded by foamy histiocytes and foreign body giant cells Chronic inflammation Fibrosis, calcification	Invasive carcinoma - "Histiocytoid" - Lobular - Apocrine - Lipid-rich Erdheim-Chester (rare)
Duct ectasia	Unilateral or bilateral non-bloody nipple discharge Nipple/skin retraction Mass	-	MMG: branching calcifications; stellate mass US: dilated subareolar ducts; mass	Dilated ducts with luminal histiocytes Periductal fibrosis Periductal chronic inflammation Intraepithelial histiocytes Calcifications in duct lumen or duct wall	Ruptured cyst Ductal dilatation due to intraductal mass
Granulomatous lobular mastitis	Mass Erythema Nipple/skin retraction Pain Draining sinus	Idiopathic *Corynebacterim* spp.	Often suspicious for malignancy MMG: ill-defined mass US: irregular hypoechoic mass; dilated ducts	Non-necrotizing granulomatous inflammation in lobules Microabscesses Suppurative granulomas with cystic vacuoles: "cystic neutrophilic granulomatous mastitis"	Granulomatous mastitis secondary to: - Infection (TB, fungal) - Sarcoidosis - Other systemic granulomatous disease
Diabetic mastopathy	Palpable mass or nodularity	Diabetes mellitus (types I > II) Autoimmune dx. Endocrine dx. (i.e., thyroid dx.)	MMG: ill-defined mass; architectural distortion US: irregular hypoechoic solid mass MRI: non-specific	Does not form well-defined mass Stromal fibrosis: dense with keloidal features and epithelioid fibroblasts Lymphocytic infiltrates in periductal, perilobular, perivascular distribution	Invasive carcinoma (apocrine or lobular) Granular cell tumor Multinucleated stromal giant cells Lymphoma Vasculitis
Breast abscess	Tender mass with redness, warmth, swelling ± Fever ± Draining sinus ± Nipple discharge	Lactational/puerperal abscess: - *S. aureus* Subareolar/ non-puerperal abscess: - SMOLD - Smoking - Trauma - Mixed flora	MMG: asymmetric mass; skin thickening US: multiloculated mass/collection	Mixed inflammatory infiltrate, mainly neutrophils Granulation tissue and chronic inflammation with resolution ± Gram-positive cocci in clusters (i.e., *S. aureus*)	Abscess secondary to granulomatous lobular mastitis or duct ectasia

MMG, mammography; US, ultrasound; spp., species; TB, tuberculosis; dx, disease; MRI, magnetic resonance imaging; SMOLD, squamous metaplasia of lactiferous ducts.

Some histiocytic processes, although rare, should also be included in the differential diagnosis of fat necrosis. Rosai-Dorfman disease is a histiocytic proliferation that rarely involves the breast and is characterized by large histiocytes accompanied by a lymphoplasmacytic infiltrate.[11] Histiocytes show emperipolesis and positive immunohistochemical staining for S100 and CD68, but negative staining for CD1a. Erdheim-Chester disease is an even rarer form of histiocytosis which may involve the breast, showing positive immunohistochemical staining for CD68 and negative staining for CD1a and S100. Patients with Erdheim-Chester disease will have involvement of other sites, most commonly the long bones, before breast involvement.[12]

Fat necrosis does not need to be excised when diagnosed via a core biopsy, unless features on imaging are suspicious for malignancy or are discordant with the pathologic diagnosis of fat necrosis.

MAMMARY DUCT ECTASIA

Mammary duct ectasia is an inflammatory condition characterized by dilatation of the central ducts with associated fibrosis and chronic inflammation. Perimenopausal and postmenopausal women are most often affected.[13-15] Duct ectasia presents as unilateral or bilateral non-bloody nipple discharge, nipple retraction, or a palpable mass that is typically subareolar and sometimes associated with pain. On mammography, duct ectasia appears as branching calcifications, ductal dilatation, or a stellate mass.[16] Ultrasound shows dilated subareolar ducts or a mass-like lesion filled with echogenic material, which may not be evident on mammography.[17] On magnetic resonance imaging (MRI), duct ectasia can present with a pattern of enhancement that can mimic DCIS.

The microscopic appearance of duct ectasia is variable and depends on the disease stage. In early stages, mild ductal dilatation

http://dx.doi.org/10.4132/jptm.2015.06.11

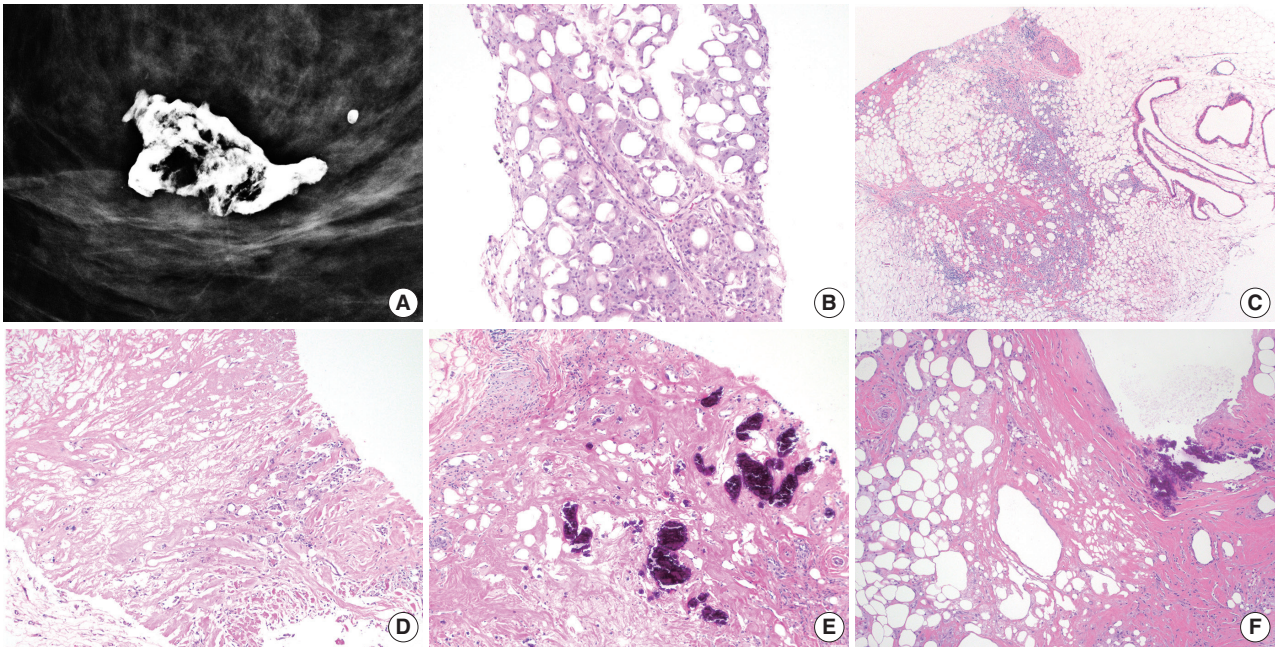

Fig. 1. Mammographic and microscopic features of fat necrosis in core biopsy samples. (A) Mammography shows a calcified lipid cyst, a characteristic feature of fat necrosis. (B) Core biopsy shows foamy histiocytes in adipose tissue. (C) Chronic inflammation is present and histiocyte-lined cysts are evident (right). (D) Necrotic adipocytes, chronic inflammation, and fibrosis are seen. (E, F) Fat necrosis is seen in stereotactic core biopsies obtained due to calcifications. (E) Calcifications formed within necrotic fat. (F) Calcified fibrous wall of a lipid cyst.

with luminal histiocytes is seen (Fig. 2A, B). Ductal epithelium is not hyperplastic and may be flattened or completely absent. Sloughed epithelium may be seen in ductal lumens (Fig. 2C). Lipid-laden foamy histiocytes can be seen within the duct lumen and in adjacent stroma. Intraepithelial histiocytes can also be seen. "Ochrocytes" refers to histiocytes in periductal stroma that show accumulation of lipofuscin pigment, which imparts a brown color to the cells (Fig. 2D).[18] A periductal chronic inflammatory cell infiltrate composed of lymphocytes and plasma cells is also present, particularly when leakage of duct contents into the surrounding stroma has occurred. In the later stages of duct ectasia, fibrosis of duct walls, sometimes accompanied by elastosis, is the predominant histologic feature. The fibrotic wall of the duct may calcify, and can result in calcifications within duct lumens (Fig. 2E). A small portion of a fibrotic duct, with or without accompanying inflammation, may be the only finding in a limited core biopsy sample. Cholesterol granulomas, or "cholesterolomas," may form within ducts and rupture, spilling contents into the surrounding stroma (Fig. 2F).

The differential diagnosis for duct ectasia includes cysts associated with fibrocystic change. Cysts are seen in terminal duct lobular units, in contrast to the subareolar duct involvement seen in duct ectasia. Making this distinction is not critical, as both lesions are typically managed conservatively. Juvenile papillomatosis is an uncommon localized lesion showing a constellation of histologic findings, including ductal stasis with luminal histiocytes. Florid ductal hyperplasia, apocrine metaplasia, papillary proliferations, and sclerosis are other characteristic findings in juvenile papillomatosis. Ductal hyperplasia and papillary epithelial hyperplasia are not seen in duct ectasia. Finally, duct ectasia occur because of duct obstruction due to an intraductal mass. If an intraductal mass is suspected and not represented in the core biopsy, excisional biopsy is necessary.

When duct ectasia is diagnosed in a screening core biopsy, excisional biopsy is not necessary, provided there is radiologic-pathologic concordance. Symptomatic cases of duct ectasia are treated by excision of the involved ducts. Duct ectasia is not associated with an elevated risk for breast carcinoma.

GRANULOMATOUS LOBULAR MASTITIS

Granulomatous mastitis have various etiologies, including infection (bacterial, fungal, mycobacterial), sarcoidosis, and other systemic granulomatous disease. After such causes are excluded, idiopathic "granulomatous lobular mastitis" describes a condition causing chronic, destructive non-necrotizing granulomatous inflammation of lobules. The etiology of granulomatous lobular mastitis is unknown, though some cases are associated with *Co-*

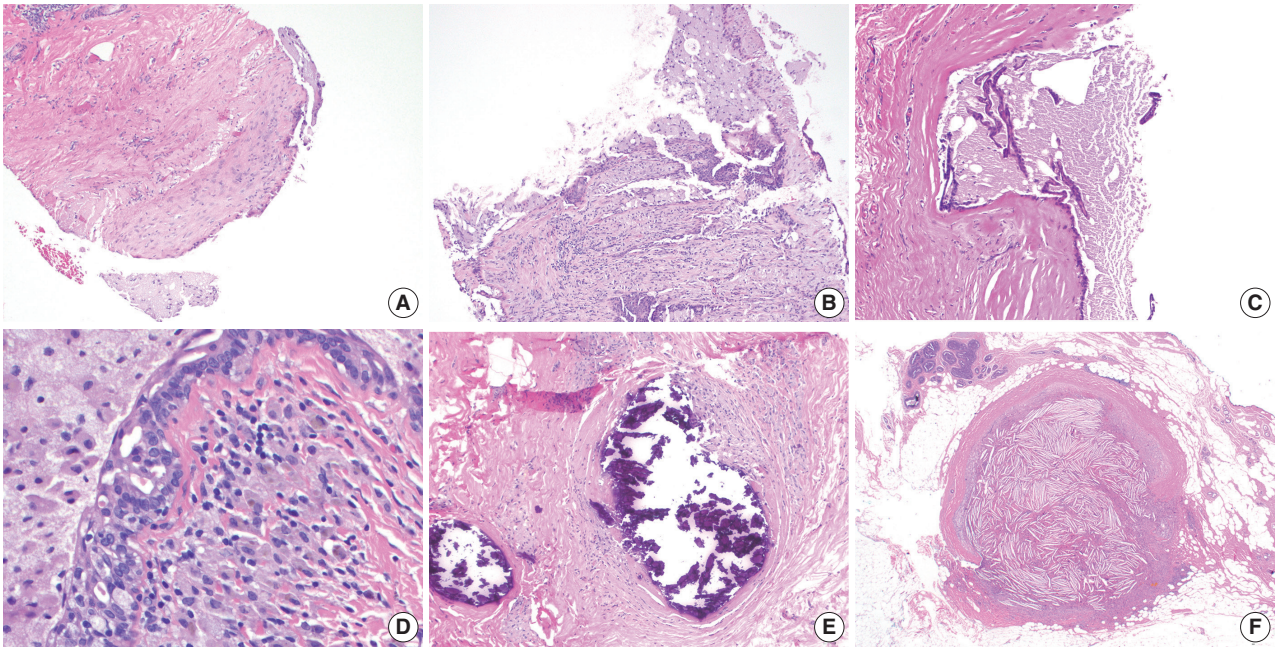

Fig. 2. Mammary duct ectasia. (A) Core biopsy performed for an "intraductal mass" shows a portion of a fibrotic duct wall lined with foamy histiocytes. (B) Disrupted/ruptured duct wall with histiocytes in periductal stroma. (C) Flattened epithelium and fragments within the proteinacious luminal contents. The sample lacks prominent inflammatory features. (D) Brown histiocytes, or "ochrocytes," are seen in the periductal stroma. Intraepithelial foamy histiocytes are also present. (E) An older lesion shows intraductal calcification. (F) Intraductal "cholesteroloma" formed within a duct with rupture into surrounding stroma.

rynebacterium infection (described below). Oral contraceptive use, smoking, and autoimmune disease do not appear to predispose women to granulomatous lobular mastitis.[19]

Most cases of granulomatous lobular mastitis occur in women of reproductive age (20s–40s). Most women have been pregnant at least once prior to presentation, though the condition does not usually occur during pregnancy or lactation.[20-23] Patients present with a unilateral palpable mass that is often accompanied by skin or nipple retraction and pain. Symptoms may be accompanied by axillary lymphadenopathy.[19,21,22] On imaging, granulomatous lobular mastitis is often suggestive of malignancy. A spiculated mass or multiple nodular masses may be seen on mammography.[22,24,25] Ultrasound often shows an irregular hypoechoic mass, fluid collection, tubular structures, or parenchymal mixed echogenicity.[21,22,24-26]

Microscopically, granulomatous lobular mastitis is characterized by non-necrotizing granulomas concentrated in lobules. The granulomas contain epithelioid histiocytes, Langhans giant cells, and lymphoplasmacytic inflammation (Fig. 3A, B). Neutrophilic microabscesses may also be seen. Granulomatous lobular mastitis may be complicated by frank abscess formation and draining skin sinuses. Cystic vacuoles, representing dissolved lipid, are often present within the granulomas, and can be lined by neutrophils; this has been termed "cystic neutrophilic granulomatous mastitis" (Fig. 3C).[27-29] In such cases, gram-positive bacilli representing *Corynebacterium* can be seen within the cystic vacuoles (Fig. 3D). The bacteria show "coryneform" features, such as arrangement into palisades and "V" shapes, as well as clubbing of the organisms. These bacteria are not readily identifiable on hematoxylin and eosin examination, and in most cases only rare (< 10) bacteria may be present in one or two vacuoles in one core biopsy sample. In fact, gram stains and microbial cultures of these samples are often negative in these cases, in part due to the fastidious nature of these organisms.[27] We recently reported on a series of twelve patients with histologically identified cystic neutrophilic granulomatous mastitis.[29] All patients presented with a unilateral breast mass that was painful in six of twelve cases. Imaging was either suspicious (BI-RADS 4) or highly suggestive of malignancy (BI-RADS 5) in over half of the studied cases. Gram-positive bacilli were identified in five of twelve cases, and all microbial cultures were negative for bacterial growth. Patients showed a variable response to treatment, with time to resolution of symptoms ranging from two weeks to six months.

Granulomatous lobular mastitis is often initially encountered in a core biopsy sample, with the differential including other

 http://dx.doi.org/10.4132/jptm.2015.06.11

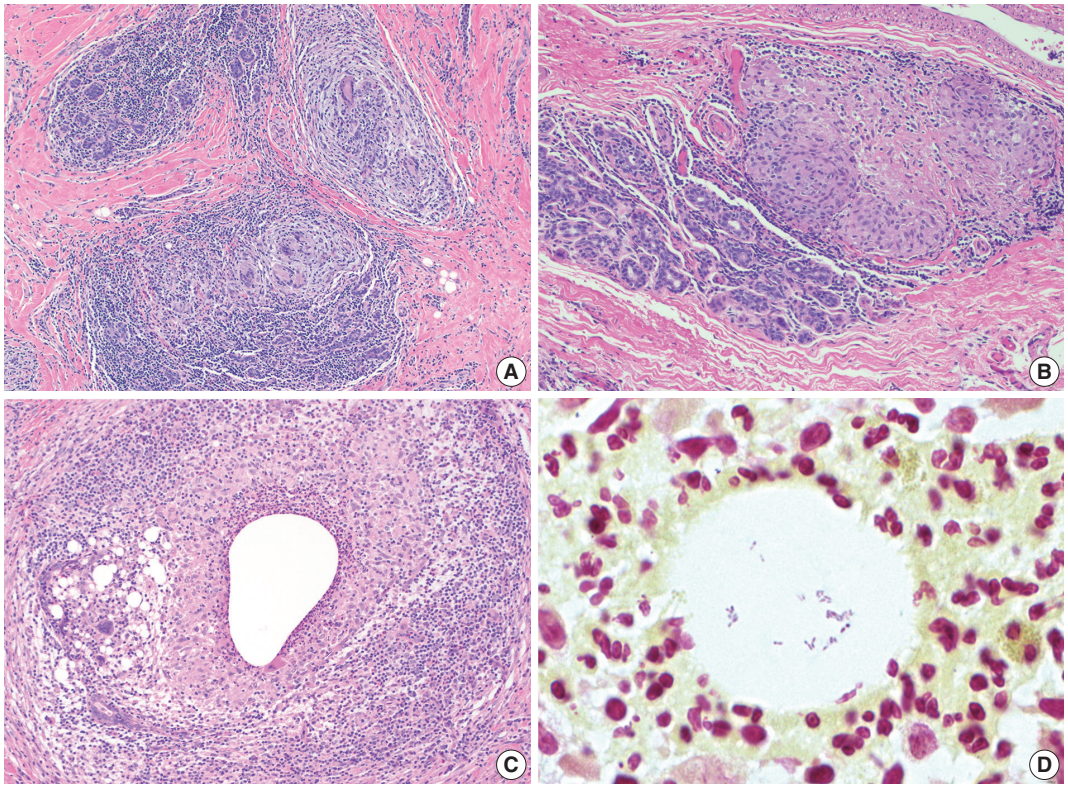

Fig. 3. Granulomatous lobular mastitis. (A, B) Non-necrotizing granulomas are centered within lobules. Granulomas contain Langhans giant cells, and are associated with lymphocytes and plasma cells. (C) Cystic neutrophilic granulomatous mastitis showing neutrophil-lined cysts within granulomas. (D) Gram-positive coryneform bacilli are present within the cysts.

causes of granulomatous lobular inflammation. Special stains should be performed to rule out infection with fungi and acid-fast bacilli as the cause of the granulomatous process. Sarcoidosis should be excluded based on clinical, imaging, and laboratory findings. Sarcoidosis involvement of the breast is uncommon, and rarely the initial site of disease detection. Sarcoid granulomas tend to show less inflammation and are not associated with abscess or microabscess formation, as in granulomatous lobular mastitis. Schaumann bodies and asteroid bodies may be identified within granulomas. In cases where cystic neutrophilic granulomatous mastitis is seen, gram stains should be performed to identify gram-positive bacilli. At our institution, when this pattern is seen on biopsy, we include a note in the pathology report stating its known association with *Corynebacterium* infection, in order to help guide treatment. Microbial cultures should be obtained in all cases of granulomatous lobular mastitis to rule out infection.

Patients with granulomatous lobular mastitis are typically treated using a combination of antibiotics and surgery. Steroids have also been shown to be effective when added to the treatment regimen or used alone.[22,23,28,30,31] Despite various treatments options, patients often experience persistent and recurrent disease, with complications including draining sinuses and abscess formation. Patients often have to undergo multiple surgical procedures and courses of antibiotics.

DIABETIC MASTOPATHY

Diabetic mastopathy, also known as "lymphocytic mastopathy" or "sclerosing lymphocytic lobulitis" is an uncommon mass-forming lesion seen in patients with insulin-dependent (type 1) diabetes mellitus, particularly in those who have long-standing disease with microvascular complications.[32-34] The characteristic histologic findings seen in diabetic mastopathy can also be seen in lesions of patients with type 2 diabetes mellitus, autoimmune diseases such as Hashimoto's thyroiditis, and even those with no history of diabetes or autoimmune disease.[34,35] The cause of diabetic mastopathy is not known. One theory is that hyperglycemia leads to stromal matrix expansion and accumulation of advanced glycosylation end products, leading ultimately to an inflammatory B-cell response.[32] It has also been suggested that diabetic mastopathy develops as a result of an immunologic re-

sponse to exogenous insulin; however, this is unlikely the sole cause, as the lesion also develops in patients who have not taken exogenous insulin.[36]

Diabetic mastopathy most often occurs in premenopausal women, although rare cases have been reported in men.[32,34,35,37] The typical presentation is a palpable unilateral mass, though screening mammography may detect the first changes. In some instances, multiple masses or ill-defined nodules are clinically detectable. The mammographic and sonographic features of diabetic mastopathy may be suspicious for malignancy: mammography may reveal an ill-defined mass, distortion, or dense glandular breast tissue;[38] ultrasound may show an irregular hypoechoic mass with posterior shadowing.[38-40] MRI shows nonspecific enhancement.[40-42]

Tomaszewski *et al*.[32] were the first to put forth criteria for the microscopic diagnosis of diabetic mastopathy. The characteristic constellation of findings includes lymphocytic lobulitis and ductitis, lymphocytic perivasculitis, and stromal fibrosis with epithelioid fibroblasts.[32] Lymphocytic infiltrates, which can be fairly dense, surround ducts, lobules, and small vessels, and may sometimes be associated with plasma cells (Fig. 4A–C). Immunohistochemical characterization of these infiltrates reveals mature B-lymphocytes with a small population of T cells.[43] Germinal centers are not typically seen here. Involved lobules may be atrophic or unremarkable. The stroma in diabetic mastopathy is dense and has a keloidal appearance. Intra-stromal epithelioid fibroblasts appear as plump cells with eosinophilic cytoplasm (Fig. 4B–D). Nuclei are oval to round with vesicular nuclei. Neither significant nuclear atypia nor mitotic figures are seen. The distribution of fibroblasts within the stroma can be heterogeneous, and show a whorled or nodular growth pattern.[35] These distinctive fibroblasts are not present in all cases of diabetic mastopathy. In a series by Ely *et al*.,[35] epithelioid fibroblasts were absent in five of 19 (26%) cases, including the two cases occurring in men. However, these fibroblasts were present in all three non-diabetic patients in their study.

The differential diagnosis for diabetic mastopathy as seen in core biopsy sample depends on which components of the lesion are present in the limited sample. If dense keloidal fibrosis is the predominant finding, fibrocystic change should be considered. It would be atypical for fibrosis to occur in diabetic mastopathy without coexisting perilobular or perivascular lymphocytic in-

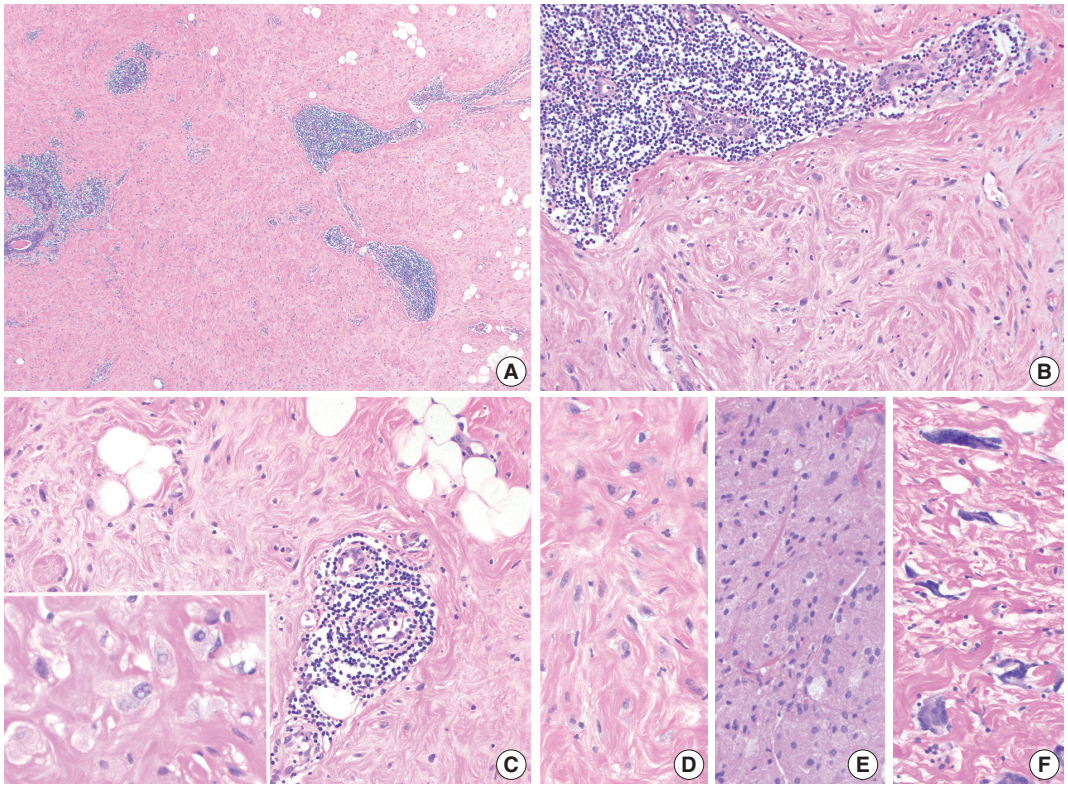

Fig. 4. Diabetic mastopathy. (A) Lymphoid infiltrates surround ducts, lobules, and small vessels. The stroma has a hyalinized appearance. (B, C) Plump epithelioid fibroblasts are present in the stroma (C inset, high power). Perilobular (B) and perivascular (C) chronic inflammation is seen. (D) Fibroblasts in diabetic mastopathy compared with granular cell tumor (E) and multinucleated stromal giant cells (F).

http://dx.doi.org/10.4132/jptm.2015.06.11

filtrates, unless the sample is quite limited. The most diagnostically relevant caveat would be to avoid misclassifying the epithelioid fibroblasts as neoplastic proliferations. Further, care should be taken to exclude carcinomas with abundant eosinophilic cytoplasm, such as pleomorphic lobular carcinomas that exhibit "histiocytoid" and/or apocrine features. These carcinomas, as in diabetic mastopathy, may not be associated with desmoplastic stroma; a broad-spectrum cytokeratin stain can be performed to rule out carcinoma in such cases. Granular cell tumors are composed of cells with abundant pink granular cytoplasm and bland nuclear features (Fig. 4E). These tumors stain positive for S100 and CD68, which helps to distinguish them from diabetic mastopathy. Multinucleated stromal giant cells, a benign incidental finding in breast tissue, can be distinguished from cells of diabetic mastopathy by their multiple hyperchromatic nuclei and scant, versus abundant, cytoplasm (Fig. 4F). Multinucleated stromal giant cells are incidental microscopic findings, while diabetic mastopathy is a mass-forming proliferation. Other mass-forming lesions with lymphoid infiltrates should be considered when lymphocytic ductitis, lobulitis, and perivasculitis are present in the absence of epithelioid fibroblasts. Lymphoma in the breast tends to diffusely infiltrate the stroma, a pattern of inflammation distinct from that seen in diabetic mastopathy. Additionally, immunostaining and molecular analysis will reveal a clonal proliferation of lymphocytes in lymphoma, but not in diabetic mastopathy.

Diabetic mastopathy is a benign condition, and patients can be managed with routine mammographic surveillance. In patients who have undergone excision of the lesion, recurrences may be ipsilateral or contralateral.[35] In a series reported by Dorokhova *et al*.,[40] five of 34 cases (15%) of diabetic mastopathy recurred (2 ipsilateral, 3 bilateral). Patients with diabetic mastopathy are not at increased risk for subsequent development of breast carcinoma. Further, the lymphocytes in diabetic mastopathy do not show evidence of clonality by immunoglobulin heavy chain gene rearrangement studies, and patients also do not appear to be at risk for developing lymphoma.[43]

ABSCESS

Breast abscesses occur most commonly during lactation, but may also occur in the subareolar breast tissue of non-lactating breasts. Abscess formation is a consequence of ductal stasis in both lactational and non-lactational breasts. Though most patients with mastitis or breast abscess are treated with empiric antibiotics, core biopsy is indicated in some cases to rule out malignancy.

Lactational abscess can develop as a complication of mastitis, which occurs in up to 10% of lactating women, most commonly during the initiation and weaning phases of breastfeeding.[44-47] The most common organism isolated from these abscesses is *S. aureus*, identified approximately 50% of the time.[46,48-50] Primiparity, prior lactational mastitis, and improper nursing technique are risk factors for the development of mastitis and abscesses.[44-46] Cracking of the nipple skin may facilitate the entry of bacteria into the ductal system. In a series reported by Dener and Inan,[46] 22 out of 128 patients (17%) with lactational abscess or mastitis had cracked nipples. Bacteria that enter the ducts are supplied with a lactose-rich environment from milk within the ductal lumen. Patients with lactational mastitis and abscess can present with redness, swelling, tenderness, or a palpable mass. Fever may additionally be present in some cases.

Subareolar, or non-puerperal abscesses, most often develop as a consequence of squamous metaplasia of lactiferous ducts. Squamous metaplasia of ducts leads to keratin accumulation with eventual rupture and spillage of duct contents into the surrounding stroma, which leads to abscess formation. This may be complicated abscess rupture and the formation of a sinus tract. The clinical scenario of recurring subareolar abscesses and sinus formation has been referred to as Zuska's Disease or periductal mastitis.[51] Patients with subareolar abscesses are typically premenopausal, though older women and men may also be affected.[49,52] Cigarette smoking is a strong risk factor for the development of subareolar abscesses, with approximately 70%–90% of patients reporting a history of smoking.[50,53,54] Diabetes and obesity are other associated risk factors.[54] Patients present with a painful subareolar or periareolar mass, with or without nipple retraction.[55] Nipple discharge, if present, may have a pasty consistency. Most cases are unilateral, but bilateral disease can also occur. In a series of 152 patients reported by Habif *et al*.,[49] 40 (26%) presented with bilateral abscesses. In contrast with lactational mastitis, the bacteria isolated from non-puerperal abscesses are most commonly mixed and predominantly anaerobic.[54] In one study, coagulase-negative staphylococci was the most common aerobic organism isolated.[56]

Mammographic features of abscesses are non-specific and may include a mass, architectural distortion, or skin thickening.[44,45] Ultrasound shows a hypoechoic mass or a multiloculated fluid collection with a thick, echogenic rim.[45,55]

Microscopically, an abscess shows a mixed inflammatory infiltrate composed mainly of neutrophils in breast tissue, which may additionally show lactational changes in a lactational abscess.

In abscess resolution, neutrophilic inflammation is replaced by granulation tissue and chronic inflammatory changes. In some cases, subareolar abscesses may show dilated ducts that contain squamous metaplasia; a foreign body giant cell reaction to keratin may also be seen within the abscess. The differential diagnosis for breast abscess includes duct ectasia and granulomatous lobular mastitis, both of which can be associated with abscess formation.

Lactational mastitis can be adequately treated with antibiotics, though surgical drainage may be necessary in unresponsive cases.[57] Nursing should be continued throughout treatment, and may in fact help resolve the infection. Treatment of subareolar abscess involves a combination of antibiotics and surgery, involving excision of the abscess and adjacent lactiferous duct. Significantly lower rates of recurrence are seen when the infected duct is also excised, compared excision of abscess alone.[50,53] Subareolar abscesses are often chronic and recurring, with longer time to resolution and higher rates of recurrence, when compared to lactational abscesses.[45,50,57]

Conflicts of Interest

No potential conflict of interest relevant to this article was reported.

REFERENCES

1. Clarke D, Curtis JL, Martinez A, Fajardo L, Goffinet D. Fat necrosis of the breast simulating recurrent carcinoma after primary radiotherapy in the management of early stage breast carcinoma. Cancer 1983; 52: 442-5.
2. Rivera R, Smith-Bronstein V, Villegas-Mendez S, *et al*. Mammographic findings after intraoperative radiotherapy of the breast. Radiol Res Pract 2012; 2012: 758371.
3. Shah C, Badiyan S, Ben Wilkinson J, *et al*. Treatment efficacy with accelerated partial breast irradiation (APBI): final analysis of the American Society of Breast Surgeons MammoSite((R)) breast brachytherapy registry trial. Ann Surg Oncol 2013; 20: 3279-85.
4. Paryani NN, Vallow L, Magalhaes W, *et al*. The incidence of fat necrosis in balloon-based breast brachytherapy. J Contemp Brachytherapy 2015; 7: 29-34.
5. Aqel NM, Howard A, Collier DS. Fat necrosis of the breast: a cytological and clinical study. Breast 2001; 10: 342-5.
6. Hogge JP, Robinson RE, Magnant CM, Zuurbier RA. The mammographic spectrum of fat necrosis of the breast. Radiographics 1995; 15: 1347-56.
7. Taboada JL, Stephens TW, Krishnamurthy S, Brandt KR, Whitman GJ. The many faces of fat necrosis in the breast. AJR Am J Roentgenol 2009; 192: 815-25.
8. Bilgen IG, Ustun EE, Memis A. Fat necrosis of the breast: clinical, mammographic and sonographic features. Eur J Radiol 2001; 39: 92-9.
9. Atasoy MM, Oren NC, Ilica AT, Güvenç İ, Günal A, Mossa-Basha M. Sonography of fat necrosis of the breast: correlation with mammography and MR imaging. J Clin Ultrasound 2013; 41: 415-23.
10. Soo MS, Kornguth PJ, Hertzberg BS. Fat necrosis in the breast: sonographic features. Radiology 1998; 206: 261-9.
11. Morkowski JJ, Nguyen CV, Lin P, *et al*. Rosai-Dorfman disease confined to the breast. Ann Diagn Pathol 2010; 14: 81-7.
12. Guo S, Yan Q, Rohr J, Wang Y, Fan L, Wang Z. Erdheim-Chester disease involving the breast: a rare but important differential diagnosis. Hum Pathol 2015; 46: 159-64.
13. Rahal RM, de Freitas-Junior R, Paulinelli RR. Risk factors for duct ectasia. Breast J 2005; 11: 262-5.
14. Thomas WG, Williamson RC, Davies JD, Webb AJ. The clinical syndrome of mammary duct ectasia. Br J Surg 1982; 69: 423-5.
15. Dixon JM. Periductal mastitis/duct ectasia. World J Surg 1989; 13: 715-20.
16. Sweeney DJ, Wylie EJ. Mammographic appearances of mammary duct ectasia that mimic carcinoma in a screening programme. Australas Radiol 1995; 39: 18-23.
17. An HY, Kim KS, Yu IK, Kim KW, Kim HH. Image presentation. The nipple-areolar complex: a pictorial review of common and uncommon conditions. J Ultrasound Med 2010; 29: 949-62.
18. Davies JD. Pigmented periductal cells (ochrocytes) in mammary dysplasias: their nature and significance. J Pathol 1974; 114: 205-16.
19. Oran EŞ, Gürdal SÖ, Yankol Y, *et al*. Management of idiopathic granulomatous mastitis diagnosed by core biopsy: a retrospective multicenter study. Breast J 2013; 19: 411-8.
20. Going JJ, Anderson TJ, Wilkinson S, Chetty U. Granulomatous lobular mastitis. J Clin Pathol 1987; 40: 535-40.
21. Ocal K, Dag A, Turkmenoglu O, Kara T, Seyit H, Konca K. Granulomatous mastitis: clinical, pathological features, and management. Breast J 2010; 16: 176-82.
22. Hovanessian Larsen LJ, Peyvandi B, Klipfel N, Grant E, Iyengar G. Granulomatous lobular mastitis: imaging, diagnosis, and treatment. AJR Am J Roentgenol 2009; 193: 574-81.
23. Pandey TS, Mackinnon JC, Bressler L, Millar A, Marcus EE, Ganschow PS. Idiopathic granulomatous mastitis: a prospective study of 49 women and treatment outcomes with steroid therapy. Breast J 2014; 20: 258-66.
24. Ozturk M, Mavili E, Kahriman G, Akcan AC, Ozturk F. Granulomatous mastitis: radiological findings. Acta Radiol 2007; 48: 150-5.
25. Al-Khawari HA, Al-Manfouhi HA, Madda JP, Kovacs A, Sheikh M,

 http://dx.doi.org/10.4132/jptm.2015.06.11

Roberts O. Radiologic features of granulomatous mastitis. Breast J 2011; 17: 645-50.
26. Joseph KA, Luu X, Mor A. Granulomatous mastitis: a New York public hospital experience. Ann Surg Oncol 2014; 21: 4159-63.
27. Renshaw AA, Derhagopian RP, Gould EW. Cystic neutrophilic granulomatous mastitis: an underappreciated pattern strongly associated with gram-positive bacilli. Am J Clin Pathol 2011; 136: 424-7.
28. Taylor GB, Paviour SD, Musaad S, Jones WO, Holland DJ. A clinicopathological review of 34 cases of inflammatory breast disease showing an association between corynebacteria infection and granulomatous mastitis. Pathology 2003; 35: 109-19.
29. D'Alfonso T, Moo TA, Arleo E, Cheng E, Antonio L, Hoda S. Cystic neutrophilic granulomatous lobular mastitis: further clinical and pathological characterization of an under-recognized entity based on eleven cases. Mod Pathol 2015; 28 Suppl 2: 40A-41A.
30. Jorgensen MB, Nielsen DM. Diagnosis and treatment of granulomatous mastitis. Am J Med 1992; 93: 97-101.
31. Akbulut S, Yilmaz D, Bakir S. Methotrexate in the management of idiopathic granulomatous mastitis: review of 108 published cases and report of four cases. Breast J 2011; 17: 661-8.
32. Tomaszewski JE, Brooks JS, Hicks D, Livolsi VA. Diabetic mastopathy: a distinctive clinicopathologic entity. Hum Pathol 1992; 23: 780-6.
33. Camuto PM, Zetrenne E, Ponn T. Diabetic mastopathy: a report of 5 cases and a review of the literature. Arch Surg 2000; 135: 1190-3.
34. Soler NG, Khardori R. Fibrous disease of the breast, thyroiditis, and cheiroarthropathy in type I diabetes mellitus. Lancet 1984; 1: 193-5.
35. Ely KA, Tse G, Simpson JF, Clarfeld R, Page DL. Diabetic mastopathy: a clinicopathologic review. Am J Clin Pathol 2000; 113: 541-5.
36. Seidman JD, Schnaper LA, Phillips LE. Mastopathy in insulin-requiring diabetes mellitus. Hum Pathol 1994; 25: 819-24.
37. Logan WW, Hoffman NY. Diabetic fibrous breast disease. Radiology 1989; 172: 667-70.
38. Moschetta M, Telegrafo M, Triggiani V, *et al*. Diabetic mastopathy: a diagnostic challenge in breast sonography. J Clin Ultrasound 2015; 43: 113-7.
39. Chan CL, Ho RS, Shek TW, Kwong A. Diabetic mastopathy. Breast J 2013; 19: 533-8.
40. Dorokhova O, Fineberg S, Koenigsberg T, Wang Y. Diabetic mastopathy, a clinicopathological correlation of 34 cases. Pathol Int 2012; 62: 660-4.
41. Tuncbilek N, Karakas HM, Okten O. Diabetic fibrous mastopathy: dynamic contrast-enhanced magnetic resonance imaging findings. Breast J 2004; 10: 359-62.
42. Wong KT, Tse GM, Yang WT. Ultrasound and MR imaging of diabetic mastopathy. Clin Radiol 2002; 57: 730-5.
43. Valdez R, Thorson J, Finn WG, Schnitzer B, Kleer CG. Lymphocytic mastitis and diabetic mastopathy: a molecular, immunophenotypic, and clinicopathologic evaluation of 11 cases. Mod Pathol 2003; 16: 223-8.
44. Mahoney MC, Ingram AD. Breast emergencies: types, imaging features, and management. AJR Am J Roentgenol 2014; 202: W390-9.
45. Trop I, Dugas A, David J, *et al*. Breast abscesses: evidence-based algorithms for diagnosis, management, and follow-up. Radiographics 2011; 31: 1683-99.
46. Dener C, Inan A. Breast abscesses in lactating women. World J Surg 2003; 27: 130-3.
47. Scott-Conner CE, Schorr SJ. The diagnosis and management of breast problems during pregnancy and lactation. Am J Surg 1995; 170: 401-5.
48. Dabbas N, Chand M, Pallett A, Royle GT, Sainsbury R. Have the organisms that cause breast abscess changed with time? Implications for appropriate antibiotic usage in primary and secondary care. Breast J 2010; 16: 412-5.
49. Habif DV, Perzin KH, Lipton R, Lattes R. Subareolar abscess associated with squamous metaplasia of lactiferous ducts. Am J Surg 1970; 119: 523-6.
50. Versluijs-Ossewaarde FN, Roumen RM, Goris RJ. Subareolar breast abscesses: characteristics and results of surgical treatment. Breast J 2005; 11: 179-82.
51. Zuska JJ, Crile G Jr, Ayres WW. Fistulas of lactifierous ducts. Am J Surg 1951; 81: 312-7.
52. Johnson SP, Kaoutzanis C, Schaub GA. Male Zuska's disease. BMJ Case Rep 2014; 2014: bcr2013201922.
53. Meguid MM, Oler A, Numann PJ, Khan S. Pathogenesis-based treatment of recurring subareolar breast abscesses. Surgery 1995; 118: 775-82.
54. Gollapalli V, Liao J, Dudakovic A, Sugg SL, Scott-Conner CE, Weigel RJ. Risk factors for development and recurrence of primary breast abscesses. J Am Coll Surg 2010; 211: 41-8.
55. Lo G, Dessauvagie B, Sterrett G, Bourke AG. Squamous metaplasia of lactiferous ducts (SMOLD). Clin Radiol 2012; 67: e42-6.
56. Walker AP, Edmiston CE Jr, Krepel CJ, Condon RE. A prospective study of the microflora of nonpuerperal breast abscess. Arch Surg 1988; 123: 908-11.
57. Kasales CJ, Han B, Smith JS Jr, Chetlen AL, Kaneda HJ, Shereef S. Nonpuerperal mastitis and subareolar abscess of the breast. AJR Am J Roentgenol 2014; 202: W133-9.

Journal of Pathology and Translational Medicine 2015; 49: 288-299
http://dx.doi.org/10.4132/jptm.2015.06.04

■ REVIEW ■

Pathology Reporting of Thyroid Core Needle Biopsy: A Proposal of the Korean Endocrine Pathology Thyroid Core Needle Biopsy Study Group

Chan Kwon Jung[1] · Hye Sook Min[2,3]
Hyo Jin Park[2] · Dong Eun Song[4]
Jang Hee Kim[5] · So Yeon Park[2]
Hyunju Yoo[6] · Mi Kyung Shin[7]
Korean Endocrine Pathology Thyroid Core Needle Biopsy Study Group

[1]Department of Hospital Pathology, College of Medicine, The Catholic University of Korea, Seoul; [2]Department of Pathology, Seoul National University College of Medicine, Seoul; [3]Department of Epidemiology and Preventive Medicine, Graduate School of Public Health, Seoul National University, Seoul; [4]Department of Pathology, University of Ulsan College of Medicine, Seoul; [5]Department of Pathology, Ajou University School of Medicine, Suwon; [6]Department of Pathology, Daerim Saint Mary's Hospital, Seoul; [7]Department of Pathology, Hallym University College of Medicine, Seoul, Korea

Received: April 16, 2015
Revised: June 2, 2015
Accepted: June 3, 2015

Corresponding Authors
Chan Kwon Jung, MD, PhD
Department of Hospital Pathology, Seoul St. Mary's Hospital, College of Medicine, The Catholic University of Korea, 222 Banpo-daero, Seocho-gu, Seoul 137-701, Korea
Tel: +82-2-2258-1622
Fax: +82-2-2258-1627
E-mail: ckjung@catholic.ac.kr

Mi Kyung Shin, MD, PhD
Department of Pathology, Hallym University Kangnam Sacred Heart Hospital, Hallym University College of Medicine, 1 Singil-ro, Yeongdeungpo-gu, Seoul 150-950, Korea
Tel: +82-2-829-5443
Fax: +82-2-829-5268
E-mail: smk0103@yahoo.co.kr

In recent years throughout Korea, the use of ultrasound-guided core needle biopsy (CNB) has become common for the preoperative diagnosis of thyroid nodules. However, there is no consensus on the pathology reporting system for thyroid CNB. The Korean Endocrine Pathology Thyroid Core Needle Biopsy Study Group held a conference on thyroid CNB pathology and developed guidelines through contributions from the participants. This article discusses the outcome of the discussions that led to a consensus on the pathology reporting of thyroid CNB.

Key Words: Thyroid nodule; Guideline; Image-guided biopsy; Preoperative period; Diagnosis

Ultrasound-guided fine needle aspiration cytology (FNAC) is the most accurate, effective and safe method for the preoperative assessment of thyroid nodules.[1] Since 2007, pathologists and clinicians have widely adopted the six-level diagnostic scheme of The Bethesda System for Reporting Thyroid Cytopathology (TBSRTC). The use of standard diagnostic categories has a significant clinical benefit in terms of risk stratification for malignancy, and enhances communication between pathologists and physi-

pISSN 2383-7837
eISSN 2383-7845

cians.[2,3] However, a major limitation of FNAC for the diagnosis of thyroid nodules, is the relatively high incidence of nondiagnostic aspirates (10%–15%) and indeterminate aspirates (10%–30%).[4,5] Patients with thyroid nodules of nondiagnostic or indeterminate aspirates typically undergo repeated aspirations for FNAC or diagnostic surgery.[1]

Ultrasound-guided core needle biopsy (CNB) has been successfully employed for the last decade as a complementary tool for the evaluation of thyroid nodules.[6-9] CNB reportedly reduces the rate of nondiagnostic or indeterminate results.[6] Therefore, CNB can be used when FNAC results are nondiagnostic or fail to correlate with clinical findings or results of ultrasound imaging studies.[4,8,10,11] Limited data suggest that CNB can be used as a first-line method for the preoperative diagnosis of thyroid nodules with a high risk of malignancy.[12] Thyroid CNB also allows ancillary immunohistochemical and molecular tests to be carried out on the tissue sample.

Ultrasound-guided thyroid CNB is a safe procedure in contrast to large CNB, which was employed in the 1990s and requires the use of a larger diameter needle.[6] The overall complication

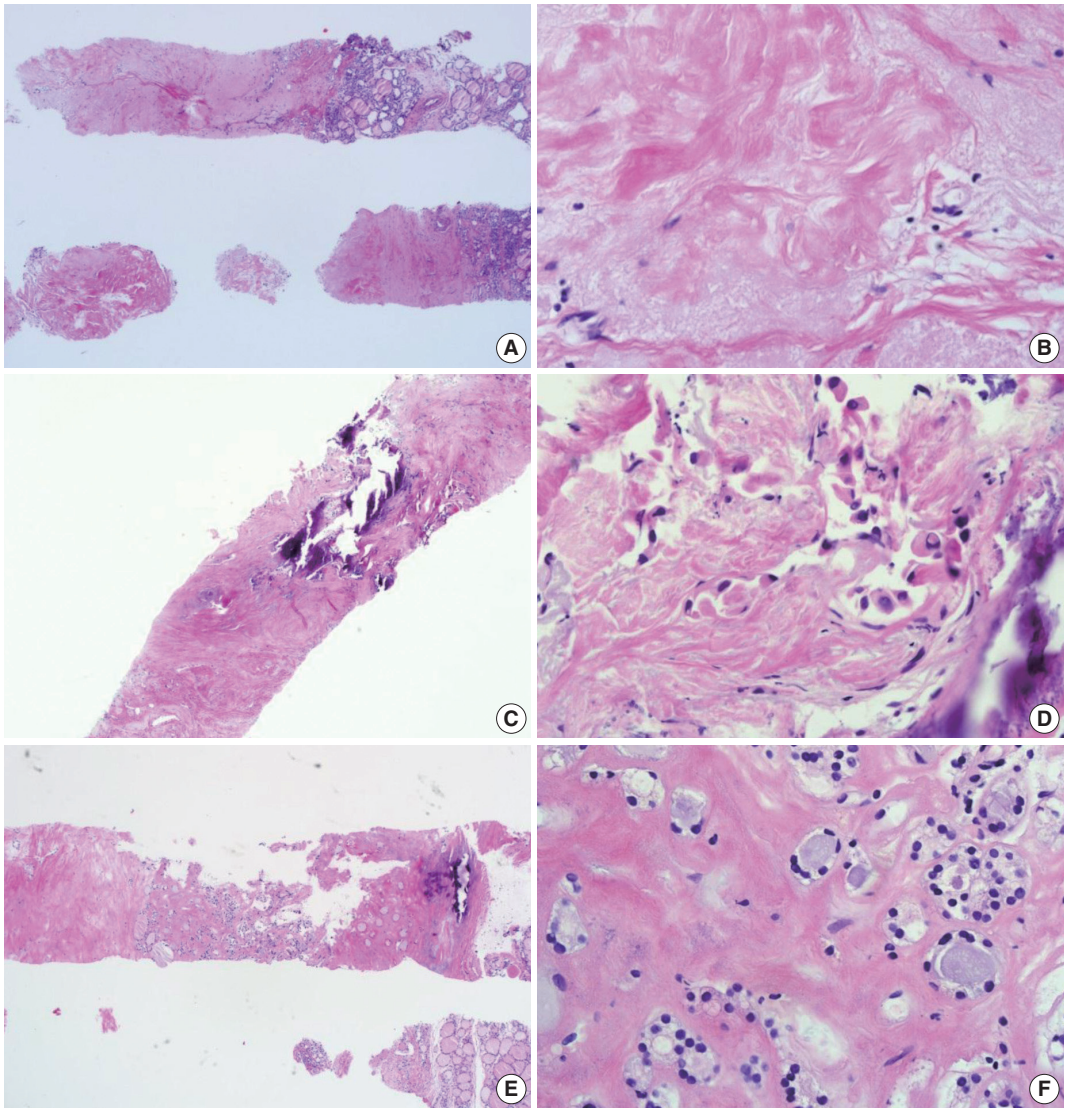

Fig. 1. Core needle biopsies of fibrotic nodules. The right column images represent the high-power views of the lesional area in the left column images. (A) The specimen consists of an acellular fibrotic lesion and adjacent normal parenchyma. (B) The fibrotic area contains no follicular cells, but contains a few lymphocytes and stromal cells. This lesion is classified in the nondiagnostic category. (C) The specimen shows a paucicellular structure with marked fibrosis and calcification. (D) Scattered atypical cells with suspicious morphological features of papillary carcinoma are embedded in the fibrosis. This lesion contains suspicious follicular cells and should therefore be diagnosed as suspicious for malignancy or as a malignancy, depending on the degree of nuclear atypia. (E) The specimen shows marked fibrosis and calcification. (F) The high-power view of the lesion shows relatively numerous benign-appearing follicular cells. This lesion can be diagnosed as a benign follicular nodule.

rate is similar to what has been reported for FNAC.[6,9,13]

The main goal of histopathologic examination by CNB is to triage patients with thyroid disease who need to be surgically managed. Through the use of CNB, a definitive diagnosis is possible in most, but not necessarily all patients. These concepts are the same as those of FNAC. However, in contrast to FNAC, there is no consensus on the diagnostic criteria for reporting thyroid CNB.

CONSENSUS CONFERENCE

Since May 2013, the Korean Endocrine Pathology Thyroid Core Needle Biopsy Study Group has held three consensus conferences on thyroid CNB pathology reporting in Seoul, Korea. The purpose of the conferences was to bring together endocrine pathologists who were thyroid specialists (1) to review existing reporting formats and published literature related to thyroid CNB, (2) to review 25 thyroid CNB specimens using virtual microscopy on each slide, (3) to reach a consensus regarding the histological diagnostic criteria and reporting format of thyroid CNB pathology, and (4) to develop a standard pathology reporting system for thyroid CNB that would be useful for clinical management and pathologic diagnosis. Twenty-one Korean endocrine pathologists participated in the conferences. In Korea, pathologists and clinicians are familiar with TBSRTC terminology and the management guidelines of each diagnostic category.[3] Therefore, all participants in the conferences agreed to use the standardized diagnostic categories for thyroid CNB.

CONTROVERSIAL SUBJECTS

Most participants decided to use the same six-level system as TBSRTC for categorizing the results of thyroid CNB. However, the following concerns exist with regard to the use of the same

Table 1. Diagnostic categories of thyroid core needle biopsy

I. Nondiagnostic or unsatisfactory
• Normal thyroid tissue only
• Extrathyroid tissue only (e.g., skeletal muscle, mature adipose tissue)
• A virtually acellular specimen
• Acellular/paucicellular fibrotic nodule
• Blood clot only
• Other
II. Benign lesion
• Benign follicular nodule or consistent with a benign follicular nodule
• Hashimoto's thyroiditis
• Granulomatous (subacute) thyroiditis
• Nonthyroidal lesion (e.g., parathyroid lesions, benign neurogenic tumors, benign lymph node)
• Other
III. Indeterminate lesion
IIIA. Indeterminate follicular lesion with nuclear atypia
• Follicular proliferative lesions with focal nuclear atypia
• Follicular proliferative lesions with equivocal or questionable nuclear atypia
• Atypical follicular cells embedded in a fibrotic stroma
IIIB. Indeterminate follicular lesion with architectural atypia
• Microfollicular proliferative lesion lacking a fibrous capsule or the adjacent nonlesional tissue in the specimen
• Solid or trabecular follicular lesion lacking a fibrous capsule or the adjacent nonlesional tissue in the specimen
• Macrofollicular proliferative lesion with a fibrous capsule
• Hürthle cell proliferative lesion lacking a fibrous capsule or the adjacent nonlesional tissue in the specimen
IIIC. Other indeterminate lesions
IV. Follicular neoplasm or suspicious for a follicular neoplasm
• Microfollicular proliferative lesion with a fibrous capsule
• Mixed microfollicular and normofollicular proliferative lesion with a fibrous capsule
• Solid/trabecular follicular proliferative lesion with a fibrous capsule
• Hürthle cell proliferative lesion with a fibrous capsule
• Follicular neoplasm with focal nuclear atypia
V. Suspicious for malignancy
• Suspicious for papillary carcinoma, medullary carcinoma, poorly differentiated carcinoma, metastatic carcinoma, lymphoma, etc.
VI. Malignant
• Papillary thyroid carcinoma, poorly differentiated carcinoma, undifferentiated (anaplastic carcinoma), medullary thyroid carcinoma, lymphoma, metastatic carcinoma, etc.
Comments
1. The core needle biopsy provides an accurate diagnosis in most cases; however, it may miss some cancers or sometimes may be inconclusive.
2. Definitive therapeutic surgery (i.e., a total thyroidectomy) should not be undertaken as a result of a category III, IV, or V core needle biopsy diagnosis.
3. The management of a thyroid lesion must be based on a multidisciplinary approach.

http://dx.doi.org/10.4132/jptm.2015.06.04

terminology: (1) some clinicians and pathologists may understand the meaning of terms in a CNB pathology report differently from the terms in an FNAC report; (2) the phrase "atypia of undetermined significance" in TBSRTC is inappropriate terminology in the field of histopathology; (3) there is no consensus regarding specimen adequacy; and (4) the sample representativity of the CNB may be different from that of the FNAC. Therefore, we recommend that the limitations of CNB should be explained in the pathology report.

Most participants in the conferences agreed that a sample composed primarily of an acellular/paucicellular fibrotic nodule should be considered nondiagnostic if it did not contain any atypical cells (Fig. 1). However, a categorical diagnosis should be rendered, irrespective of the number of follicular cells, if a sample contains atypical cells (Fig. 1).

Another dilemma is the differential diagnosis of follicular proliferative lesions without nuclear atypia in a CNB sample. Histologically, hyperplastic nodules are usually found in multiples and are partially encapsulated by a fibrous capsule. Follicular adenoma is a completely encapsulated follicular nodule that is mostly solitary and has microscopic features that are different from those of the surrounding normal thyroid tissue.[14] Fibrous

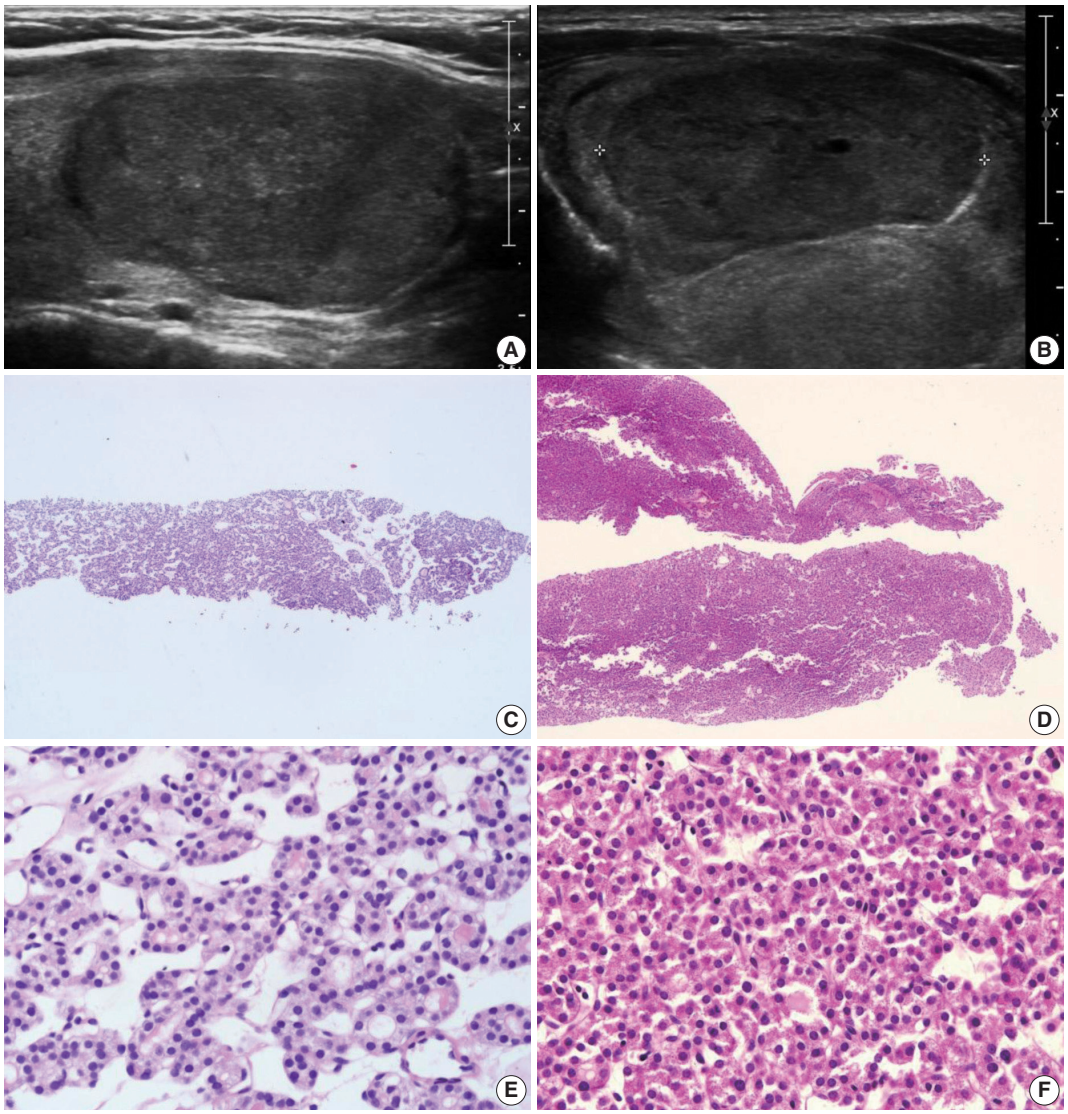

Fig. 2. (A, B) The ultrasound images show well-circumscribed solid, homogeneous, nodules with peripheral hypoechoic rims. (C, D) The core needle biopsies show only microfollicular proliferation. These specimens do not contain a fibrous capsule or adjacent normal tissue that is required to make a diagnosis of follicular neoplasm. (E, F) Images are the high-power views of Fig. 2C and D, respectively. No nuclear atypia is present. The left and right columns show the conventional and Hürthle cell types, respectively. Typical ultrasound features of follicular neoplasms, when present, can lead to the diagnosis of follicular neoplasms, even when specimens are not contained in a fibrous capsule.

capsules of follicular neoplasms vary in thickness. Tumor capsules are usually thin on follicular adenomas and tend to be thicker on follicular carcinomas.[14] It is not possible to differentiate between follicular adenoma and carcinoma using FNAC or CNB samples because the diagnosis of follicular carcinoma is based on the presence of tumor capsular invasion or vascular invasion. Nonetheless, in CNB samples, it may be possible to determine whether a nodule is a follicular neoplasm or a non-neoplastic lesion.[15] Most participants agreed that a diagnosis of "follicular neoplasm or suspicious for a follicular neoplasm" is appropriate when a follicular proliferative lesion is separated from the surrounding thyroid parenchyma by a definite fibrous capsule, has features that are architecturally and cytologically different from the adjacent thyroid glands, and lacks the nuclear features of a papillary carcinoma. However, the CNB specimen of a widely invasive follicular carcinoma may not show a fibrous

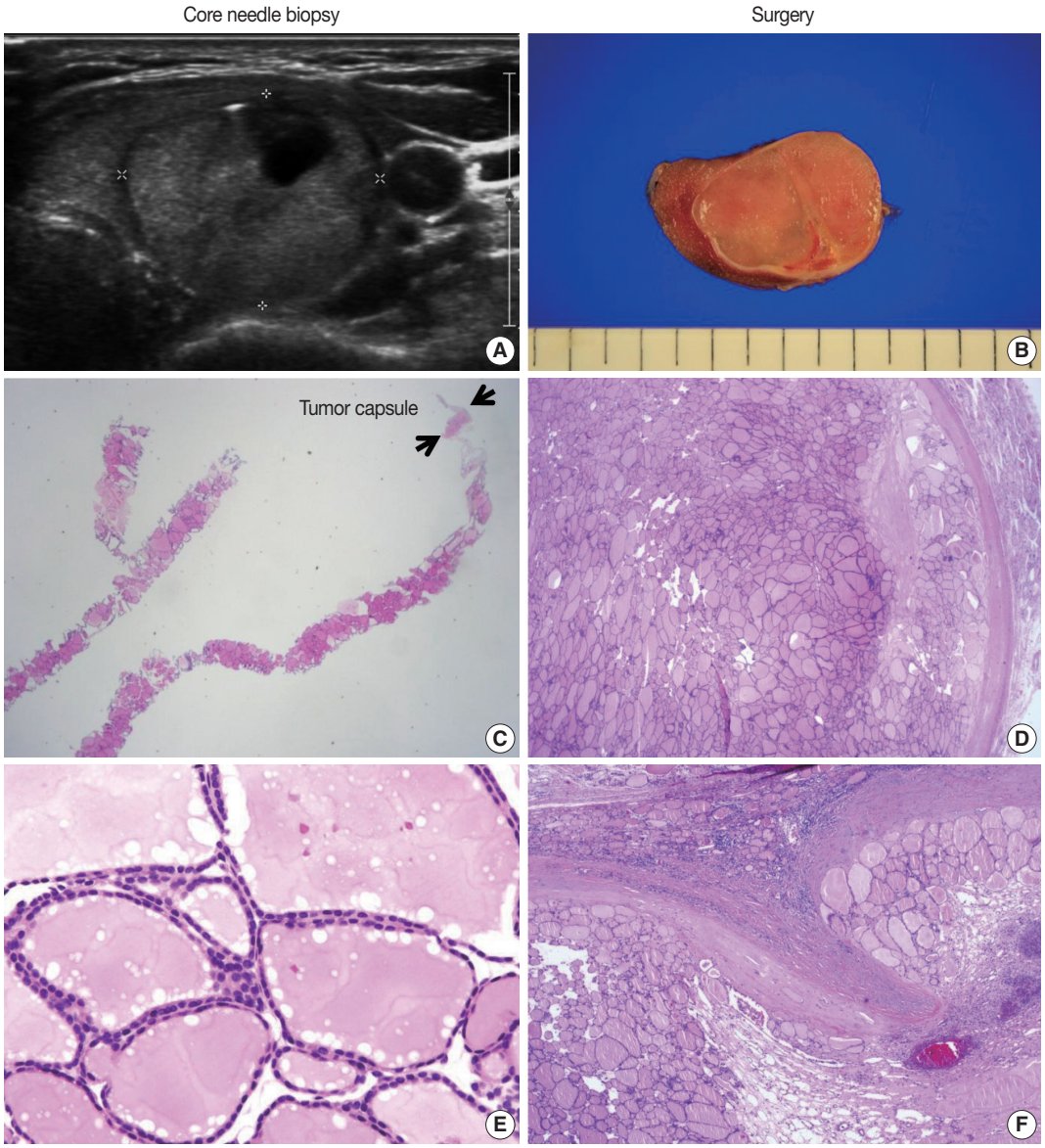

Fig. 3. Core needle biopsy findings of a follicular neoplasm with a macrofollicular growth pattern. The images in the left column and the right column show the core needle biopsy specimen and the resected specimen, respectively. (A) The ultrasound image shows a well-circumscribed, isoechoic, ovoid nodule with a peripheral hypoechoic rim. A focal cystic change is present. (B) The surgical specimen exhibits a thick fibrotic capsule surrounding the nodule. (C) The core needle biopsy shows a macrofollicular proliferative lesion with a fibrous capsule (arrows). (E) The high-power view of the biopsy specimen shows benign-appearing follicular cells. The typical ultrasound features and thick fibrous capsule can lead to a diagnosis of follicular neoplasm, even in a macrofollicular lesion. The microscopic examination of the surgical specimen shows that the tumor is well encapsulated (D) and capsular invasion is minimal (F).

http://dx.doi.org/10.4132/jptm.2015.06.04

capsule because the tumor is not encapsulated although it has invaded into the thyroid parenchyma and extrathyroidal tissue. Some hyperplastic nodules have a cellular microfollicular or solid growth pattern and a fibrous capsule. Therefore, misdiagnosing a widely invasive follicular carcinoma as a benign follicular lesion or a hyperplastic nodule as a follicular neoplasm on the CNB specimens remains a concern.

No study has yet been conducted to define the number of tissue cores that are required for an accurate diagnosis of a thyroid nodule. However, most conference participants agreed that two cores are adequate to diagnose a lesion.

CONSENSUS DIAGNOSTIC CATEGORIES

In the histologic examination of CNB samples, a diagnostic category is selected from the following six standardized options. This proposal was approved by the Korean Endocrine Pathology Thyroid Core Needle Biopsy Study Group (Table 1).

I. Nondiagnostic or unsatisfactory

This category includes specimens with an insufficient number of follicular cells to provide an appropriate diagnosis or when the specimen is not representative of the ultrasound image of the lesion. This diagnosis is subjective; and therefore, the report should explain why the sample is nondiagnostic or unsatisfactory. For example, the sample may be normal thyroid tissue only, extrathyroid tissue only (e.g., skeletal muscle and mature adipose tissue), a virtually acellular specimen, an acellular/paucicellular fibrotic nodule, a blood clot only, or it may show other nondiagnostic or unsatisfactory findings. However, any CNB specimen containing atypical cells should not be considered nondiagnostic or unsatisfactory.

Normal thyroid tissue or extrathyroid tissue only implies that the thyroid lesion has not been sampled. For some benign follicular lesions with normofollicular structures, it may be difficult to assess specimen adequacy. It is important to find the transition between the follicular lesion and the surrounding normal parenchyma and compare between the pathologic finding and its ultrasound images.

II. Benign

This category includes all benign thyroidal and nonthyroidal diseases. A CNB specimen can be classified, based on the specific diagnosis for the lesion, as benign. For example, the sample may

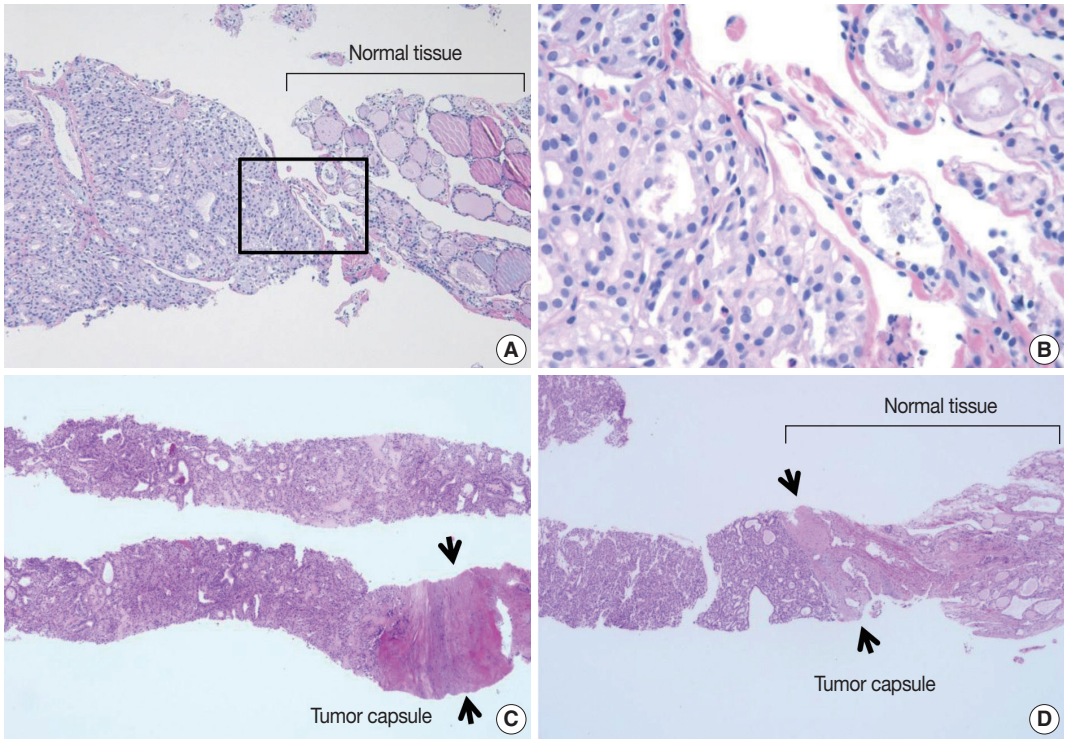

Fig. 4. (A) The core needle biopsy shows a microfollicular proliferative lesion and surrounding normal tissue. (B) The high-power view of the boxed area in Fig. 4A shows that the lesion has no nuclear atypia or fibrous capsule. This lesion should be diagnosed as a benign follicular nodule. (C, D) When microfollicular proliferative lesions show a definite fibrous capsule (arrows) in the core needle biopsy, the specimens should be diagnosed as a follicular neoplasm.

be a benign follicular nodule or consistent with a benign follicular nodule, Hashimoto's thyroiditis, subacute granulomatous thyroiditis, a nonthyroidal lesion (e.g., a parathyroid lesion, benign neurogenic tumors, and benign lymph node), or another benign lesion.

A benign follicular nodule encompasses nodular hyperplasias (adenomatoid nodule), colloid nodules, a nodule in Graves' disease, nodular Hashimoto's thyroiditis, and a subset of follicular adenomas. CNB specimens of these lesions show a benign-appearing normofollicular or macrofollicular structure and do not have a well-defined fibrous capsule.

III. Indeterminate lesion

The cytologic atypia and histologic growth patterns in this category are of uncertain significance and insufficient to be classified under other diagnostic categories. The diagnostic category III "indeterminate lesion" corresponds to "atypia of undetermined significance" or "follicular lesion of undetermined signif-

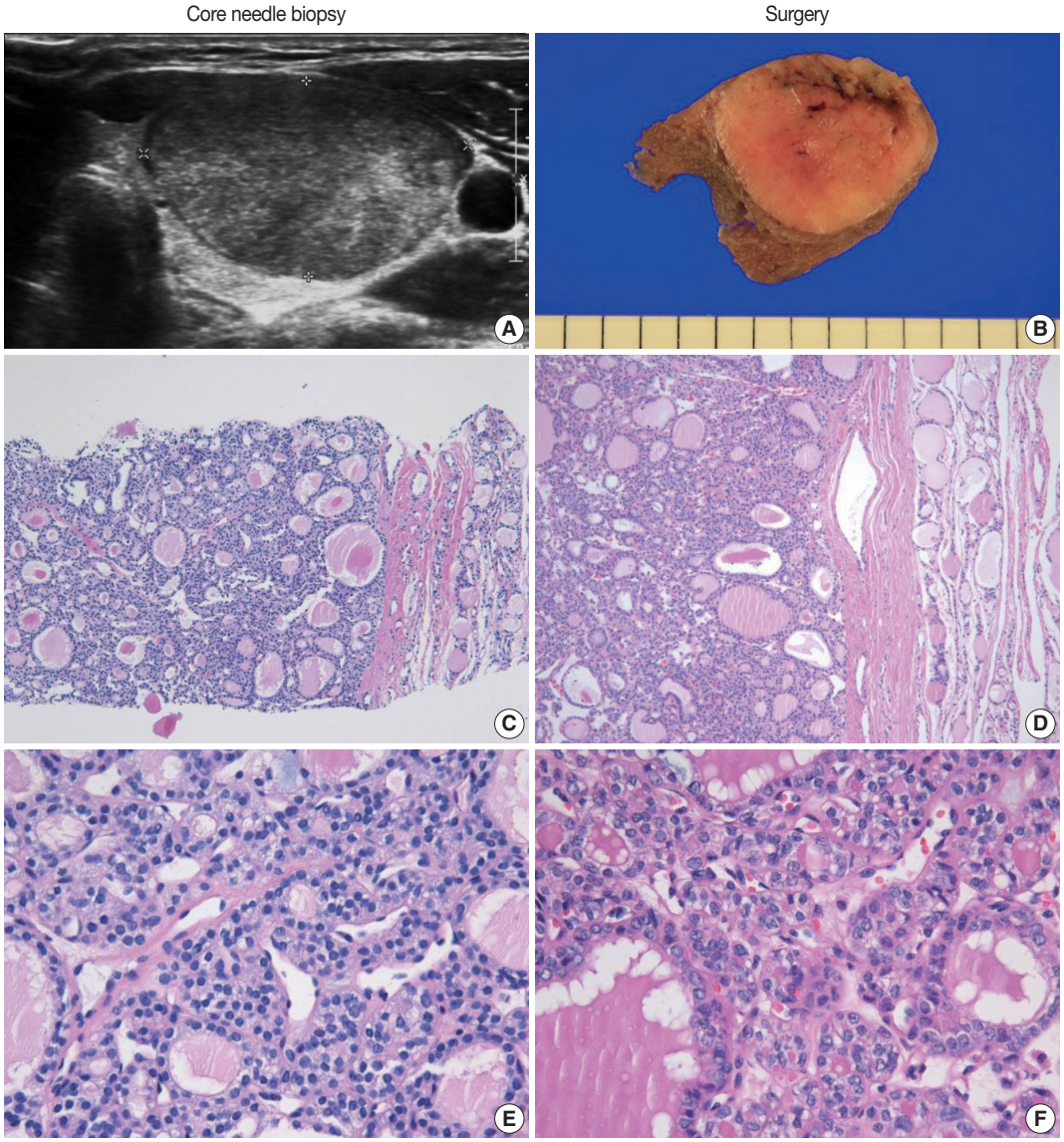

Fig. 5. The core needle biopsy of a follicular neoplasm with focal nuclear atypia. The images in the left and right columns show the findings of the core needle biopsy and the corresponding surgical specimen, respectively. (A) The ultrasound image shows a solid, homogeneous, hypoechoic, ovoid nodule with a peripheral halo. (B) The cut surface of the resected specimen corresponds to the ultrasound image in Fig. 5A. (C, D) The low-power view shows a follicular proliferative lesion with a fibrous capsule. (E) The high-power view of Fig. 5C reveals focal nuclear atypia. (F) The corresponding image in the surgical specimen more definitely shows the morphological features (e.g., nuclear enlargement, irregularity, clearing, and grooves) of a follicular variant of papillary carcinoma.

http://dx.doi.org/10.4132/jptm.2015.06.04

icance" in TBSRTC. However, it was considered inappropriate to use the term "atypia of undetermined significance" in the histopathologic diagnosis of CNB specimens.

The diagnosis of category III is appropriate when a follicular proliferative lesion shows focal nuclear atypia such as nuclear enlargement with pale chromatin, irregular nuclear membranes, and nuclear grooves in a background of predominantly benign-appearing follicles. If a microfollicular proliferative lesion is separated by a fibrous capsule from the surrounding normal parenchyma it is diagnosed as a follicular neoplasm (see category IV). If a fibrous capsule or adjacent nonlesional tissue is not identified in a CNB specimen that shows a predominantly microfollicular or trabecular growth pattern, it is reasonable to classify the lesion as diagnostic category III because it cannot be determined whether the nodule has a fibrous capsule. However, if sonographic features suggest a follicular neoplasm in such lesions, the sample can be considered a category IV, "follicular neoplasm" (Fig. 2).[15] A multidisciplinary approach to a thyroid nodule can improve the preoperative diagnostic accuracy of FNAC and CNB specimens.[16]

FNAC specimens of macrofollicular lesions are usually diagnosed as benign. However, when ultrasound images show the typical features of a follicular neoplasm and the CNB specimen microscopically shows a fibrous capsule, then the CNB specimen can be diagnosed as a follicular neoplasm, even in a macrofollicular lesion (Fig. 3). However, in surgical pathologies, most participants agreed that category III is appropriate in a macrofollicular proliferative lesion with a definite fibrous capsule (Fig. 3).

The following are common scenarios that may be encountered in case of follicular proliferative lesions:

IIIA. Indeterminate follicular lesion with nuclear atypia

Examples in this category are follicular proliferative lesions with focal nuclear atypia, follicular proliferative lesions with equivocal or questionable nuclear atypia, and atypical follicular cells embedded in fibrotic stroma.

IIIB. Indeterminate follicular lesion with architectural atypia

Examples in this category are microfollicular proliferative lesions lacking a fibrous capsule or the adjacent nonlesional tissue in the specimen; solid or trabecular follicular lesions lacking a fibrous capsule or the adjacent nonlesional tissue in the specimen; macrofollicular proliferative lesions with a fibrous capsule; Hürthle cell proliferative lesions lacking a fibrous capsule or the

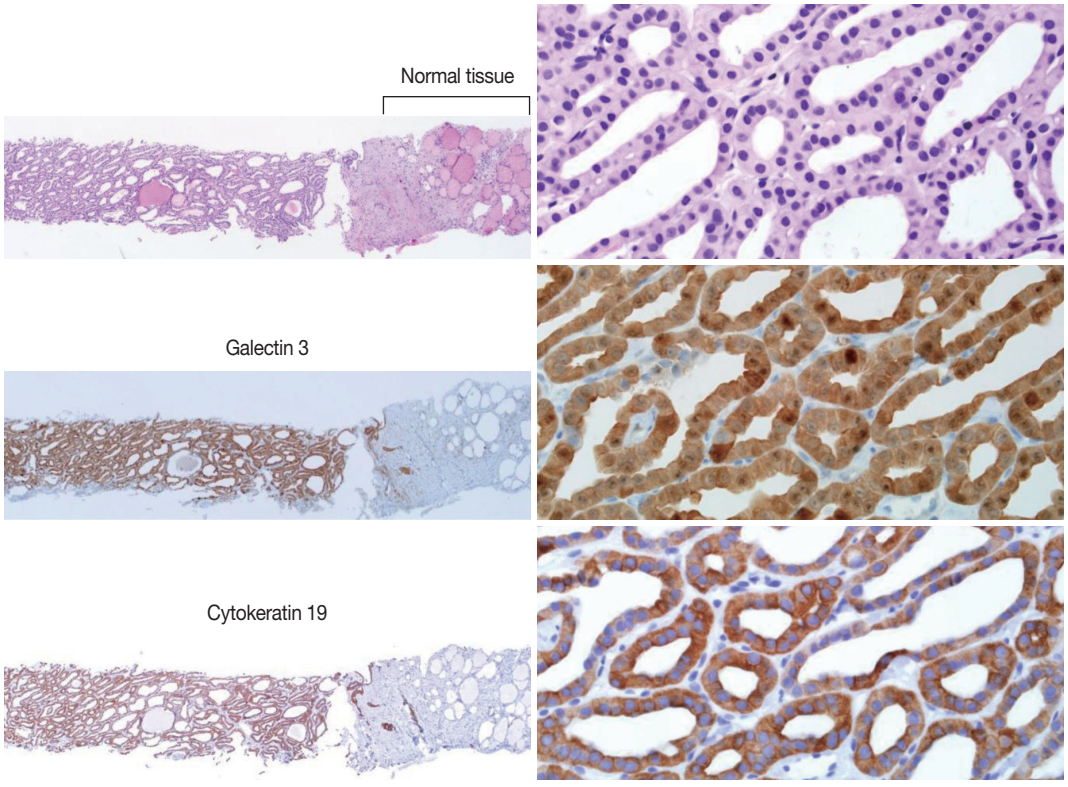

Fig. 6. The core needle biopsy shows a follicular proliferative lesion with nuclear atypia and diffuse strong immunohistochemical staining for galectin 3 and cytokeratin 19 in the tumor cells. Images in the left and right columns show the low magnification and high magnification views, respectively, of the samples.

adjacent nonlesional tissue in the specimen.

IIIC. Other indeterminate lesions

IV. Follicular neoplasm or suspicious for a follicular neoplasm

In CNB and FNAC, the term "follicular neoplasm or suspicious for a follicular neoplasm" is used to encompass neoplastic lesions with follicular proliferative patterns (e.g., follicular adenoma, follicular carcinoma, follicular variant of papillary carcinoma, follicular variant of medullary carcinoma).[2,3] The histologic diagnosis of "follicular neoplasm or suspicious for a follicular neoplasm" in a CNB specimen is based on the presence of a fibrous capsule and microscopic features that differ from the adjacent thyroid parenchyma (Fig. 4). Follicular cells do not show the typical nuclear features of papillary carcinomas. It is important to identify a well-formed fibrous capsule in the CNB specimen. The FNAC diagnosis for follicular neoplasm is primarily based on the presence of microfollicular or trabecular architecture and the lack of colloid. In a CNB specimen, the growth patterns of a follicular neoplasm can be microfollicular, normofollicular, solid, or trabecular when a fibrous tumor capsule is identified in the sample. Examples in this category include microfollicular proliferative lesions with fibrous capsules, mixed microfollicular and

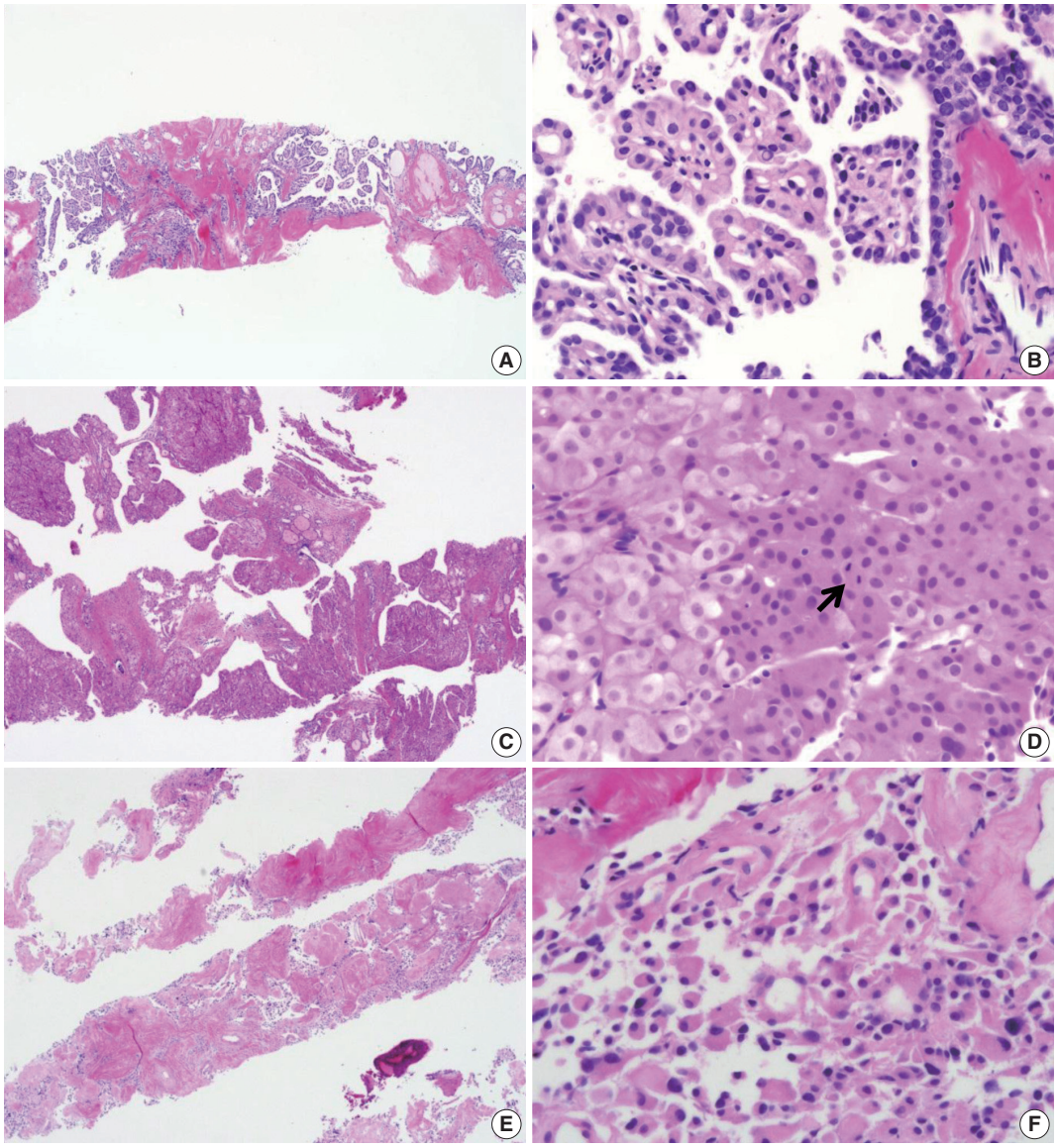

Fig. 7. Core needle biopsies of malignant thyroid nodules. (A, B) The biopsy specimen maintains the typical morphological features of papillary carcinoma. Poorly differentiated carcinoma shows solid, trabecular, and insular growth patterns (C) and mitosis (arrow) (D) under the high-power view. The medullary carcinoma shows the typical morphological features under the low-power view (E) and the high-power view (F).

http://dx.doi.org/10.4132/jptm.2015.06.04

normofollicular proliferative lesions with fibrous capsules, solid or trabecular follicular lesions with fibrous capsules, Hürthle cell proliferative lesions with fibrous capsules, and follicular neoplasms or samples suspicious for follicular neoplasms with focal nuclear atypia.

A recent study reported that the neoplasm or malignancy rate was not different among these architectural patterns of follicular lesions.[15] A CNB cannot discriminate between a follicular carcinoma and a follicular adenoma because the diagnosis of these neoplasms requires examination of the entire thick fibrous capsule. However, in a subset of this category, focal nuclear atypia raises the possibility of a follicular variant of papillary carcinoma (Fig. 5).[15,17,18] A follicular variant of papillary carcinoma is reportedly the most common malignancy found after surgery of thyroid nodules with a preoperative diagnosis of follicular neoplasm.[17,18]

Histological findings of a follicular neoplasm on the CNB sample should be correlated with ultrasound imaging features. Typical ultrasound images of a follicular neoplasm show a well-circumscribed, solid, ovoid or round mass with a surrounding halo or a hypoechoic rim around the thyroid nodule (Figs. 3, 5).[19,20] The neoplasm can be hypoechoic, isoechoic, hyperechoic, or mixed.[20] The sonographic halo corresponds with the fibrous capsule surrounding the follicular lesion (Figs. 3, 5).[19,20] Focal cystic change can be present, but calcification is rare.[20]

V. Suspicious for malignancy

The "suspicious for malignancy" diagnosis is given when histologic features are strongly suspicious for malignancy, but they are insufficient for a definitive diagnosis of malignancy. In this category, a lesion may be suspicious for papillary thyroid carcinoma, suspicious for medullary thyroid carcinoma, suspicious for poorly differentiated thyroid carcinoma, suspicious for metastatic carcinoma, suspicious for lymphoma, or show other suspicious findings.

Ancillary immunohistochemical or molecular studies can be helpful for the diagnosis of CNB specimens with findings that are suspicious for malignancy. An immunostaining panel consisting of galectin-3, HBME1, cytokeratin 19, or CD56 is helpful in the diagnosis of lesions suspicious for papillary thyroid carcinoma (Fig. 6).[21-23] A combination of at least two immunostaining markers is recommended to improve the diagnostic ac-

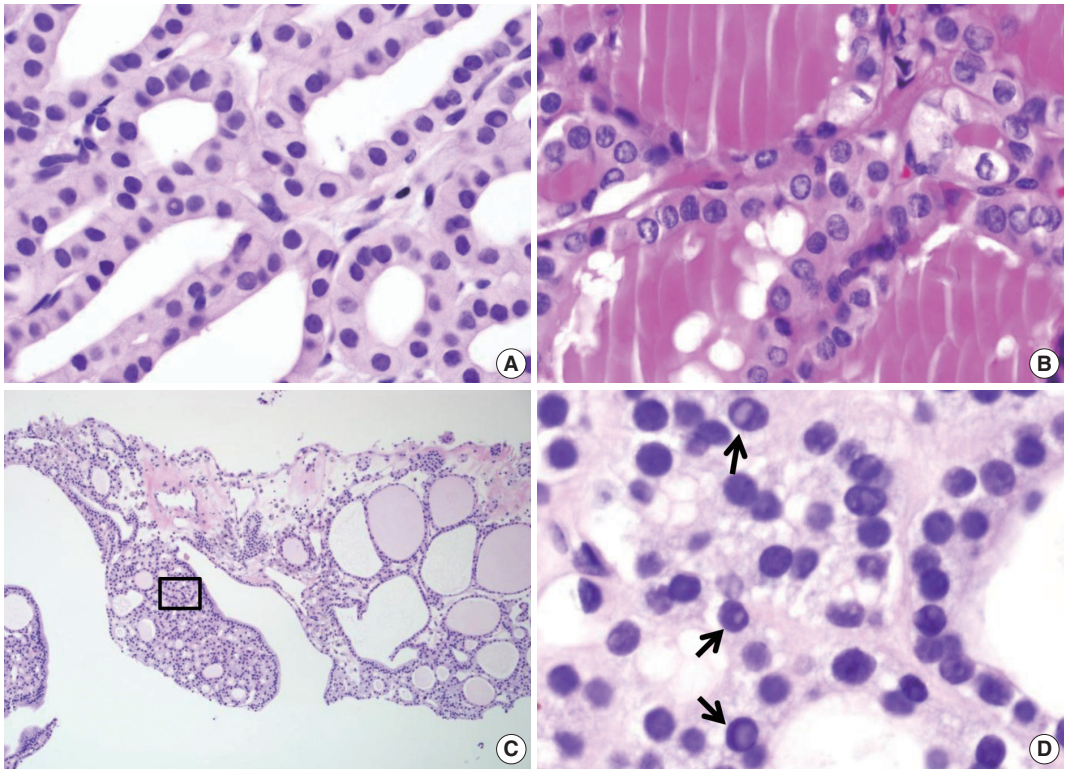

Fig. 8. Diagnostic pitfalls in thyroid core needle biopsy. Follicular cells are smaller and darker in core needle biopsies in comparison (A) to resected specimens (B). These images have been obtained from the same patient as those pictured in Fig. 6. (C) The core needle biopsy shows the histologic features of a benign follicular nodule. (D) The high-power view of the boxed area in Fig. 8C shows nuclear vacuoles that mimic intranuclear cytoplasmic pseudoinclusions in papillary carcinoma (arrows).

curacy.[22] Presence of the *BRAF* V600E mutation, detected by molecular test or immunostaining, strongly suggests a diagnosis of the papillary carcinoma.[21]

A diagnosis of medullary thyroid carcinoma can be confirmed with positive immunostaining for calcitonin on a CNB specimen. A diagnosis of lymphoma can be rendered using immunophenotyping studies on a CNB specimen that is suspicious for lymphoma.[5]

VI. Malignant

Most thyroid malignancies, except for follicular carcinoma, have typical histologic features and are easily diagnosed as a malignancy on a CNB specimen. The following diagnoses are included in this category: papillary thyroid carcinoma (Fig. 7A, B), poorly differentiated carcinoma (Fig. 7C, D), undifferentiated (anaplastic) carcinoma, medullary thyroid carcinoma (Fig. 7E, F), lymphoma, and metastatic carcinoma.

COMMON PITFALLS OF A DIAGNOSIS OF CORE NEEDLE BIOPSY

The follicular cells in a CNB specimen appear smaller and show darker chromatin than in typical surgical specimens (Fig. 8A, B). Nuclear artifacts that mimic intranuclear cytoplasmic pseudoinclusions in papillary carcinoma may also be present in benign follicular cells (Fig. 8C, D). The artifactual vacuoles are irregularly shaped and appear pale on staining, whereas pseudoinclusions in papillary carcinoma are round and sharply delineated by the rim of the nuclear membrane.

Conflicts of Interest

No potential conflict of interest relevant to this article was reported.

Acknowledgments

The authors would like to thank the members of the Endocrine Pathology Study Group of the Korean Society of Pathologists for their valuable expertise and suggestions throughout this study. This research was supported by the Korean Society of Pathologists Grant 2013 and Basic Science Research Program through the National Research Foundation of Korea (NRF) funded by the Ministry of Science, ICT and future planning (2013R1A2A2A01068570).

REFERENCES

1. American Thyroid Association (ATA) Guidelines Taskforce on Thyroid Nodules and Differentiated Thyroid Cancer, Cooper DS, Doherty GM, *et al*. Revised American Thyroid Association management guidelines for patients with thyroid nodules and differentiated thyroid cancer. Thyroid 2009; 19: 1167-214.
2. Ali SZ. Thyroid cytopathology: Bethesda and beyond. Acta Cytol 2011; 55: 4-12.
3. Cibas ES, Ali SZ; NCI Thyroid FNA State of the Science Conference. The Bethesda System for Reporting Thyroid Cytopathology. Am J Clin Pathol 2009; 132: 658-65.
4. Lee SH, Kim MH, Bae JS, Lim DJ, Jung SL, Jung CK. Clinical outcomes in patients with non-diagnostic thyroid fine needle aspiration cytology: usefulness of the thyroid core needle biopsy. Ann Surg Oncol 2014; 21: 1870-7.
5. Hahn SY, Shin JH, Han BK, Ko EY, Ko ES. Ultrasonography-guided core needle biopsy for the thyroid nodule: does the procedure hold any benefit for the diagnosis when fine-needle aspiration cytology analysis shows inconclusive results? Br J Radiol 2013; 86: 20130007.
6. Trimboli P, Crescenzi A. Thyroid core needle biopsy: taking stock of the situation. Endocrine 2015; 48: 779-85.
7. Sung JY, Na DG, Kim KS, *et al*. Diagnostic accuracy of fine-needle aspiration versus core-needle biopsy for the diagnosis of thyroid malignancy in a clinical cohort. Eur Radiol 2012; 22: 1564-72.
8. Na DG, Kim JH, Sung JY, *et al*. Core-needle biopsy is more useful than repeat fine-needle aspiration in thyroid nodules read as nondiagnostic or atypia of undetermined significance by the Bethesda system for reporting thyroid cytopathology. Thyroid 2012; 22: 468-75.
9. Baek JH, Na DG, Lee JH, *et al*. Core needle biopsy of thyroid nodules: consensus statement and recommendations. J Korean Soc Ultrasound Med 2013; 32: 95-102.
10. Ha EJ, Baek JH, Lee JH, *et al*. Core needle biopsy can minimise the non-diagnostic results and need for diagnostic surgery in patients with calcified thyroid nodules. Eur Radiol 2014; 24: 1403-9.
11. Yeon JS, Baek JH, Lim HK, *et al*. Thyroid nodules with initially nondiagnostic cytologic results: the role of core-needle biopsy. Radiology 2013; 268: 274-80.
12. Trimboli P, Nasrollah N, Guidobaldi L, *et al*. The use of core needle biopsy as first-line in diagnosis of thyroid nodules reduces false negative and inconclusive data reported by fine-needle aspiration. World J Surg Oncol 2014; 12: 61.
13. Nasrollah N, Trimboli P, Rossi F, *et al*. Patient's comfort with and tolerability of thyroid core needle biopsy. Endocrine 2014; 45: 79-83.
14. Baloch ZW, LiVolsi VA. Our approach to follicular-patterned lesions of the thyroid. J Clin Pathol 2007; 60: 244-50.

http://dx.doi.org/10.4132/jptm.2015.06.04

15. Min HS, Kim JH, Ryoo I, Jung SL, Jung CK. The role of core needle biopsy in the preoperative diagnosis of follicular neoplasm of the thyroid. APMIS 2014; 122: 993-1000.
16. Yassa L, Cibas ES, Benson CB, *et al*. Long-term assessment of a multidisciplinary approach to thyroid nodule diagnostic evaluation. Cancer 2007; 111: 508-16.
17. Bae JS, Choi SK, Jeon S, *et al*. Impact of *NRAS* mutations on the diagnosis of follicular neoplasm of the thyroid. Int J Endocrinol 2014; 2014: 289834.
18. Ustun B, Chhieng D, Van Dyke A, *et al*. Risk stratification in follicular neoplasm: a cytological assessment using the modified Bethesda classification. Cancer Cytopathol 2014; 122: 536-45.
19. Sillery JC, Reading CC, Charboneau JW, Henrichsen TL, Hay ID, Mandrekar JN. Thyroid follicular carcinoma: sonographic features of 50 cases. AJR Am J Roentgenol 2010; 194: 44-54.
20. Reading CC, Charboneau JW, Hay ID, Sebo TJ. Sonography of thyroid nodules: a "classic pattern" diagnostic approach. Ultrasound Q 2005; 21: 157-65.
21. Crescenzi A, Guidobaldi L, Nasrollah N, *et al*. Immunohistochemistry for *BRAF*(V600E) antibody VE1 performed in core needle biopsy samples identifies mutated papillary thyroid cancers. Horm Metab Res 2014; 46: 370-4.
22. Alshenawy HA. Utility of immunohistochemical markers in diagnosis of follicular cell derived thyroid lesions. Pathol Oncol Res 2014; 20: 819-28.
23. El Demellawy D, Nasr AL, Babay S, Alowami S. Diagnostic utility of CD56 immunohistochemistry in papillary carcinoma of the thyroid. Pathol Res Pract 2009; 205: 303-9.

Journal of Pathology and Translational Medicine 2015; 49: 300-309
http://dx.doi.org/10.4132/jptm.2015.06.16

REVIEW

The Utilization of Cytologic Fine-Needle Aspirates of Lung Cancer for Molecular Diagnostic Testing

Michael H. Roh

Department of Pathology, University of Michigan Health System, Ann Arbor, MI, USA

Received: May 6, 2015
Revised: June 10, 2015
Accepted: June 16, 2015

Corresponding Author
Michael H. Roh, MD, PhD
Department of Pathology, University of Michigan Health System, 1500 E. Medical Center Drive, Ann Arbor, MI 48109-5054, USA
Tel: +1-734-936-6776
Fax: +1-734-763-4095
E-mail: mikro@med.umich.edu

In this era of precision medicine, our understanding and knowledge of the molecular landscape associated with lung cancer pathogenesis continues to evolve. This information is being increasingly exploited to treat advanced stage lung cancer patients with tailored, targeted therapy. During the management of these patients, minimally invasive procedures to obtain samples for tissue diagnoses are desirable. Cytologic fine-needle aspirates are often utilized for this purpose and are important not only for rendering diagnoses to subtype patients' lung cancers, but also for ascertaining molecular diagnostic information for treatment purposes. Thus, cytologic fine-needle aspirates must be utilized and triaged judiciously to achieve both objectives. In this review, strategies in utilizing fine-needle aspirates will be discussed in the context of our current understanding of the clinically actionable molecular aberrations underlying non-small cell lung cancer and the molecular assays applied to these samples in order to obtain treatment-relevant molecular diagnostic information.

Key Words: Lung neoplasms; Cytology; Biopsy, fine-needle; Molecular testing; Precision medicine

During this current era of precision medicine, our current knowledge regarding the molecular drivers underlying cancer continues to evolve. Therefore, anatomic pathology specimens are becoming increasingly utilized for molecular diagnostic assays in order to detect clinically actionable genetic abnormalities in addition to routine diagnoses. This allows for tailored, personalized therapy in a subset of patients afflicted with malignancies harboring actionable genetic mutations for which approved targeted therapeutic agents exist. Molecular testing is therefore most relevant in the context of high-stage, surgically unresectable cancers. In this setting, minimally invasive small biopsy procedures are preferable in that they are associated with low risk of complications for the patient. Cytologic fine-needle aspiration (FNA) specimens are especially suitable, in this regard, as FNA procedures represent rapid, efficient, and minimally invasive means to sample superficial and deep lesions. Technological advances in imaging modalities and instruments such as computed tomography and endobronchial ultrasound (EBUS) have facilitated accurate and precise sampling of the latter. This constellation of circumstances poses unique challenges and opportunities for pathologists as FNA samples must be judiciously utilized, not only for rendering accurate cytologic diagnoses, but also effectively preserved and triaged for anticipated, relevant downstream molecular diagnostic assays.

In the past decade, significant strides have been made in further optimizing the use of small biopsy specimens and FNAs of non-small cell lung carcinomas (NSCLCs), especially adenocarcinomas and mixed histological subtypes with a component of adenocarcinomatous differentiation, for molecular studies.[1] One commonly held misconception is that FNAs are generally insufficient for the performance of molecular assays. However, for instance, we and others have observed and demonstrated that cellularity on the order of 100–500 cells are sufficient for DNA sequencing-based assays.[2,3] For fluorescence *in-situ* hybridization (FISH) assays, 100 analyzable tumor cell nuclei are generally sufficient.[3]

Successfully integrating molecular ancillary techniques into routine cytology practice is essential in facilitating the appropriate management of advanced stage cancer patients by their oncologists.[4,5] The purpose of this review is to describe the approach to processing lung cancer FNA specimens at our institution, within the contexts of our current understanding of clinically actionable genetic abnormalities in NSCLCs and diverse cytopreparatory platforms on which molecular diagnostic tests are performed.

pISSN 2383-7837
eISSN 2383-7845

FINE-NEEDLE ASPIRATION SPECIMEN PROCESSING

FNAs represent an advantageous, effective means to obtain diagnostic cellular material as they can often sample a wide area of the target lesion, acquire tumor cells with lower contamination by background stromal connective tissue elements, and allow for immediate assessment during rapid on-site evaluation (ROSE). During the on-site assessment, a member of the cytopathology team is present and prepares direct smears, using the contents expelled from the needle, at the location of the procedure. This is advantageous for three reasons: each needle pass can be examined to determine tumor cell adequacy; there is an opportunity to engage the clinical care provider in a conversation regarding the preliminary diagnosis and relevant molecular diagnostic tests; and the cytopathology team member can help ensure that the specimen is processed in a manner that optimizes judicious triage for ancillary tests, including molecular studies.[4,5] FNAs can be performed without ROSE and in this setting, the contents of the FNA needles are typically expelled and rinsed in a cell preservative solution for use in liquid-based cytology (LBC) preparations. Examples of LBC preparations include ThinPrep (Hologic, Bedford, MA, USA), SurePath (Becton Dickinson, Franklin Lakes, NJ, USA), thin-layer advanced cytology assay system (TACAS, MBL, Tokyo, Japan), and Liqui-PREP (LGM International Inc., Ft. Lauderdale, FL, USA). Nonetheless, ROSE is an effective means to maximize the chances of success in acquiring adequate tumor cells for diagnosis and anticipated molecular studies. The ultimate goal is to prevent unnecessary repeat procedures to obtain additional tissue just for molecular studies which can lead to delays in treatment.

For patients afflicted with lung cancer at our institution, we perform ROSE for cytopathologist-performed FNAs and for EBUS-guided FNAs, performed by our clinical colleagues. The contents of each needle pass are expelled onto a slide which is utilized to prepare direct smears. The needle is then rinsed into buffered media; we utilize RPMI media for this purpose. Commonly, a pair of direct smears is prepared per needle pass; one is air-dried and the other is immediately alcohol-fixed. The air-dried smear is stained on-site with the Diff-Quik (Romanowsky) stain and the stained slide can be examined under the microscope immediately thereafter. The alcohol-fixed smear is stained later in the cytopathology laboratory with the Papanicolaou stain. Alternatively, the needle contents can be distributed over multiple smears allowing for flexibility in the utilization of direct smears for cytomorphologic evaluation and ancillary studies (Fig. 1).[4,5] Based on the findings in the Diff-Quik stained smears, the determination can be made to perform additional needle passes to ob-

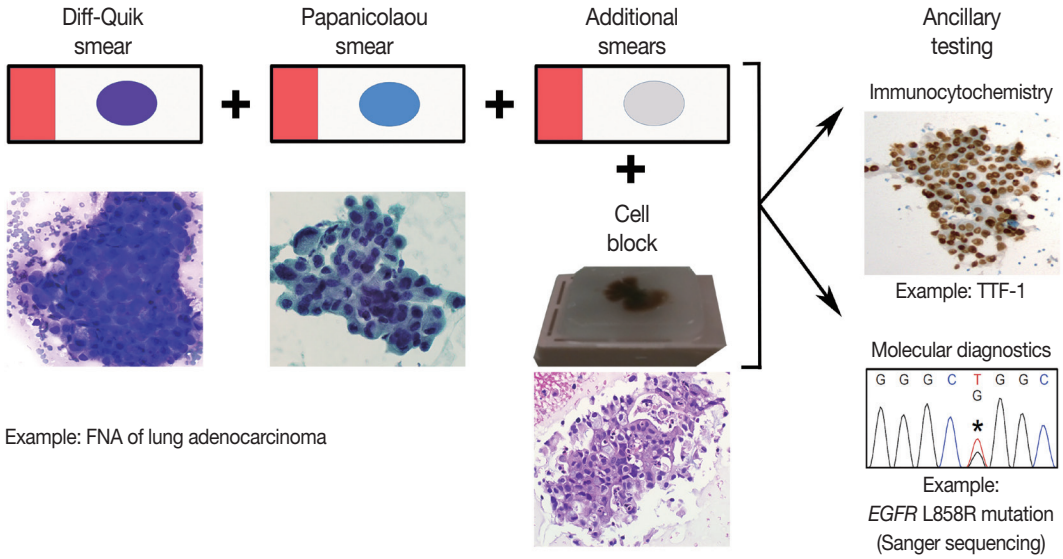

Fig. 1. Example of fine-needle aspiration (FNA) processing workflow. The contents of a needle pass, obtained during an FNA procedure, are expelled onto a slide to prepare smears. Typically, a pair of smears (one Diff-Quik stained and one Papanicolaou stained) is prepared per needle pass. However, additional smears can be prepared from a single needle pass by distributing the cellular material across more than two slides. The additional smears can be directly triaged for ancillary studies. For instance, an unstained smear can be sent to the Immunohistochemistry Laboratory for immunostaining (e.g., thyroid transcription factor-1 [TTF-1] immunocytochemistry). Also, a stained smear can be directly triaged to the Molecular Diagnostics Laboratory for tumor cell macro- or microdissection, nucleic acid isolation, and subsequent molecular testing (e.g., epidermal growth factor receptor [*EGFR*] mutation analysis).

tain more tumor cells for diagnosis and/or anticipated ancillary studies while the patient is still accessible. For instance, additional direct smears can be prepared and/or dedicated needle passes for the rinse solution (i.e., the needle contents are rinsed in the RPMI solution without the preparation of smears for those needle passes) obtained for the cell block preparation. This overall approach is flexible, forgiving, and engages the cytopathology team in maximizing the chance of success in obtaining adequate cellular material for diagnosis and ancillary studies. This approach can help minimize the chances of encountering the scenario in which diagnostic cellular material is present on only one smear; microdissection of the cells for molecular studies can result in sacrificing this only diagnostic slide in this context, which can have medico-legal consequences.[6] If this scenario is encountered, however, this risk can be mitigated by digital archiving prior to microdissection either via digital slide scanning and/or obtaining photomicrographs.[7] After immediate assessment of the cytomorphologic findings on the Diff-Quik stained smears, a preliminary diagnosis can be rendered by the cytopathologist and communicated to the clinical care providers.

After the conclusion of the procedure, the needle rinse solution, containing a suspension of aspirated cells, is centrifuged in the cytopathology laboratory to pellet the cells. Once the supernatant is removed, the cell pellet is congealed in a matrix; an agar-like substance such as HistoGel (Thermo Scientific, Waltham, MA, USA) can be used or the cells can be mixed with plasma and thrombin to create a clot. At our institution, we employ HistoGel for this purpose. The resulting cell button is then placed in a cassette. Commonly, this cassette is fixed in formalin and processed to ultimately create a formalin-fixed, paraffin-embedded (FFPE) cell block. This is analogous to a FFPE block of small biopsy tissue, which can be sectioned for evaluation via the hematoxylin and eosin stain and ancillary tests such as immunocytochemistry or molecular diagnostic assays. It should be noted that heavy metal fixatives such as Zenker's fixative and acid-zinc-formalin, acidic fixatives such as Bouin's solution, or decalcification solutions should generally be avoided as these render specimens unusable for molecular testing.[3]

Cell blocks are traditionally utilized for ancillary immunocytochemistry and molecular diagnostic assays. The main advantage of using cell blocks is that the majority of ancillary tests are validated for FFPE sections; FFPE cell blocks are treated similarly to traditional surgical pathology FFPE blocks. Furthermore, multiple serial sections from cell blocks can be utilized to perform a battery of ancillary studies. There are two main disadvantages associated with cell blocks, however. First, adequate cellularity in cell blocks is not guaranteed at the time of the procedure. Performing dedicated needle passes, for the needle rinse solution during the FNA procedure, may improve the chances of obtaining a sufficiently cellular cell block but still does not guarantee success.[4] In addition, for hypocellular cell blocks, there is a risk of depleting the cells of interest upon deeper sectioning for molecular tests. Second, the cell block is derived from a needle rinse solution which is a pooled specimen that contains contents of all the needle passes. Thus, if one or more needle passes contain tumor cells but other needle passes contain abundant benign background cellular elements, the tumor cells will be diluted by these benign cells in the cell block.[4] In addition to the above disadvantages, DNA extracted from FFPE cell blocks may produce sequencing artifacts as formalin fixation leads to the cross-linking of nucleic acids and proteins and the possibility of sequence alterations.[8]

Recently, given the shortcomings of cell blocks, there has been an increasing appreciation of alternative cytopreparatory platforms for molecular testing such as direct smears and LBC samples. In the subsequent sections below, the utilization of these cytopreparatory platforms will be discussed in the context of the clinically relevant mutations and translocations analyzed during molecular diagnostic testing of NSCLCs.

EPIDERMAL GROWTH FACTOR RECEPTOR

The epidermal growth factor receptor (*EGFR*) gene encodes a transmembrane growth factor receptor that exhibits tyrosine kinase activity. Upon activation, intracellular signaling is mediated by cytoplasmic effectors in the RAS-RAF-MEK-ERK, PI3K-AKT, and STAT pathways.[8] Approximately 10%–15% of NSCLC harbor clinically relevant, sensitizing mutations in *EGFR*. *EGFR* mutations are predominantly observed in lung adenocarcinomas; the L858R substitution and small in-frame deletions in exon 19 are the most commonly observed mutations and account for up to 90% of all *EGFR* mutations in this setting.[3,9] These mutations are more commonly associated with East Asian ethnicity, female gender, and non-smoking history. However, these are not absolute rules and clinical characteristics should not be used to exclude lung cancer patients from mutation testing.[10] Lung adenocarcinomas harboring these sensitizing mutations in *EGFR* have been shown to respond to EGFR tyrosine kinase inhibitors (TKIs). The first-line TKIs include erlotinib and gefitinib. In clinical trials, TKI therapy has been demonstrated to result in improved progression-free survival, compared to standard chemotherapy, for patients with lung adenocarcinoma har-

http://dx.doi.org/10.4132/jptm.2015.06.16

boring *EGFR* mutations.[11-16]

EGFR mutation analysis is commonly performed via polymerase chain reaction (PCR) and sequencing-based approaches; advances in the development of testing modalities have afforded a multitude of methodologies.[1,17,18] Sanger sequencing is considered the gold standard as this involves direct DNA sequence acquisition and can provide information regarding the presence of all potential mutations including common, known mutations and novel mutations. Nonetheless, this test requires a relatively higher enrichment of tumor cell DNA content in the sample. The typical analytic sensitivity for Sanger sequencing is 15%–20% mutant allele, which equates to 30%–40% tumor cells assuming that the genetic mutation is a heterozygous event without amplification.[17] This can be problematic in both small biopsy and cytology specimens, especially cell blocks, in which the tumor cell population can be diluted by background benign cellular elements such as inflammatory cells, bronchial epithelial cells, and/or stromal mesenchymal cells. Especially in this setting, a negative mutation result can be either due to the true absence of the mutation in the tumor cells or insufficient percent tumor cellularity that falls below the analytic sensitivity threshold thereby resulting in the failure to detect the mutation even despite the presence of the mutation.[4,9,17,19] Therefore, often times, there is more reliance on tumor cell enrichment by either macrodissection or microdissection to obtain a reliable result.[7,9,17,20] Sanger sequencing is also relatively more labor intensive and time consuming than targeted methods and can lead to longer turnaround times.[18] In contrast to the general Sanger sequencing approach, targeted mutation detection methods such as PCR-restriction fragment length polymorphism, real-time PCR, pyrosequencing, high resolution melting analysis (HRMA), and PCR fragment analysis can be utilized.[17] The advantages of these approaches include their improved analytic sensitivity and less time-consuming nature leading to reduced turnaround times. At our institution, we utilize a multiplex PCR fragment analysis assay for *EGFR* mutation testing; this allows for the simultaneous assessment of the two most commonly observed *EGFR* mutations (Fig. 2). The analytic sensitivity of this method is better than that of Sanger sequencing; a minimum of only 10% tumor cells is required. In the past decade, myriad studies have been reported demonstrating that a variety of cytologic samples and cytopreparatory platforms can be effectively utilized for *EGFR* mutational analysis. These have been reviewed elsewhere[18,21] but salient examples will be discussed below.

As mentioned previously, FFPE cell blocks represent the traditional cytopreparatory platform on which ancillary molecular diagnostic tests are performed. Much of the reasoning behind this lies in that FFPE cell blocks best approximate FFPE blocks containing tissue specimens and the majority of the molecular assays are validated using FFPE material. Nonetheless, in light of the inherent disadvantages of cell blocks mentioned previously, investigation into other cytopreparatory platforms for molecular diagnostic assays have been performed by our group and many others. Cytopathology specimen preparation is diverse and ver-

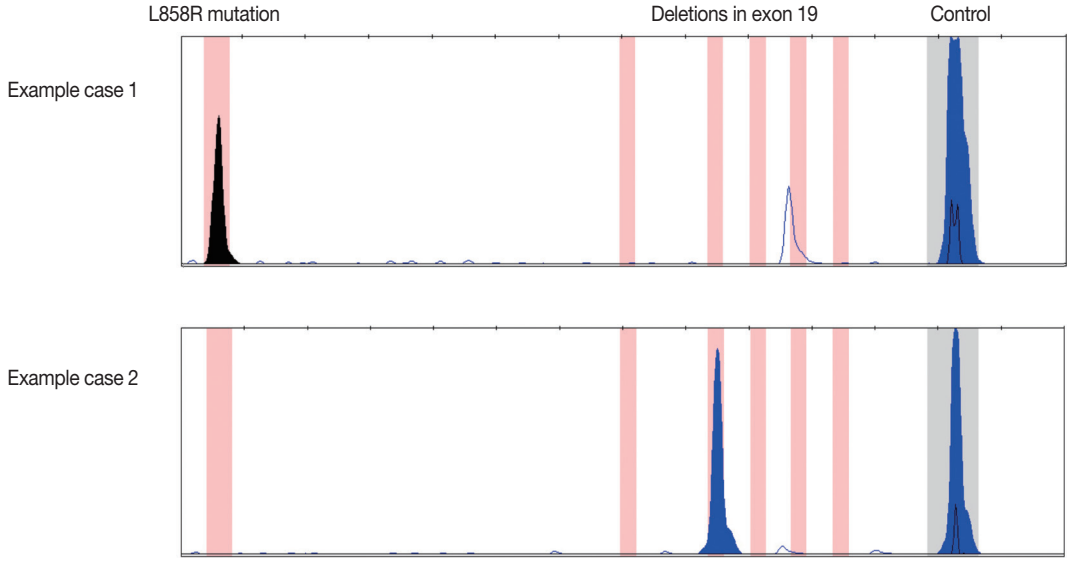

Fig. 2. Examples of epidermal growth factor receptor (*EGFR*) mutations detected by the polymerase chain reaction based fragment analysis assay utilized at our institution. Our assay is a multiplex assay designed to detect the two most common mutations in *EGFR*: the L858R substitution (case 1) and small deletions within exon 19 (case 2).

satile; the consequence of this is that each type of cytologic analyte platform needs to be carefully validated for any given molecular test. Cytologic direct smears may ultimately prove to be the cytologic platform best suited for PCR-based analysis due to the high quality of nucleic acids and immediate nature of specimen assessment for tumor cell adequacy[4,17] Cells on direct smears are not exposed to formalin but rather undergo an alcohol-based fixation process prior to staining; thus, the negative effects of formalin fixation on nucleic acid quality is non-contributory for direct smears. Furthermore, the tumor cells of interest can be directly visualized on the direct smear and isolated for nucleic acid extraction and molecular analysis; in essence, "what you see is what you get." We have previously demonstrated that uncoverslipped and previously coverslipped/decoverslipped Diff-Quik stained smears are robust sources of cellular material for PCR-based mutational analysis such as *EGFR* mutation testing of lung adenocarcinoma and *BRAF* mutation testing of metastatic melanoma FNA specimens.[9,19,22] We and others have observed that destaining the smears is not necessary for successful DNA extraction and PCR.[9,21] Our preference in utilizing Diff-Quik stained smears over Papanicolaou stained smears is rooted in the following observations: (1) cellular material on a Diff-Quik stained smear can be easily visualized without a coverslip and immediately triaged for molecular diagnostic testing;[4] and (2) the report by Killian *et al*.[23] that nucleic acids extracted from Diff-Quik stained smears show better preservation and integrity than DNA extracted from Papanicolaou stained smears. With respect to the latter point, others have pointed out that Papanicolaou stained smears are just as feasible for PCR-based molecular tests.[7,21,24] Multiple groups have successfully demonstrated the utilization of cytologic direct smears for *EGFR* mutation testing of lung adenocarcinomas[2,9,25-36] with low failure rates and high degree of concordance with *EGFR* molecular testing results from corresponding histologic specimens, when available. In our experience, 100 to 200 tumor cells are sufficient for successful DNA isolation and *EGFR* mutation analysis and this is congruent with the observations from others.[2,21]

LBC samples have also been investigated for *EGFR* mutation testing and have been shown to be an effective analyte for this purpose. This is valuable when a member of the cytopathology team is not available for ROSE.[37] Several LBC technologies have been developed including ThinPrep, SurePath, TACAS, and Liqui-PREP. Of these, the emerging literature, to date, on the utilization of LBC samples for molecular testing of NSCLC have predominantly focused on Cytolyt (Cytyc Corp., Marlborough, MA, USA) cell suspensions and ThinPrep slides. Collecting FNA samples in the methanol-based Cytolyt solution results in reduction of background blood as the Cytolyt solution exhibits hemolytic properties.[7] The cell suspension can be divided and an aliquot is used to prepare a ThinPrep slide that is stained via the Papanicolaou method, similar to alcohol-fixed Papanicolaou stained direct smears. Tumor cells can be isolated from the ThinPrep slide and used for DNA isolation and *EGFR* mutation analysis.[38,39] Furthermore, the cell suspension aliquot that is not used to prepare a ThinPrep slide can be centrifuged and the cell pellet itself can be used as an analyte for mutation testing.[38-40] Similar to the needle rinse cell suspension utilized to prepare cell blocks, the Cytolyt cell suspension is a pooled specimen if multiple needle passes are expelled and rinsed into Cytolyt. Thus, if one or more needle passes are high in tumor cell content whereas other needle passes contain a high proportion of benign cellular elements, the tumor cells in the final pooled cell suspension will be diluted.[4] This is not necessarily an insurmountable challenge for two reasons. First, targeted methods for detecting *EGFR* mutations with improved analytic sensitivity, relative to Sanger sequencing, can be utilized.[38] Second, tumor cell enrichment from the ThinPrep slide can be accomplished by laser capture microdissection (LCM). To illustrate these points, Malapelle *et al*.[39] directly compared the performance of *EGFR* mutation analysis by Sanger sequencing using paired samples for each case analyzed: (1) pelleted cells from the Cytolyt suspension and (2) tumor cells obtained from the ThinPrep slide via LCM. They observed that *EGFR* mutations were more reliably identified in the latter rather than the former. This difference was minimized when utilizing more sensitive *EGFR* mutation analytic approaches which included HRMA and PCR fragment analysis assays.[38] Based on these studies, the authors speculated that coupling the use of highly sensitive *EGFR* mutation detection assays and Cytolyt derived cell pellets may be sufficient obviating the need for microscopy. Nonetheless, it must be emphasized that any negative molecular testing result should carefully be reconciled with the analyte input utilized for the mutation assay. This is essential to determine whether the negative result represents a true negative or potentially a false-negative, necessitating possible retesting. In this regard, the utilization of microscopy still remains an essential pre-analytic quality assurance activity to best ensure that the input analyte is of sufficient tumor cellularity to maximize confidence in the results of the mutation assay. Of note, a follow-up study by Bellevicine *et al*.[6] compared the utility of direct smears versus ThinPrep slides. They observed that the direct smears exhibited significantly higher cellularity than ThinPrep slides, on average. Accordingly, the average yield of DNA extracted from direct smears was significantly higher than that

 http://dx.doi.org/10.4132/jptm.2015.06.16

from ThinPrep slides.

As the L858R substitution and deletions in exon 19 represent approximately 90% of all *EGFR* mutations in lung adenocarcinoma,[41] rabbit monoclonal antibodies have been recently developed and investigated. One antibody is specific for the exon 21 L858R mutation and the other specific for the 15-base pair/5-amino acid deletion (E746_A750del) in exon 19 (clone 6B6). The immunohistochemical approach to detecting mutant EGFR proteins using these antibodies has been examined in several studies on lung cancer tissues as well as cytologic and small biopsy samples.[42-48] The sensitivity of these assays range from 47%–92% but their high positive predictive value and specificity supports the feasibility of utilizing this approach as a first-line screening approach.[3] Two cautionary points are worth mentioning with regards to this approach. First, immunohistochemistry should be performed after careful validation and formulation of immunostain scoring criteria. The significance of how best to interpret equivocal staining results should be clarified as overinterpreting weak immunoreactivity as a positive mutation result can lead to increased false positives and decreased specificity. Second, the clone 6B6 antibody best detects the 15-base pair (E746_A750del) *EGFR* deletion mutant protein but demonstrates variable immunoreactivity for the EGFR mutant proteins resulting from non-15-base pair deletions in exon 19.[43]

ANAPLASTIC LYMPHOMA KINASE

The anaplastic lymphoma kinase (ALK) protein is a receptor tyrosine kinase and rearrangements involving the *ALK* gene locus is observed in approximately 5% of lung adenocarcinomas.[49,50] These mutations are more commonly observed in younger age patients who are never-smokers. However, there can be exceptions to this and clinical characteristics should not be used to exclude lung cancer patients for *ALK* rearrangement testing.[10] Most *ALK* rearrangements in lung adenocarcinoma result from interstitial deletions and small inversions within the short arm of chromosome 2. This results in the fusion of portions of the echinoderm microtubule-associated protein-like 4 (*EML4*) and *ALK* genes.[50,51] The fusion gene product displays oncogenic activity that drives these *ALK* rearranged lung adenocarcinomas.[50] Other less common *ALK* rearrangements involve fusions between *ALK* and other genes, such as *KIF5B* and *TFG*.[10] *ALK* rearranged lung adenocarcinoma has been recognized as a legitimate target for small molecular inhibitor therapy; crizotinib was shown to be efficacious in treating patients with these cancers. In a phase 1 study evaluating 143 patients, an overall response rate of 61% and estimated overall survival rates of 74.8% at 12 months were observed.[52] Therefore, the evaluation of lung adenocarcinoma FNA samples for *ALK* rearrangements, in addition to *EGFR* mutations, has become increasingly incorporated into patient management algorithms.

FISH is currently the preferred approach to assaying lung adenocarcinomas for *ALK* rearrangements according to expert recommendations based on review of the literature.[10] In the United States of America, there is only one test approved by the Food and Drug Administration (FDA) for this purpose. This assay utilizes a dual *ALK* breakapart probe strategy in which orange and green labeled probes hybridize to the highly conserved translocation breakpoint region in the *ALK* gene. *ALK* gene loci that have not undergone rearrangement typically display fused orange and green signals (yellow) or juxtaposed touching orange and green signals. When an *ALK* rearrangement occurs, the orange and green signals become separated. However, as the majority of the *ALK* rearrangements involve a small inversion within chromosome 2p, rather than a rearrangement involving another chromosome, the extent to which the two signals are split is finite. In order to score a nucleus as positive for the *ALK* rearrangement, the orange and green signals must be separated by a distance of >2 signal diameters (Fig. 3); a nucleus can also be scored positive if a single orange signal without a corresponding green signal is observed.[53] Typically, up to 100 tumor cell nuclei are scored in this assay and a lung adenocarcinoma is considered positive for the *ALK* rearrangement if at least 15% of the nuclei are scored as positive for the rearrangement.[53,54]

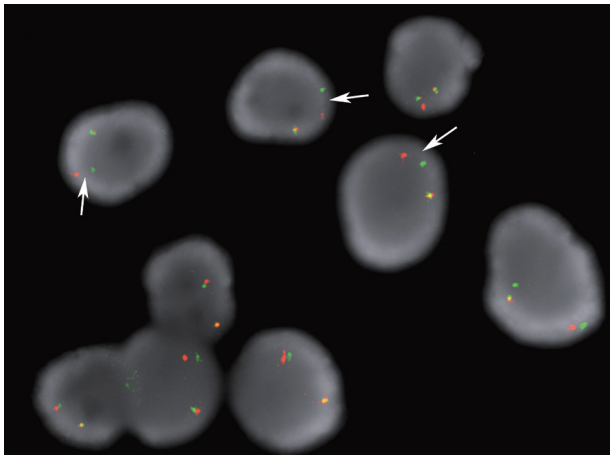

Fig. 3. Example case of anaplastic lymphoma kinase (*ALK*) rearrangement fluorescence *in-situ* hybridization assay performed on a direct smear containing lung adenocarcinoma cells. The arrows point to the split orange and green signals that are separated by a distance of >2 signal diameters. These nuclei would be scored as positive for the *ALK* rearrangement.

The FDA has approved this dual breakapart probe set for use on paraffin embedded tissue sections. As mentioned previously, paraffin embedded cell blocks are processed similarly to paraffin embedded tissue blocks; thus, cell blocks are traditionally used for the performance of *ALK* rearrangement FISH assays.[55] Nonetheless, there is an observed noticeable failure rate when using and relying on cell blocks for these assays due to insufficient tumor cell material in a significant proportion of cases.[4,54] Thus, we and others have investigated alternative cytopreparatory platforms for *ALK* FISH. In our study, we demonstrated the effective use of Diff-Quik stained direct smears for this purpose and observed that the performance of this assay using direct smears was better than the performance using cell blocks.[53] Proietti *et al*.[56] also examined the use of Papanicolaou stained direct smears and observed that the failure rate due to insufficient cellularity was significantly higher for cell blocks than for direct smears. Therefore, the utilization of both Diff-Quik and Papanicolaou stained smears are feasible analytes for *ALK* FISH. Recently, ThinPrep slides have also been shown to be a feasible platform for *ALK* FISH.[54] The advantage of utilizing cytologic preparation platforms such as direct smears and ThinPrep slides for this purpose is that entire tumor cell nuclei are being analyzed. FISH evaluation on paraffin sections derived cell blocks and other FFPE blocks are prone to signal loss in some of the tumor cells due to section truncation artifacts.[53,54]

In addition, alternative methods to FISH have been the subject of recent investigation. Immunohistochemistry utilizing antibodies directed against ALK is an attractive alternative as it is simpler, quicker, and less expensive.[10] The challenge associated with this approach is that the ALK protein is expressed at much lower levels in *ALK* rearranged lung tumors than in anaplastic large cell lymphoma, the prototypical *ALK* rearranged tumor.[10] Fortunately, monoclonal anti-ALK antibodies (clones D5F3, D9E4, and 5A4) have been shown to exhibit high sensitivity and specificity.[10,57] Immunohistochemistry using the D5F3 and 5A4 monoclonal antibodies on cytologic specimens have been recently described and shown to exhibit a high degree of concordance with *ALK* FISH testing.[54,58] This supports the feasibility of utilizing an immunohistochemical approach as a first-line screening methodology to select specimens for *ALK* FISH testing. Of note, the mouse monoclonal anti-ALK1 antibody (CD246) typically used for the diagnosis of anaplastic large cell lymphoma is less reliable for identifying *ALK* rearrangements in lung adenocarcinoma; this is most likely attributable to the limited sensitivity of this particular antibody in detecting the lower expression levels of the ALK fusion proteins in lung adenocarcinoma relative to anaplastic large cell lymphoma.[10] Finally, the application of reverse transcriptase PCR (RT-PCR) to cytologic direct smears for *ALK* rearrangement analysis has been recently reported.[31] When evaluating a cohort of paired cytologic-histologic specimens by RT-PCR, Mitiushkina and colleagues observed a 100% concordance of results. Nonetheless, as a cautionary note, there is a high degree of variability in *EML4-ALK* fusion events with at least 13 variants of *EML4-ALK* being reported.[10] Furthermore, other fusion partners to *ALK* such as *TFG* and *KIF5B* can be observed. Therefore, an RT-PCR approach may not capture all clinically relevant *ALK* rearrangements.[10]

EMERGING MOLECULAR GENETIC BIOMARKERS

While *EGFR* mutations and *ALK* rearrangements represent the two best characterized, clinically actionable molecular alterations in NSCLC, other molecular markers are becoming increasingly appreciated and investigated. *ROS1* encodes a receptor tyrosine kinase and is rearranged in approximately 2% of lung adenocarcinomas.[59] Early data seem to indicate that these tumors are responsive to crizotinib. *MET* encodes another receptor tyrosine kinase, hepatocyte growth factor receptor, and is amplified in a subset of NSCLC; a significant proportion of these cases are seen in context of acquired resistance to EGFR TKIs.[1] As crizotinib also targets this receptor, studies are under way to determine whether this agent will be effective in *MET* amplified lung cancers. Next, mutations in *BRAF* are seen in approximately 3% of lung adenocarcinomas.[60] Therapeutic agents targeting BRAF, such as dabrafenib, are currently being investigated in clinical trials.[61] In addition, gene rearrangements involving the *RET* tyrosine kinase gene (e.g., *KIF5B-RET*) have been observed in approximately 2% of lung adenocarcinomas; RET specific TKIs such as sunitinib, sorafenib, and vandetanib may be useful in treating patients with these lung cancers.[3] Finally, amplification of *FGFR1* and mutations in *PIK3CA* have been observed in some lung squamous cell carcinomas and agents targeting these gene products are also under investigation.[1] The above mentioned molecular genetic markers highlight the distinct molecular profiles that are becoming increasingly appreciated for different subtypes of NSCLC, especially adenocarcinomas and squamous cell carcinomas. Therefore, efforts to correctly subtype cases of NSCLC are important, including challenging cases of poorly-differentiated NSCLC.[10] At our institution, if the subtyping of NSCLC is deemed to be challenging based on cytomorphologic evaluation alone, immunocytochemistry is utilized; we have de-

http://dx.doi.org/10.4132/jptm.2015.06.16

monstrated that this can be accomplished using smears as well as cell blocks.[4] For example, Napsin-A and thyroid transcription factor-1 are often positive in lung adenocarcinomas and can be utilized for confirming this subtype of NSCLC. In contrast, p63 and p40 are useful markers for confirming a diagnosis of squamous cell carcinoma. Ultimately, utilizing FNA samples of NSCLC for immunocytochemistry must be judiciously leveraged to ensure that sufficient material still exists for molecular ancillary testing.

CONCLUDING THOUGHTS

Given the continuously evolving landscape in our understanding of the genetic events responsible for lung cancer pathogenesis, the integration between anatomic pathology, particularly cytopathology, and molecular diagnostics will become even more essential. Emerging molecular technological advances, such as next generation sequencing (NGS), that allow for high-throughput, high-sensitivity molecular analyses will likely play an important role in the management of patients with NSCLC. Cytologic specimens, based on recent reports, represent a robust source of cellular material for NGS.[62-65]

Conflicts of Interest

No potential conflict of interest relevant to this article was reported.

Acknowledgments

I wish to thank my colleague in the Molecular Diagnostics Laboratory at University of Michigan Health System, Dr. Bryan Betz, for providing the images pertaining to molecular diagnostic assays displayed in this review.

REFERENCES

1. Aisner DL, Marshall CB. Molecular pathology of non-small cell lung cancer: a practical guide. Am J Clin Pathol 2012; 138: 332-46.
2. Allegrini S, Antona J, Mezzapelle R, *et al*. Epidermal growth factor receptor gene analysis with a highly sensitive molecular assay in routine cytologic specimens of lung adenocarcinoma. Am J Clin Pathol 2012; 138: 377-81.
3. Dacic S. Molecular genetic testing for lung adenocarcinomas: a practical approach to clinically relevant mutations and translocations. J Clin Pathol 2013; 66: 870-4.
4. Knoepp SM, Roh MH. Ancillary techniques on direct-smear aspirate slides: a significant evolution for cytopathology techniques. Cancer Cytopathol 2013; 121: 120-8.
5. Roh MH. Triage of cytologic direct smears for ancillary studies: a case-based illustration and review. Arch Pathol Lab Med 2013; 137: 1185-90.
6. Bellevicine C, Malapelle U, Vigliar E, de Luca C, Troncone G. Epidermal growth factor receptor test performed on liquid-based cytology lung samples: experience of an academic referral center. Acta Cytol 2014; 58: 589-94.
7. Bellevicine C, Malapelle U, de Luca C, Iaccarino A, Troncone G. EGFR analysis: current evidence and future directions. Diagn Cytopathol 2014; 42: 984-92.
8. da Cunha Santos G, Shepherd FA, Tsao MS. *EGFR* mutations and lung cancer. Annu Rev Pathol 2011; 6: 49-69.
9. Betz BL, Roh MH, Weigelin HC, *et al*. The application of molecular diagnostic studies interrogating *EGFR* and *KRAS* mutations to stained cytologic smears of lung carcinoma. Am J Clin Pathol 2011; 136: 564-71.
10. Lindeman NI, Cagle PT, Beasley MB, *et al*. Molecular testing guideline for selection of lung cancer patients for EGFR and ALK tyrosine kinase inhibitors: guideline from the College of American Pathologists, International Association for the Study of Lung Cancer, and Association for Molecular Pathology. J Mol Diagn 2013; 15: 415-53.
11. Han JY, Park K, Kim SW, *et al*. First-SIGNAL: first-line single-agent iressa versus gemcitabine and cisplatin trial in never-smokers with adenocarcinoma of the lung. J Clin Oncol 2012; 30: 1122-8.
12. Katayama T, Matsuo K, Kosaka T, Sueda T, Yatabe Y, Mitsudomi T. Effect of gefitinib on the survival of patients with recurrence of lung adenocarcinoma after surgery: a retrospective case-matching cohort study. Surg Oncol 2010; 19: e144-9.
13. Maemondo M, Inoue A, Kobayashi K, *et al*. Gefitinib or chemotherapy for non-small-cell lung cancer with mutated *EGFR*. N Engl J Med 2010; 362: 2380-8.
14. Mitsudomi T, Morita S, Yatabe Y, *et al*. Gefitinib versus cisplatin plus docetaxel in patients with non-small-cell lung cancer harbouring mutations of the epidermal growth factor receptor (WJTOG3405): an open label, randomised phase 3 trial. Lancet Oncol 2010; 11: 121-8.
15. Mok TS, Wu YL, Thongprasert S, *et al*. Gefitinib or carboplatin-paclitaxel in pulmonary adenocarcinoma. N Engl J Med 2009; 361: 947-57.
16. Zhang L, Ma S, Song X, *et al*. Gefitinib versus placebo as maintenance therapy in patients with locally advanced or metastatic non-small-cell lung cancer (INFORM; C-TONG 0804): a multicentre, double-blind randomised phase 3 trial. Lancet Oncol 2012; 13: 466-75.
17. Aisner DL, Sams SB. The role of cytology specimens in molecular testing of solid tumors: techniques, limitations, and opportunities. Diagn Cytopathol 2012; 40: 511-24.
18. Ellison G, Zhu G, Moulis A, Dearden S, Speake G, McCormack R.

EGFR mutation testing in lung cancer: a review of available methods and their use for analysis of tumour tissue and cytology samples. J Clin Pathol 2013; 66: 79-89.
19. Hookim K, Roh MH, Willman J, *et al*. Application of immunocytochemistry and *BRAF* mutational analysis to direct smears of metastatic melanoma. Cancer Cytopathol 2012; 120: 52-61.
20. Chowdhuri SR, Xi L, Pham TH, *et al*. *EGFR* and *KRAS* mutation analysis in cytologic samples of lung adenocarcinoma enabled by laser capture microdissection. Mod Pathol 2012; 25: 548-55.
21. da Cunha Santos G, Saieg MA, Geddie W, Leighl N. *EGFR* gene status in cytological samples of nonsmall cell lung carcinoma: controversies and opportunities. Cancer Cytopathol 2011; 119: 80-91.
22. Bernacki KD, Betz BL, Weigelin HC, *et al*. Molecular diagnostics of melanoma fine-needle aspirates: a cytology-histology correlation study. Am J Clin Pathol 2012; 138: 670-7.
23. Killian JK, Walker RL, Suuriniemi M, *et al*. Archival fine-needle aspiration cytopathology (FNAC) samples: untapped resource for clinical molecular profiling. J Mol Diagn 2010; 12: 739-45.
24. Dejmek A, Zendehrokh N, Tomaszewska M, Edsjö A. Preparation of DNA from cytological material: effects of fixation, staining, and mounting medium on DNA yield and quality. Cancer Cytopathol 2013; 121: 344-53.
25. Billah S, Stewart J, Staerkel G, Chen S, Gong Y, Guo M. *EGFR* and *KRAS* mutations in lung carcinoma: molecular testing by using cytology specimens. Cancer Cytopathol 2011; 119: 111-7.
26. Boldrini L, Gisfredi S, Ursino S, *et al*. Mutational analysis in cytological specimens of advanced lung adenocarcinoma: a sensitive method for molecular diagnosis. J Thorac Oncol 2007; 2: 1086-90.
27. Bozzetti C, Negri FV, Azzoni C, *et al*. Epidermal growth factor receptor and Kras gene expression: reliability of mutational analysis on cytological samples. Diagn Cytopathol 2013; 41: 595-8.
28. Bruno P, Mariotta S, Ricci A, *et al*. Reliability of direct sequencing of *EGFR*: comparison between cytological and histological samples from the same patient. Anticancer Res 2011; 31: 4207-10.
29. Khode R, Larsen DA, Culbreath BC, *et al*. Comparative study of epidermal growth factor receptor mutation analysis on cytology smears and surgical pathology specimens from primary and metastatic lung carcinomas. Cancer Cytopathol 2013; 121: 361-9.
30. Lozano MD, Zulueta JJ, Echeveste JI, *et al*. Assessment of epidermal growth factor receptor and K-ras mutation status in cytological stained smears of non-small cell lung cancer patients: correlation with clinical outcomes. Oncologist 2011; 16: 877-85.
31. Mitiushkina NV, Iyevleva AG, Poltoratskiy AN, *et al*. Detection of *EGFR* mutations and *EML4-ALK* rearrangements in lung adenocarcinomas using archived cytological slides. Cancer Cytopathol 2013; 121: 370-6.
32. Nomoto K, Tsuta K, Takano T, *et al*. Detection of *EGFR* mutations in archived cytologic specimens of non-small cell lung cancer using high-resolution melting analysis. Am J Clin Pathol 2006; 126: 608-15.
33. Pang B, Dettmer M, Ong CW, *et al*. The positive impact of cytological specimens for *EGFR* mutation testing in non-small cell lung cancer: a single South East Asian laboratory's analysis of 670 cases. Cytopathology 2012; 23: 229-36.
34. Smith GD, Chadwick BE, Willmore-Payne C, Bentz JS. Detection of epidermal growth factor receptor gene mutations in cytology specimens from patients with non-small cell lung cancer utilising high-resolution melting amplicon analysis. J Clin Pathol 2008; 61: 487-93.
35. Sun PL, Jin Y, Kim H, Lee CT, Jheon S, Chung JH. High concordance of *EGFR* mutation status between histologic and corresponding cytologic specimens of lung adenocarcinomas. Cancer Cytopathol 2013; 121: 311-9.
36. van Eijk R, Licht J, Schrumpf M, *et al*. Rapid *KRAS, EGFR, BRAF* and *PIK3CA* mutation analysis of fine needle aspirates from non-small-cell lung cancer using allele-specific qPCR. PLoS One 2011; 6: e17791.
37. Lee YS, Jin GY, Han YM, Chung MJ, Park HS. Computed tomography-guided transthoracic needle aspiration biopsy of intrapulmonary lesions: utility of a liquid-based cytopreparatory technique. Acta Cytol 2008; 52: 665-70.
38. Malapelle U, de Rosa N, Bellevicine C, *et al*. *EGFR* mutations detection on liquid-based cytology: is microscopy still necessary? J Clin Pathol 2012; 65: 561-4.
39. Malapelle U, de Rosa N, Rocco D, *et al*. *EGFR* and *KRAS* mutations detection on lung cancer liquid-based cytology: a pilot study. J Clin Pathol 2012; 65: 87-91.
40. Reynolds JP, Tubbs RR, Minca EC, *et al*. *EGFR* mutational genotyping of liquid based cytology samples obtained via fine needle aspiration (FNA) at endobronchial ultrasound of non-small cell lung cancer (NSCLC). Lung Cancer 2014; 86: 158-63.
41. Sharma SV, Bell DW, Settleman J, Haber DA. Epidermal growth factor receptor mutations in lung cancer. Nat Rev Cancer 2007; 7: 169-81.
42. Ambrosini-Spaltro A, Campanini N, Bortesi B, *et al*. *EGFR* mutation-specific antibodies in pulmonary adenocarcinoma: a comparison with DNA direct sequencing. Appl Immunohistochem Mol Morphol 2012; 20: 356-62.
43. Brevet M, Arcila M, Ladanyi M. Assessment of *EGFR* mutation status in lung adenocarcinoma by immunohistochemistry using antibodies specific to the two major forms of mutant *EGFR*. J Mol Diagn 2010; 12: 169-76.
44. Hasanovic A, Ang D, Moreira AL, Zakowski MF. Use of mutation specific antibodies to detect EGFR status in small biopsy and cytol-

 http://dx.doi.org/10.4132/jptm.2015.06.16

ogy specimens of lung adenocarcinoma. Lung Cancer 2012; 77: 299-305.
45. Kato Y, Peled N, Wynes MW, *et al*. Novel epidermal growth factor receptor mutation-specific antibodies for non-small cell lung cancer: immunohistochemistry as a possible screening method for epidermal growth factor receptor mutations. J Thorac Oncol 2010; 5: 1551-8.
46. Kitamura A, Hosoda W, Sasaki E, Mitsudomi T, Yatabe Y. Immunohistochemical detection of *EGFR* mutation using mutation-specific antibodies in lung cancer. Clin Cancer Res 2010; 16: 3349-55.
47. Kozu Y, Tsuta K, Kohno T, *et al*. The usefulness of mutation-specific antibodies in detecting epidermal growth factor receptor mutations and in predicting response to tyrosine kinase inhibitor therapy in lung adenocarcinoma. Lung Cancer 2011; 73: 45-50.
48. Yu J, Kane S, Wu J, *et al*. Mutation-specific antibodies for the detection of *EGFR* mutations in non-small-cell lung cancer. Clin Cancer Res 2009; 15: 3023-8.
49. Rodig SJ, Mino-Kenudson M, Dacic S, *et al*. Unique clinicopathologic features characterize ALK-rearranged lung adenocarcinoma in the western population. Clin Cancer Res 2009; 15: 5216-23.
50. Soda M, Choi YL, Enomoto M, *et al*. Identification of the transforming *EML4-ALK* fusion gene in non-small-cell lung cancer. Nature 2007; 448: 561-6.
51. Thunnissen E, Bubendorf L, Dietel M, *et al*. *EML4-ALK* testing in non-small cell carcinomas of the lung: a review with recommendations. Virchows Arch 2012; 461: 245-57.
52. Camidge DR, Bang YJ, Kwak EL, *et al*. Activity and safety of crizotinib in patients with ALK-positive non-small-cell lung cancer: updated results from a phase 1 study. Lancet Oncol 2012; 13: 1011-9.
53. Betz BL, Dixon CA, Weigelin HC, Knoepp SM, Roh MH. The use of stained cytologic direct smears for *ALK* gene rearrangement analysis of lung adenocarcinoma. Cancer Cytopathol 2013; 121: 489-99.
54. Minca EC, Lanigan CP, Reynolds JP, *et al*. ALK status testing in non-small-cell lung carcinoma by FISH on ThinPrep slides with cytology material. J Thorac Oncol 2014; 9: 464-8.
55. Neat MJ, Foot NJ, Hicks A, *et al*. *ALK* rearrangements in EBUS-derived transbronchial needle aspiration cytology in lung cancer. Cytopathology 2013; 24: 356-64.
56. Proietti A, Alì G, Pelliccioni S, *et al*. Anaplastic lymphoma kinase gene rearrangements in cytological samples of non-small cell lung cancer: comparison with histological assessment. Cancer Cytopathol 2014; 122: 445-53.
57. Mino-Kenudson M, Chirieac LR, Law K, *et al*. A novel, highly sensitive antibody allows for the routine detection of *ALK*-rearranged lung adenocarcinomas by standard immunohistochemistry. Clin Cancer Res 2010; 16: 1561-71.
58. Savic S, Bode B, Diebold J, *et al*. Detection of ALK-positive non-small-cell lung cancers on cytological specimens: high accuracy of immunocytochemistry with the 5A4 clone. J Thorac Oncol 2013; 8: 1004-11.
59. Bergethon K, Shaw AT, Ou SH, *et al*. *ROS1* rearrangements define a unique molecular class of lung cancers. J Clin Oncol 2012; 30: 863-70.
60. Paik PK, Arcila ME, Fara M, *et al*. Clinical characteristics of patients with lung adenocarcinomas harboring *BRAF* mutations. J Clin Oncol 2011; 29: 2046-51.
61. Luk PP, Yu B, Ng CC, *et al*. *BRAF* mutations in non-small cell lung cancer. Transl Lung Cancer Res 2015; 4: 142-8.
62. Gailey MP, Stence AA, Jensen CS, Ma D. Multiplatform comparison of molecular oncology tests performed on cytology specimens and formalin-fixed, paraffin-embedded tissue. Cancer Cytopathol 2015; 123: 30-9.
63. Hovelson DH, McDaniel AS, Cani AK, *et al*. Development and validation of a scalable next-generation sequencing system for assessing relevant somatic variants in solid tumors. Neoplasia 2015; 17: 385-99.
64. Kanagal-Shamanna R, Portier BP, Singh RR, *et al*. Next-generation sequencing-based multi-gene mutation profiling of solid tumors using fine needle aspiration samples: promises and challenges for routine clinical diagnostics. Mod Pathol 2014; 27: 314-27.
65. Karnes HE, Duncavage EJ, Bernadt CT. Targeted next-generation sequencing using fine-needle aspirates from adenocarcinomas of the lung. Cancer Cytopathol 2014; 122: 104-13.

Journal of Pathology and Translational Medicine 2015; 49: 310-317
http://dx.doi.org/10.4132/jptm.2015.05.13

ORIGINAL ARTICLE

Analysis of Histologic Features Suspecting Anaplastic Lymphoma Kinase (ALK)-Expressing Pulmonary Adenocarcinoma

In Ho Choi · Dong Won Kim
Sang Yun Ha[1] · Yoon-La Choi[1]
Hee Jeong Lee[2] · Joungho Han[1]

Department of Pathology,
Soonchunhyang University Seoul Hospital,
Soonchunhyang University College of Medicine,
Seoul; [1]Department of Pathology, Samsung Medical Center, Sungkyunkwan University School of Medicine, Seoul; [2]Department of Pathology, Gwangmyeong Sungae Hospital, Gwangmyeong, Korea

Received: March 3, 2015
Revised: May 10, 2015
Accepted: May 12, 2015

Corresponding Author
Joungho Han, MD, PhD
Department of Pathology, Samsung Medical Center,
Sungkyunkwan University School of Medicine,
81 Irwon-ro, Gangnam-gu, Seoul 135-710, Korea
Tel: +82-2-3410-2800
Fax: +82-2-3410-0025
E-mail: hanjho@skku.edu

Background: Since 2007 when anaplastic lymphoma kinase (*ALK*) rearrangements were discovered in non-small cell lung cancer, the *ALK* gene has received attention due to *ALK*-targeted therapy, and a notable treatment advantage has been observed in patients harboring the *EML4*/*ALK* translocation. However, using ALK-fluorescence *in situ* hybridization (FISH) as the standard method has demerits such as high cost, a time-consuming process, dependency on interpretation skill, and tissue preparation. We analyzed the histologic findings which could complement the limitation of ALK-FISH test for pulmonary adenocarcinoma. **Methods:** Two hundred five cases of ALK-positive and 101 of ALK-negative pulmonary adenocarcinoma from January 2007 to May 2013 were enrolled in this study. The histologic findings and ALK immunohistochemistry results were reviewed and compared with the results of ALK-FISH and *EGFR*/*KRAS* mutation status. **Results:** Acinar, cribriform, and solid growth patterns, extracellular and intracellular mucin production, and presence of signet-ring-cell element, and psammoma body were significantly more often present in ALK-positive cancer. In addition, the presence of goblet cell-like cells and presence of nuclear inclusion and groove resembling papillary thyroid carcinoma were common in the ALK-positive group. **Conclusions:** The above histologic parameters can be helpful in predicting *ALK* rearranged pulmonary adenocarcinoma, leading to rapid FISH analysis and timely treatment.

Key Words: Lung; Adenocarcinoma; Anaplastic large cell lymphoma kinase; Anaplastic lymphoma kinase; *In situ* hybridization, fluorescence

Two major genetic mutations in non-small cell lung carcinomas (NSCLCs), epidermal growth factor receptor (*EGFR*) and *KRAS*, have been well studied. Since 2007 when Soda *et al*.[1] discovered rearrangements of anaplastic lymphoma kinase (*ALK*) in NSCLC, the *ALK* gene has received attention as being responsible for another molecular subtype of lung cancer, accounting for about 3% to 6% of NSCLCs.[1,2] It is important that the presence of *ALK* gene rearrangement can be an indication for targeted therapy, like *EGFR*-tyrosine kinase inhibitor (ex. gefitinib) as first-line therapy in patients with advanced pulmonary adenocarcinoma. Moreover, studies have shown that the *ALK*-targeted inhibitor 'crizotinib' produces a notable positive effect in patients harboring the *EML4*/*ALK* translocation.[3]

For the most effective use of *ALK* inhibitor, an accurate method to detect *ALK* gene rearrangement should be performed. To date, fluorescence *in situ* hybridization (FISH) is the universally accepted standard method for detecting *ALK* rearrangement, with immunohistochemistry (IHC) used as a screening method for identifying *ALK* rearrangement.[4,5] However, there is a need for a more rapid method to detect *ALK* rearrangement due to the highly time-consuming nature of FISH. We encountered a patient who showed a dramatic response to crizotinib treatment before confirming *ALK* rearrangement by FISH based only IHC-positive results for ALK and suspicious histological findings from a biopsy. Therefore, we were curious whether the combination of IHC and suspicious histological findings can improve upon the shortcomings of FISH. Additionally, limited specimen obtained by biopsy is common and often results in lack of remaining tissue for *ALK* study after the two major mutation tests (*EGFR* and *KRAS*) for lung cancer. If the histologic finding is more suggestive of *ALK* mutation,[6] priority can be given to the *ALK* mutation test because *EGFR, KRAS*, and *ALK* are known to be virtually mutually exclusive.

Our study aimed to investigate the characteristic histologic

pISSN 2383-7837
eISSN 2383-7845

features of ALK-positive pulmonary adenocarcinoma, in order to identify important histologic findings in small biopsied specimens whose architecture is difficult to assess and to evaluate whether the combination of these morphologic features and IHC results can overcome the shortcomings of FISH.

MATERIALS AND METHODS

Case selection

Two hundred five ALK-positive cases identified using IHC or FISH on biopsied and resected specimens from Samsung Medical Center were enrolled from January 2007 to May 2013. The basic characteristics of these cases (age, sex, and tumor stage), method of sampling (biopsy or operation), and results of IHC and FISH were investigated.

As a control group for comparing the histologic findings, all consecutive cases of pulmonary resection performed during 2012 were collected. The ALK-IHC had been performed in all cases of the control group, regardless of *EGFR* and *KRAS* analyses or microscopic findings.

The Institutional Review Board of Samsung Medical Center approved this study (IRB No. 2014-01-146).

Review of the histological findings

All resected tumors were classified according to histologic subtype based on the new International Association for the Study of Lung Cancer (IASLC)/American Thoracic Society (ATS)/European Respiratory Society (ERS) classification; the predominant pattern was determined as lepidic, acinar, papillary, solid, and invasive mucinous. All other components (> 5% of tumors) were also noted, including the cribriform growth pattern. Presence of extracellular and intracellular mucin, presence of signet-ring-cells, abrupt presence of goblet cell-like cells that contain amphophilic mucin like those in the intestinal mucosa, and presence of psammoma body, nuclear inclusion and groove, bizarre nuclei and multilobated nuclei were evaluated. As one of the other cytomorphological parameters, presence of prominent large eosinophilic nucleoli was investigated using a cut-off value of > 30% for tumor cells. In the biopsied specimens, we did not determine the predominant subtype, but we recorded all identifiable growth patterns, nuclear features and presence of psammoma body, bizarre nuclei, and nuclear inclusion and groove. We applied the parameter of 'nuclear inclusion and groove' to cells showing cytomorphologic features of thyroid papillary carcinoma. All cytomorphological features in all presented growth components were evaluated in three fields of each growth pattern using high magnification (×400).

IHC and scoring for ALK

IHC for *ALK* fusion was performed using formalin-fixed paraffin-embedded (FFPE) tumor tissue (4-μm thickness) and an antibody to NCL-*ALK* (1:30, clone 5A4, Novocastra, Newcastle upon Tyne, UK). The interpretation of IHC results was based on the a four-tier scoring system: 0 (none), 1+ (faint cytoplasmic staining, ≥10% of tumor cells), 2+ (moderate, smooth cytoplasmic staining), and 3+ (intense, granular cytoplasmic staining). IHC scores of 2+ or 3+ were regarded as ALK-positive results.[5]

FISH of ALK

The FISH analysis for *ALK* rearrangement on FFPE tissue was examined using a probe specific to the *ALK* locus (Vysis LSI *ALK* dual-color, Break-Apart Rearrangement Probe, Abbott Molecular, Abbott Park, IL, USA). At least 50 nonoverlapping tumor cells were examined, and the cut-off value for positive *ALK* rearrangement was defined as > 15% of tumor cells showing split signals or lone 3′ (orange color) signals (Fig. 1).

EGFR and *KRAS* mutation status

EGFR and *KRAS* mutation data of *ALK*-negative and *ALK*-positive groups were investigated. The mutation analyses of *EGFR* (exon 18, 19, 20, and 21) and *KRAS* (exons 2 and 3) were examined using direct sequencing-polymerase chain reaction

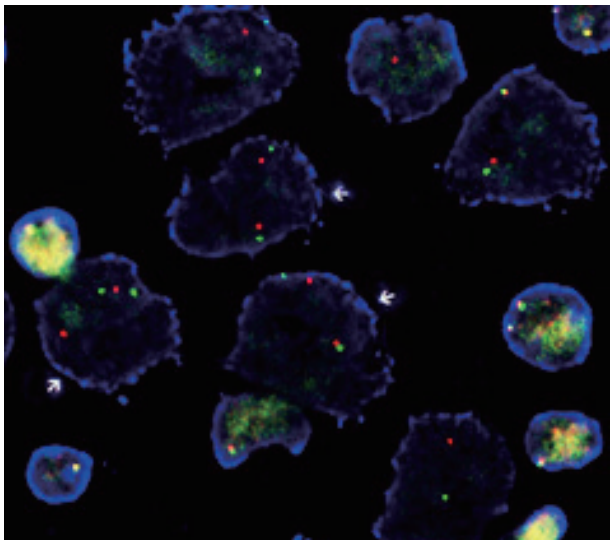

Fig. 1. Fluorescence *in situ* hybridization (FISH) of anaplastic lymphoma kinase (*ALK*)-rearranged pulmonary adenocarcinoma. Rearranged tumor nuclei show split signals (arrows) of 3′ (orange color) and 5′ (green color) ends of the gene hybridized using a dual-color ALK break-apart FISH probe (Vysis LSI ALK Dual Color, Break Apart Rearrangement Probe, Abbott Molecular).

(PCR). Genomic DNA was extracted from the FFPE tissue and purified with a QIAquick PCR purification kit (Qiagen, Hilden, Germany). Bidirectional sequencing was performed using the BigDye Terminator v 1.1 kit (Applied Biosystems, Foster City, CA, USA) on an ABI 3130xl genetic analyzer (Applied Biosystems).

Statistical analysis

Fisher exact test was used to compare the features of ALK-positive pulmonary adenocarcinoma according to sex, and linear by linear association was used for age and tumor stage. Normal distribution according to age in each group was tested by Kolmogorove-Smirnove and Shapiro-Wilk test. Chi-square test/Fisher exact test, independent samples t test, and logistic regression analysis were applied where appropriate in order to determine the relationship between morphological features and ALK positivity. A p-value of < .05 was considered to be statistically significant in all statistical tests. All analyses were performed using SPSS ver. 18.0 (SPSS Inc., Chicago, IL, USA).

RESULTS

Comparison of ALK-IHC and ALK-FISH

The status of ALK-FISH and ALK-IHC was compared in 78 cases (Table 1). Among 69 ALK-FISH positive cases, 63 cases showed 2+ or 3+ positivity in ALK-IHC staining; therefore, the sensitivity of ALK-IHC (2+ and 3+) was determined to be 91.3% (63/69).

Characteristics of patients with ALK-positive pulmonary adenocarcinoma

We settled ALK-positive group (n = 205) as ALK-IHC or ALK-FISH positive cases, including 127 cases of ALK-IHC positive (2+ or 3+) without ALK-FISH examination, 63 cases of positive ALK-IHC and ALK-FISH, 9 cases of positive ALK-IHC and not detected or failed ALK-FISH, and 6 cases of nega-

Table 1. Arrangement of ALK-FISH results according to ALK-IHC and sampling method

	ALK-FISH			No. of cases (n = 78)
	Rearranged (n = 69)	Not detected (n = 6)	Failed (n = 3)	
ALK-IHC				
Negative	1 (1.4)	0	0	1
1+	3 (4.3)	0	0	3
2+	42 (60.9)	3 (50.0)	3 (100)	48
3+	21 (30.4)	3 (50.0)	0	24
Failed	2 (2.9)	0	0	2
Sampling method				
Biopsy	56 (81.2)	2 (33.3)	0	58
Resection	13 (18.8)	4 (66.7)	3 (100)	20

Values are presented as number (%).
ALK, anaplastic lymphoma kinase; FISH, fluorescence *in situ* hybridization; IHC, immunohistochemistry.

Table 2. Characteristics of patients with ALK-positive and -negative pulmonary adenocarcinoma

Total cases (n=306)		ALK-positive			ALK-negative	p-value
		Biopsy (n = 129)	Resection (n = 76)	Total (n = 205)	Resection (n = 101)	
Sex (M:F)		47:82	36:40	83:122	53:48	.047[a]
						.501[b]
Age (yr)		53.9 ± 11.5	55.1 ± 11.7	54.4 ± 11.5	61.7 ± 8.8	< .001[a]
						< .001[b,c]
TNM stage, n (%)	a	1 (0.8)	29 (38.2)	30 (14.6)	20 (19.8)	.234[b,d]
	1b	1 (0.8)	4 (5.3)	5 (2.4)	14 (13.9)	
	2a	4 (3.1)	8 (10.5)	12 (5.9)	12 (11.9)	
	2b	1 (0.8)	0	1 (0.5)	8 (7.9)	
	3a	7 (5.4)	23 (30.3)	30 (14.6)	32 (31.7)	
	3b	9 (7.0)	3 (3.9)	12 (5.9)	1 (1.0)	
	4	106 (82.2)	9 (11.8)	115 (56.1)	14 (13.9)	

ALK, anaplastic lymphoma kinase; M, male; F, female.
[a]p-value between the ALK-positive and -negative group; [b]p-value between the ALK-positive and -negative resected group; [c]p-value by Student's t test; [d]Linear by linear association by chi-square test.

http://dx.doi.org/10.4132/jptm.2015.05.13

tive (0 or 1+) or failed ALK-IHC and positive ALK-FISH.

The characteristics of patients in the ALK-positive group and control group are presented in Table 2. The ALK-positive group consisted of 129 biopsy cases and 76 resection cases. The sex ratio in the ALK-positive group was male:female = 83:122 in contrast to 53:48 in the ALK-negative group. This finding was statistically significant (p = .047) and suggested that ALK-positive pulmonary adenocarcinoma occurs more frequently in women, with odds ratio of 1.623. ALK-positive cancer occurred in patients 7.3 years younger than the ALK-negative group, and this difference was statistically significant (p < .001). The distribution of tumor stage in the ALK-positive biopsy group was one-sided in stage 4 (82.2%). However, a statistically significant difference was not noted between the ALK-positive and -negative resection groups (p = .234).

Histological type and characteristic microscopic findings in ALK-positive pulmonary adenocarcinoma

Histologic subtypes based on predominant growth pattern were investigated in the ALK-positive and -negative resection groups, but there was no statistically significant histologic subtype of ALK-positive pulmonary adenocarcinoma (Table 3). However, acinar, solid, micropapillary, and cribriform growth patterns were more frequent in ALK-positive lung cancer based on the examination of growth patterns (p = .035, p = .002, p = .004, and p < .001 respectively) (Table 3, Fig. 2A, B). The ALK-positive group showed more variable growth patterns at a statistically significant level; 77.7% of cases in the ALK-positive group showed more than 3 types of growth patterns (mean, 3.3). However, cases in the ALK-negative group usually contained 2 or 3 types of growth patterns (75.2%; mean, 2.4) (p < .001) (Table 3, Fig. 2A).

Table 3. Correlation of histologic findings in resection groups according to ALK positivity

	ALK-positive resection (n = 76)	ALK-negative resection (n = 101)	p-value
Histololologic subtype (predominant)			
Acinar	31 (40.8)	35 (34.7)	.403
Papillary	24 (31.6)	36 (35.6)	.572
Solid	19 (25.0)	23 (22.8)	.730
Micropapillary	0	3 (3.0)	.130
Lepidic	0	3 (3.0)	.130
Invasive mucinous	2 (2.3)	1 (1.0)	.402
Growth pattern (>5% of entire tumor)			
Acinar	65 (85.5)	73 (72.3)	.035
Papillary	52 (68.4)	66 (65.3)	.668
Solid	45 (59.2)	36 (35.6)	.002
Micropapillary	31 (40.8)	21 (20.8)	.004
Lepidic	7 (9.2)	20 (19.8)	.052
Cribriform	51 (67.1)	29 (28.7)	< .001
No. of growth patterns[a]			
1	3 (3.9)	14 (13.9)	< .001[b]
2	14 (18.4)	44 (43.6)	
3	26 (34.2)	32 (31.7)	
4	23 (30.3)	9 (8.9)	
5	10 (13.2)	1 (1.0)	
6	0	1 (1.0)	
Microscopic findings			
Presence of signet-ring-cell element	20 (26.3)	4 (4.0)	< .001
Extracellular mucin production	34 (44.7)	18 (17.8)	< .001
Intracellular mucin content	58 (76.3)	57 (56.4)	.006
Hobnail cells with abundant cytoplasm	4 (5.3)	35 (34.7)	< .001
Abrupt presence of goblet cell-like cells	49 (64.5)	33 (32.7)	< .001
Psammoma body	33 (43.4)	5 (5.0)	< .001
Presence of bizarre cells	19 (25.0)	43 (42.6)	.015
Presence of multilobated cells	5 (6.6)	6 (5.9)	.862
Nuclear inclusion and groove	16 (21.1)	10 (9.9)	.038
Prominent macronucleoli	58 (46.6)	78 (53.4)	.034

Values are presented as number (%).
ALK, anaplastic lymphoma kinase.
[a]Number of all presented growth patterns presented in 'Growth pattern (>5% of entire tumor)'; [b]p-value by Student's t-test.

Among the examined cytomorphologic parameters, extracellular and intracellular mucin production (Fig. 2C), presence of signet-ring-cell element (Fig. 2D), presence of psammoma body (Fig. 2E), abrupt presence of goblet cell-like cells (Fig. 2F), and presence of nuclear inclusion and groove (Fig. 2G) were significantly more frequent in the ALK-positive resection group. Hobnail cells with abundant cytoplasm, bizarre cells, and presence of macronucleoli were more frequently observed in the ALK-neg-

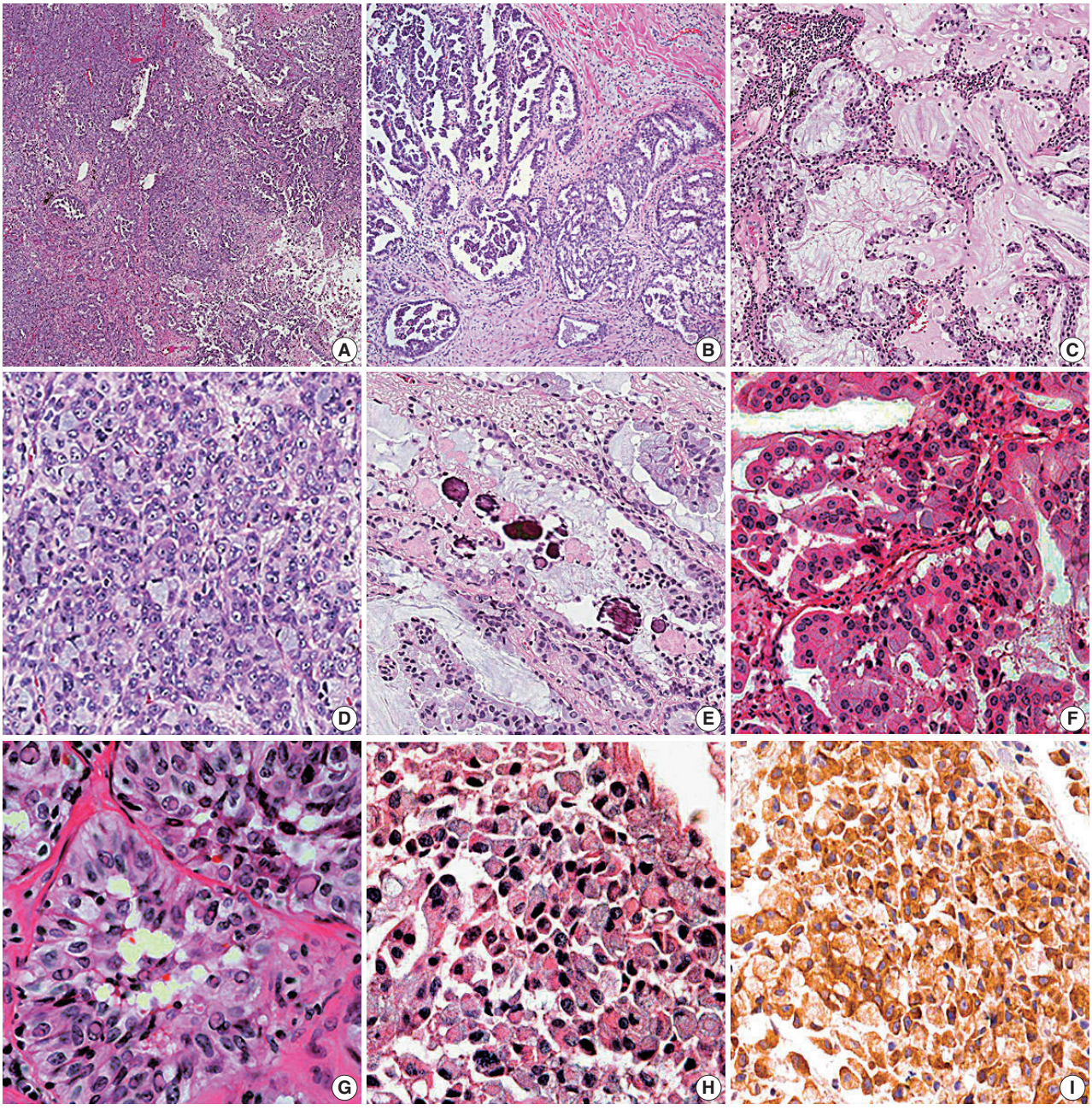

Fig. 2. Histologic features of anaplastic lymphoma kinase (*ALK*)-rearranged pulmonary adenocarcinoma. (A) *ALK*-rearranged tumors show variable growth patterns. At low magnification, the tumor shows solid, acinar, and papillary growth patterns. (B) Cribriform and micropapillary patterns are more frequent in ALK-positive pulmonary adenocarcinoma. (C) Tumors have frequent extracellular and intracellular mucin production. (D) Solid growth is frequently found to contain signet-ring-cells. (E) A few psammoma bodies are noted in the background of mixed tumor and extracellular mucin. (F) Some tumors contain goblet cell-like cells. (G) Intranuclear inclusion and nuclear groove resembling papillary thyroid carcinoma are frequently found. (H) On the biopsied specimen from the patient showing dramatic response to *ALK*-targeted therapy before ALK-fluorescence *in situ* hybridization, many signet-ring-cells are found. (I) Tumor cells in Fig. 2H show 3+ ALK-immunohistochemistry score.

http://dx.doi.org/10.4132/jptm.2015.05.13

Table 4. Multivariate analysis: histologic findings in ALK-positive or -negative resection groups

	ALK-positive resection (n=76)	ALK-negative resection (n=101)	Odds ratio	95% CI
Growth pattern (>5% of entire tumor)				
Acinar	65 (85.5)	73 (72.3)	3.178	1.298–7.779
Solid	45 (59.2)	36 (35.6)	2.694	1.301–5.577
Micropapillary	31 (40.8)	21 (20.8)	3.414	1.581–7.372
Cribriform	51 (67.1)	29 (28.7)	3.771	1.877–7.575
Microscopic findings				
Presence of signet-ring-cell element	20 (26.3)	4 (4.0)	5.466	1.488–20.080
Extracellular mucin production	34 (44.7)	18 (17.8)	3.372	1.411–8.057
Hobnail cells with abundant cytoplasm	4 (5.3)	35 (34.7)	0.096	0.026–0.356
Psammoma body	33 (43.4)	5 (5.0)	16.548	5.303–51.641

Values are presented as number (%).
ALK, anaplastic lymphoma kinase; CI, confidence interval.

Table 5. Correlation of morphologic features between ALK-positive biopsy and resection groups

	ALK-positive biopsy (n=129)	ALK-positive resection (n=76)	p-value
Presence of signet-ring-cell element	40 (31.0)	20 (26.3)	.476
Extracellular mucin production	15 (11.6)	34 (44.7)	<.001
Intracellular mucin content	101 (78.3)	58 (76.3)	.743
Hobnail cells with abundant cytoplasm	5 (3.9)	4 (5.3)	.640
Abrupt presence of goblet cell-like cells	69 (53.5)	49 (64.5)	.124
Psammoma body	20 (15.5)	33 (43.4)	<.001
Nuclear inclusion and groove	7 (5.4)	16 (21.1)	.001

Values are presented as number (%).
ALK, anaplastic lymphoma kinase.

ative group.

According to logistic regression analysis (Table 4), acinar, solid, micropapillary, and cribriform growth patterns were more frequent in ALK-positive group, and the significant cytomorphologic features included presence of signet-ring-cell elements, extracellular mucin production, hobnail cells with abundant cytoplasm, and psammoma body.

Morphological features of small biopsy specimens compared with resection specimens

To evaluate whether ALK-specific morphologic features in the resection group can be applied to small biopsy specimens, cytomorphologic findings were compared between the ALK-positive biopsy and resection groups (Table 5). The parameters except for extracellular mucin production, psammoma body, and nuclear inclusion and groove showed no differences between the biopsy and resection groups ($p > .05$).

DISCUSSION

Since the presence of *ALK* rearrangement has become an important predictive biomarker for the use of the *ALK*-targeted inhibitor 'crizotinib' for NSCLC, the detection of *ALK* rearrangements is also becoming increasingly important. However, ALK-FISH as a standard method for detecting *ALK* rearrangement is expensive, time-consuming, and influenced by many factors (skill and material). On the other hand, ALK-IHC has been used as a screening method due to its lower specificity compared to ALK-FISH. We evaluated the histologic findings that can be helpful in predicting *ALK* rearrangement and in saving time until *ALK*-targeted inhibitor treatment.

Although there might have been a selection bias due to the excessive number of biopsied cases in stage IV, the ALK-positive group showed more frequent occurrence of lung adenocarcinoma in an advanced tumor stage than did the ALK-negative group (stage IV: 56.1% vs 13.9%). Although the ALK-positive resection group showed no statistically significant difference in the distribution of tumor stage compared with the ALK-negative group ($p = .234$), ALK-positive lung cancer is suspected to show more aggressive behavior, considering that ALK-positive lung cancer presents in an advanced stage with low resectability, leading to the need for chemotherapy or palliative therapy instead of surgical treatment.

There have been several studies on the morphologic findings of *ALK*-rearranged NSCLCs. Some authors[7-9] have suggested that acinar growth pattern and extracellular mucin production

are typical of ALK-rearranged pulmonary adenocarcinoma. Another author recommended signet-ring-cell elements associated with solid growth as a feature of *ALK*-rearranged pulmonary adenocarcinoma.[10] In the present study, histologic subtype based on 'predominant' growth pattern was not effective in discriminating between the ALK-positive and -negative groups. However, ALK-positive pulmonary adenocarcinoma showed more variable growth patterns (Fig. 2A) with significantly more frequent presence of acinar, solid, micropapillary, and cribriform growth patterns (Fig. 2A, B, D) compared with non-*ALK* rearranged adenocarcinoma (Table 3).

As reported by Jokoji *et al*.[7] and Inamura *et al*.,[9] who observed that mucin production was one of the important findings of *EML4-ALK*-positive lung adenocarcinoma, our study also showed that extracellular mucin production was statistically significant in the ALK-positive resection group ($p < .001$).

Rodig *et al*.[10] showed that tumor cells forming a solid or sheet-like pattern were easily distinguishable from other growth patterns in *ALK*-rearranged adenocarcinoma, and that the majority (56%) of *ALK*-rearranged tumors showed a solid growth pattern with > 10% signet-ring cells. Our study also showed frequent solid growth (45/76 cases, 59.2%) in the ALK-positive resection group, and signet-ring-cell elements were extremely frequent in the ALK-positive resection group (20/76 cases, 26.3% vs 4/101 cases, 4.0%) (Table 3, Fig. 2D). Indeed, the signet-ring-cell element was significantly more frequent in the ALK-positive resection group showing solid growth than in the ALK-negative group (odds ratio, 21.9 vs 1.9).

A recent study about histomorphologic features of *ALK*-rearranged lung adenocarcinoma by Kim *et al*.[11] showed several significant microscopic features, including cribriform formation, presence of extracellular mucin, presence of mucin-containing cells, close relation to adjacent bronchioles, presence of psammoma body, presence of cholesterol cleft, and solid predominant pattern. Their data are similar to those of the present study except for two parameters that we did not evaluate close relation to adjacent bronchioles and presence of cholesterol cleft. However, we are more interested in the abrupt presence of goblet cell-like cells and presence of nuclear inclusion and groove resembling papillary thyroid carcinoma.

Abrupt presence of goblet cell-like cells (Fig. 2F) was frequent in the ALK-positive resection group (64.5% vs 32.7%, $p < .001$). We also found that many cases with a signet-ring-cell element in the ALK-positive resection group showed abrupt presence of goblet cell-like cells (16/20 cases, 80.0%). Considering the cytomorphologic similarity between signet-ring cells and goblet cell-like cells, we supposed that presence of goblet cell-like cells is part of a process to form signet-ring-cell and is predictive parameter for ALK-positive pulmonary adenocarcinoma. However, this relation was not statistically significant ($p = .091$).

One of the notable findings of our study was that the presence of nuclear inclusion and groove resembling papillary thyroid carcinoma (Fig. 2G) was noted more often observed in the ALK-positive lung cancer cases compared to the negative cases. We hypothesized that this feature is valuable in predicting ALK-positive lung cancer. However, there is no available data on why papillary thyroid carcinoma-like features are more frequent in ALK-positive lung cancer, suggesting additional study cases are needed.

On the correlation between biopsy and resection cases in ALK-positive tumors (Table 5), we found that some parameters, such as presence of signet-ring-cell elements, intracellular mucin content, and presence of goblet cell-like cells, showed no statistically significant differences between the biopsy and resection groups. However, these features are believed to be helpful for predicting ALK positivity in small biopsy specimens. Furthermore, presence of signet-ring-cell, psammoma body, nuclear inclusion and groove, and goblet cell-like cells are meaningful in small biopsy sections, if present (Fig. 2H).

Paik *et al*.[4] reported that the sensitivity and specificity of ALK-IHC was 100% and 95.8%, respectively, with a well-organized interpretation flow and concluded that ALK-IHC might be useful as a screening method to identify *ALK* rearrangements; a 91.3% sensitivity of ALK-IHC was noted in our study. However, ALK-IHC alone is not yet adequate to replace ALK-FISH and is applicable only as a screening method. For example, we excluded 4 cases showing discordance between the result of *ALK* and that of *EGFR* and *KRAS* before the present study. These cases included three *EGFR*-mutated cases (two ALK-IHC- and *EGFR*-positive cases with no examination by ALK-FISH and one concurrent *EGFR*-mutated and ALK-FISH-positive case) and one concurrent ALK-IHC- and *KRAS*-positive case without examination by ALK-FISH; *KRAS* missense mutation in the 12th codon : c.34G > T (p.G12C). Upon reviewing a case showing *EGFR* missense mutation in exon 18 (G719X), ALK-IHC-positivity (2+), and ALK-FISH-positivity, there was a suspicion of over-interpretation of ALK-FISH analysis; about 20% of tumor cells showed only 'lone 3´ (orange color) signals' without 'split signals.' The reasons for the other three false positive cases by ALK-IHC could not be determined, although they showed definite 2+ and 3+ ALK-IHC scoring.

However, ALK-FISH has some demerits, such as high cost,

http://dx.doi.org/10.4132/jptm.2015.05.13

time-consuming process, dependency on many conditions, including skill of interpretation, and preparation of material such as quantity and quality of tumor cells. In our study, 9 cases showed no detection or failed results on ALK-FISH, and they were all negative for *EGFR* and *KRAS*, despite having 2+ or 3+ ALK-IHC scores (Table 1). After review of ALK-IHC and ALK-FISH results, the 6 cases with no detection were also confirmed as failures due to interpretation difficulty of ALK-FISH caused by excessive mucin content and low cellularity. In the practice, ALK-FISH is usually the second choice after analyses of both major mutations (*EGFR* and *KRAS*), and it leads to scarcity of tissue availability for testing from small biopsied specimens. Therefore, we believe that ALK-FISH could be complemented for rapid treatment, and the microscopic findings might be predictors of *ALK* rearrangement. If the morphologic findings are suggestive of *ALK*-rearranged pulmonary adenocarcinoma and are supported by a positive result in ALK-IHC, the patients can benefit from timely treatment. For example, we encountered a patient who showed dramatic response to 'crizotinib' before confirmation by ALK-FISH using only positive ALK-IHC and suspicious histological findings via biopsy (Fig. 2H, I).

Conclusively, we found that acinar, micropapillary, cribriform, and solid growth patterns with intracellular mucin content, signet-ring-cell element, and psammoma body were useful in predicting *ALK* rearrangement. Indeed, the notable findings of our study were that presence of goblet cell-like cells or nuclear inclusion or groove resembling papillary thyroid carcinoma was more common in *ALK*-positive adenocarcinoma of the lung, although these findings should be evaluated further. In the biopsied specimens, presence of signet-ring-cell elements, goblet cell-like cells, intracellular mucin content, and psammoma body can be helpful in predicting *ALK* rearrangement. Additionally, there is a limitation of our study as the histologic comparison between FISH-positive cases and IHC-positive cases could not be made due to weighted biopsied specimens.

We hope to clarify the histologic findings of *ALK* rearrangement in a prospective cohort study and to evaluate the histologic findings with newly appearing genes in *ALK* rearrangement.

Conflicts of Interest

No potential conflict of interest relevant to this article was reported.

REFERENCES

1. Soda M, Choi YL, Enomoto M, *et al*. Identification of the transforming *EML4-ALK* fusion gene in non-small-cell lung cancer. Nature 2007; 448: 561-6.
2. Sun JM, Lira M, Pandya K, *et al*. Clinical characteristics associated with *ALK* rearrangements in never-smokers with pulmonary adenocarcinoma. Lung Cancer 2014; 83: 259-64.
3. O'Bryant CL, Wenger SD, Kim M, Thompson LA. Crizotinib: a new treatment option for ALK-positive non-small cell lung cancer. Ann Pharmacother 2013; 47: 189-97.
4. Paik JH, Choe G, Kim H, *et al*. Screening of anaplastic lymphoma kinase rearrangement by immunohistochemistry in non-small cell lung cancer: correlation with fluorescence *in situ* hybridization. J Thorac Oncol 2011; 6: 466-72.
5. Yi ES, Boland JM, Maleszewski JJ, *et al*. Correlation of IHC and FISH for *ALK* gene rearrangement in non-small cell lung carcinoma: IHC score algorithm for FISH. J Thorac Oncol 2011; 6: 459-65.
6. Yoshida A, Tsuta K, Nakamura H, *et al*. Comprehensive histologic analysis of *ALK*-rearranged lung carcinomas. Am J Surg Pathol 2011; 35: 1226-34.
7. Jokoji R, Yamasaki T, Minami S, *et al*. Combination of morphological feature analysis and immunohistochemistry is useful for screening of *EML4-ALK*-positive lung adenocarcinoma. J Clin Pathol 2010; 63: 1066-70.
8. Inamura K, Takeuchi K, Togashi Y, *et al*. *EML4-ALK* fusion is linked to histological characteristics in a subset of lung cancers. J Thorac Oncol 2008; 3: 13-7.
9. Inamura K, Takeuchi K, Togashi Y, *et al*. *EML4-ALK* lung cancers are characterized by rare other mutations, a TTF-1 cell lineage, an acinar histology, and young onset. Mod Pathol 2009; 22: 508-15.
10. Rodig SJ, Mino-Kenudson M, Dacic S, *et al*. Unique clinicopathologic features characterize *ALK*-rearranged lung adenocarcinoma in the western population. Clin Cancer Res 2009; 15: 5216-23.
11. Kim H, Jang SJ, Chung DH, *et al*. A comprehensive comparative analysis of the histomorphological features of *ALK*-rearranged lung adenocarcinoma based on driver oncogene mutations: frequent expression of epithelial-mesenchymal transition markers than other genotype. PLoS One 2013; 8: e76999.

Journal of Pathology and Translational Medicine 2015; 49: 318-324
http://dx.doi.org/10.4132/jptm.2015.06.01

■ ORIGINAL ARTICLE ■

Cancers with Higher Density of Tumor-Associated Macrophages Were Associated with Poor Survival Rates

Kyong Yeun Jung[1,2] · Sun Wook Cho[1,3]
Young A Kim[4] · Daein Kim[3]
Byung-Chul Oh[5] · Do Joon Park[1]
Young Joo Park[1]

[1]Department of Internal Medicine, Seoul National University College of Medicine, Seoul; [2]Department of Internal Medicine, Eulji University School of Medicine, Seoul; [3]Department of Internal Medicine, National Medical Center, Seoul; [4]Department of Pathology, SMG-SNU Boramae Medical Center, Seoul; [5]Lee Gil Ya Cancer and Diabetes Institute, Gachon University Graduate School of Medicine, Incheon, Korea

Received: May 21, 2015
Accepted: June 1 2015

Corresponding Author
Young Joo Park, MD, PhD
Department of Internal Medicine, Seoul National University College of Medicine, 101 Daehak-ro, Jongno-gu, Seoul 110-799, Korea
Tel: +82-2-2072-4183
Fax: +82-2-764-2199
E-mail: yjparkmd@snu.ac.kr

Background: Macrophages are a component of a tumor's microenvironment and have various roles in tumor progression and metastasis. This study evaluated the relationships between tumor-associated macrophage (TAM) density and clinical outcomes in 14 different types of human cancers. **Methods:** We investigated TAM density in human tissue microarray sections from 14 different types of human cancers (n = 266) and normal thyroid, lung, and breast tissues (n = 22). The five-year survival rates of each cancer were obtained from the 2011 Korea Central Cancer Registry. **Results:** Among 13 human cancers, excluding thyroid cancer, pancreas, lung, and gallbladder cancers had the highest density of CD163-positive macrophages (7.0 ± 3.5%, 6.9 ± 7.4%, and 6.9 ± 5.5%, respectively). The five-year relative survival rates of these cancers (pancreas, 8.7%; lung, 20.7%; gallbladder, 27.5%) were lower than those of other cancers. The histological subtypes in thyroid cancer exhibited significantly different CD163-positive macrophages densities (papillary, 1.8 ± 1.6% vs anaplastic, 22.9 ± 17.1%; p < .001), but no significant difference between histological subtypes was detected in lung and breast cancers. Moreover, there was no significant difference in CD163-positive macrophages densities among the TNM stages in lung, breast, and thyroid cancers. **Conclusions:** Cancers with higher TAM densities (pancreas, lung, anaplastic thyroid, and gallbladder) were associated with poor survival rate.

Key Words: Tumor-associated macrophage; Prognosis; Neoplasms

The tumor microenvironment includes cancer cells and various stromal cells, including immune cells, fibroblasts, and vascular endothelial cells.[1] Tumor-associated macrophages (TAMs) are also present in the tumor microenvironment and are important in tumor progression and metastasis.[2] TAMs can induce neoplastic cell transformation, elicit tumor destructive reactions, and have either negative or positive effects on tumor growth.[3] Several reports have suggested that TAMs are associated with tumor growth, disease progression, and poor prognosis in some human cancers.[4-6] Moreover, high densities of TAMs are present in the more advanced stages of cancers that have poor prognoses, such as breast,[7] lung,[8] thyroid,[5] and bladder[3] cancers. In contrast, several reports, including those on colorectal,[9] stomach,[10] lung,[11,12] and endometrial[13] cancers, have shown that a high density of TAMs is associated with a high survival rate. Collectively, these results suggest that TAMs can have either positive or negative effects depending on the specific tissue type, tumor location, and tumor stage. The aim of this study was to evaluate the relationship between TAM density and clinical outcome in various human cancers.

MATERIALS AND METHODS

Study subjects and tissue microarrays

We purchased 14 different type of human cancer human tissue microarray sections (lung, 49; breast, 49; thyroid, 10; pancreas, 10; gallbladder, 9; larynx, 9; esophagus, 10; liver, 10; cervix, 10; ovary, 10; stomach, 10; prostate, 9; kidney, 9; and endometrium, 9 sections) and normal tissues (lung, 9; breast, 8 sections) from SuperBioChips Laboratories (Seoul, Korea). The supplier pro-

pISSN 2383-7837
eISSN 2383-7845

vided the clinical information associated with each section, including age at surgery; gender; pathologic diagnosis; TNM staging for cancers; survival/death follow-up result for lung and breast cancers; and estrogen receptor (ER), progesterone receptor (PR), p53, and C-erbB2 expression for breast cancers. Thyroid microarrays contained normal thyroid (n = 5), papillary thyroid cancer (PTC; n = 35), and anaplastic thyroid cancer (ATC; n = 18), and one of the thyroid microarray slides was used in a previous study.[14] Clinical and pathologic data for the thyroid samples were obtained from medical records at Seoul National University Hospital and SMG-SNU Boramae Medical Center. The five-year cancer relative survival rates were obtained from the 2011 annual report of cancer statistics in Korea.[15]

Immunohistochemistry on tissue array blocks

CD68 and CD163 were used as TAM markers. Immunohistochemical (IHC) staining for CD68 and CD163 was performed using the BenchMark XT Slide Preparation System (Ventana Medical Systems, Tucson, AZ, USA) and CD68 (ready-to-use, 514H12, Novocastra, Newcastle upon Tyne, UK) and CD163 (1:200, 10D6, ER2, Novocastra). The proportion of CD163-positive area in each tumor was evaluated after IHC staining (Fig. 1). We divided the area of each tissue core into quarters and a central area and randomly chose all five fragments to determine the positive stain proportion (Fig. 1A). Areas of fibrosis or tumor necrosis among the randomly chosen fragments were excluded. We used a color deconvolution plug-in for Image J software to identify the positive stains and to calculate the percent CD163-positive area (Fig. 1B, C). TAM density was determined by calculating the average CD163-positive area (%) at a minimum of four different sites in each tissue.

Statistical analysis

The CD163-positive macrophages density (%) is presented as mean ± standard deviation. Differences in CD163-positive macrophages densities among TNM cancer stages, histological subtypes, and pathological characteristics were determined using one-way analysis of variance (ANOVA) or Student's t test. Statistical significance is indicated by a p-value less than .05. All data were analyzed with IBM SPSS Statistics ver. 20.0 (SPSS Inc., Chicago, IL, USA).

Ethics statement

This study was approved by the Institutional Review Boards of Seoul National University Hospital (1107-060-369) and SMG-SNU Boramae Medical Center (06-2010-176). The need for informed consent was waived by those boards.

RESULTS

CD163-positive macrophage densities and prognoses in human cancers

The average CD163-positive area was significantly correlated with the average CD68-positive area (%) in thyroid ($r = 0.775$, $p < .001$) (Appendix 1A), breast ($r = 0.806$, $p < .001$) (Appendix 1B), and lung ($r = 0.780$, $p < .001$) (Appendix 1C) cancers. Therefore, our remaining IHC assessments were performed with CD163 data.

The CD163-positive macrophages densities and the five-year relative survival rates in the 14 different types of human cancers are summarized in Fig. 2. Excluding thyroid cancer, of the 13 other human cancers, pancreas, lung, and gallbladder cancers had the highest density of CD163-positive macrophages (7.0 ±

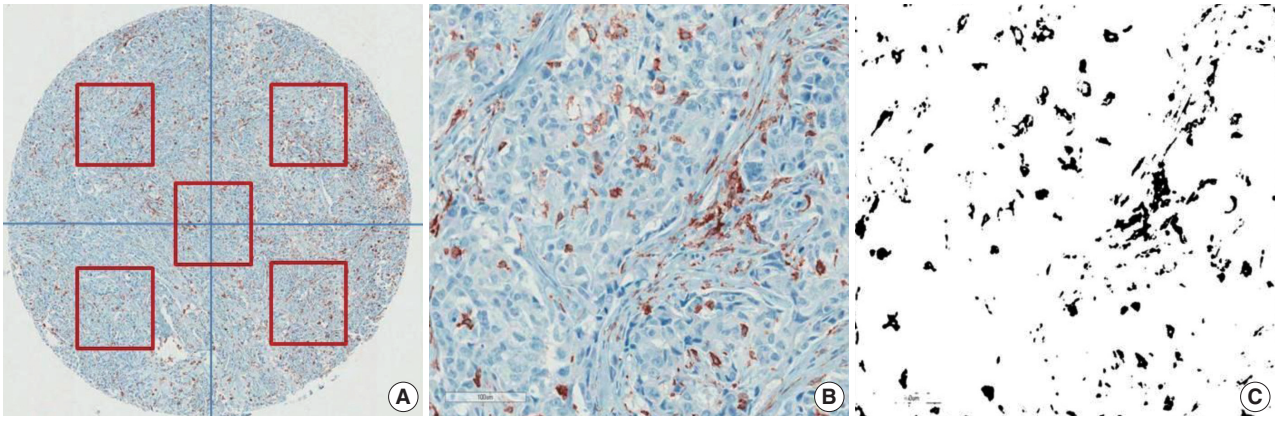

Fig. 1. Immunohistochemical staining for CD163 in breast cancer. Representative CD163 staining in breast cancer. TAM density was measured by averaging the CD163-positive area (%) of five different sites in each tissue (A). The positive IHC staining area (%) was separated and calculated using the Image J color deconvolution plugin (B, C).

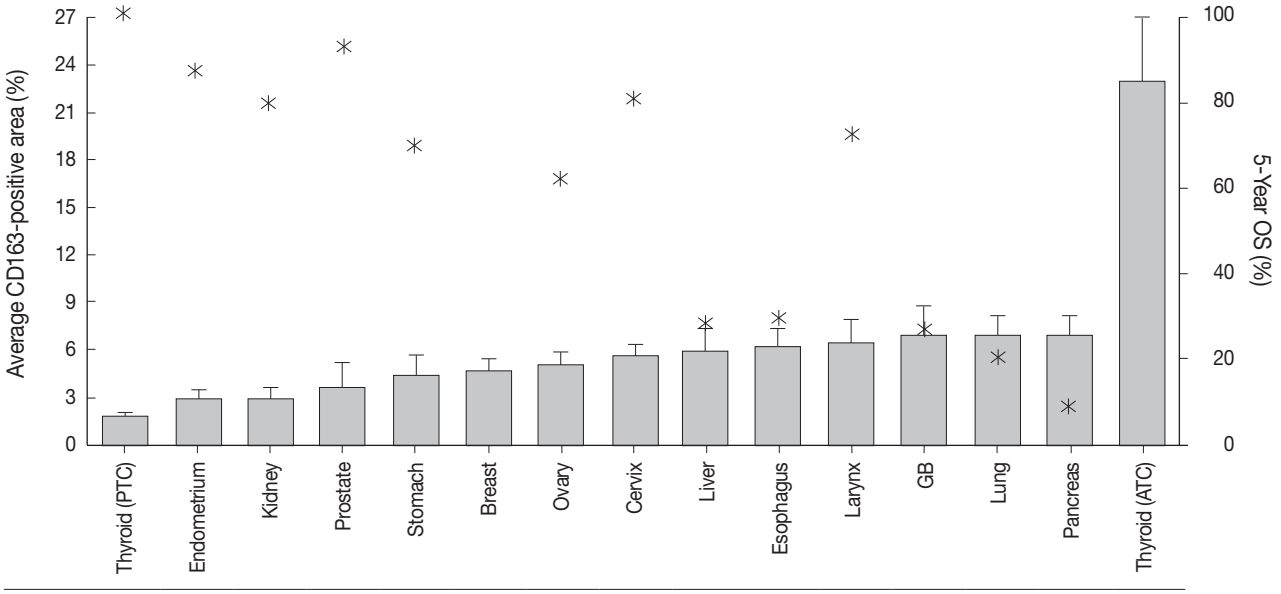

	Thyroid (PTC)	Endometrium	Kidney	Prostate	Stomach	Breast	Ovary	Cervix	Liver	Esophagus	Larynx	GB	Lung	Pancreas	Thyroid (ATC)
CD163 (%)	1.8	2.8	2.8	3.6	4.4	4.7	5.0	5.6	5.9	6.1	6.3	6.9	6.9	7.0	22.9
5-Yr OS	100	86.5	78.8	92	69.4	91.3	61.6	80.1	28.6	30.2	71.7	27.5	20.7	8.7	NA

Fig. 2. CD163-positive macrophage densities and five-year survival rates in 14 different types of human cancers. Left axis and bar graphs represent the average CD163-positive area (%) as mean ± standard error. Right axis and star-shaped markers represent the five-year overall survival (OS, %) obtained from the 2011 Annual Report of Cancer Statistics in Korea. PTC, papillary thyroid cancer; GB, gallbladder; ATC, anaplastic thyroid cancer; NA, not acquired.

3.5%, 6.9 ± 7.4%, and 6.9 ± 5.5%, respectively). In contrast, endometrium, prostate, and kidney cancers had the lowest densities of CD163-positive macrophages (3.6 ± 4.6%, 2.8 ± 2.5%, and 2.8 ± 1.8%, respectively). Interestingly, among the tested cancers, five-year relative survival rate (%) was inversely correlated with CD163-positive macrophages density. The five-year overall survival rates of the cancers with highest TAM densities (pancreas, 8.7%; lung, 20.7%; gallbladder and biliary tract, 27.5%) were lower than those of the cancers with the lowest TAM densities (endometrial, 86.5%; kidney, 78.8%; prostate, 92%).

Of the 14 cancers assessed, thyroid cancer exhibited an extremely wide range of TAM densities that varied according to pathologic subtype (Fig. 3). The ATC cases had the highest density of CD163-positive macrophages (22.9 ± 17.1%), whereas the PTC cases had the lowest CD163-positive macrophage density (1.8 ± 1.3%).

Clinicopathological correlations with TAM density in thyroid, lung, and breast cancers

To investigate the role of TAMs in human cancers, we evaluated the correlations between TAM density and clinicopathological features in lung, breast, and PTC cancers. The CD163-positive macrophage density was significantly higher in cancer tissues

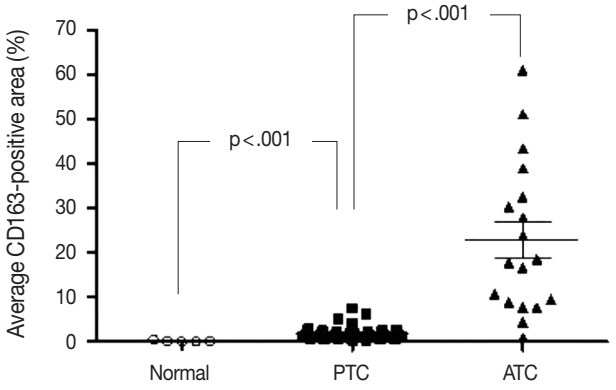

Fig. 3. The CD163-positive macrophage densities of normal tissue, papillary thyroid cancer (PTC) and anaplastic thyroid cancer (ATC).

than normal tissues in breast (4.7 ± 4.5% vs 0.6 ± 0.2%; p < .001), lung (6.9 ± 7.4% vs 1.6 ± 1.6%; p < .001), and thyroid (PTC, 1.8 ± 1.3% vs normal, 0.2 ± 0.2%; p < .001) tissues (Fig. 3). Among the histological subtypes of lung (adenocarcinoma, 5.8 ± 4.4% vs squamous cell carcinoma, 5.9 ± 4.5% vs large cell carcinoma, 8.7 ± 7.3%; p = .428) and breast cancers (infiltrating ductal carcinoma, 4.0 ± 3.4% vs medullary carcinoma, 9.3 ± 3.4%; p = .055), there were no significant differences in CD163-positive macrophages density (Appendix 2). Differences among TNM stages were ev-

http://dx.doi.org/10.4132/jptm.2015.06.01

aluated by assessing adenocarcinoma and squamous cell carcinoma of lung cancer, infiltrating ductal carcinoma of breast cancer, and PTC. There were no significant differences in CD163-positive macrophage density associated with TNM stage in lung ($p = .821$), breast ($p = .060$), or thyroid (PTC, $p = .943$) cancer (Appendix 2). Within the breast cancer samples, several prognostic markers including ER, PR, p53, and C-erbB2 were analyzed. The ER-positive ($3.4 \pm 4.5\%$ vs $5.6 \pm 4.8\%$; $p = .182$) and PR-positive ($3.7 \pm 4.4\%$ vs $5.4 \pm 4.9\%$; $p = .319$) breast cancers showed non-significant trends toward lower CD163-positive macrophages density than those in the ER- or PR-negative breast cancers. In contrast, p53-positive ($5.9 \pm 5.9\%$ vs $4.2 \pm 3.6\%$; $p = .269$) and C-erbB2-positive ($6.4 \pm 6.8\%$ vs $4.4 \pm 3.8\%$; $p = .233$) breast cancer showed nonsignificant trends toward higher CD163-positive macrophage density than those in p53- or C-erbB2-negative breast cancers.

DISCUSSION

Our results demonstrate that CD163-positive macrophage density is inversely correlated with five-year cancer survival rate in a variety of human cancers. This finding suggests the presence of a potential pro-tumorigenic role of TAMs in some human cancers. Among the 14 different types of human cancers assessed, ATC, the most aggressive cancer in humans,[16,17] had the highest CD163-positive macrophages density (23%), which was markedly higher than the second highest TAM density (7%) detected in the pancreas cancer samples. ATC accounts for up to 2% of thyroid cancers and is characterized by an extremely poor survival rate with a one-year average survival rate of 20% and a median survival duration of five months.[18,19] In contrast, the most common well-differentiated thyroid cancer, PTC, had the lowest CD163-positive macrophages density (1.8%). PTC is associated with lower recurrence and mortality rates[20] than other solid and relatively indolent tumors and has a five-year survival rate higher than 90%.[15] Since the differentiation of pathologic subtypes is distinctive and survival rates markedly differ among subtypes, our observation of a striking difference in CD163-positive macrophages density between two thyroid cancer subtypes led us to hypothesize that TAM density is a potential prognostic factor in human cancers.

In contrast, histological subtypes of lung and breast cancers did not exhibit significant differences in CD163-positive macrophage density. Correlations between TAM density and clinicopathological features have been reported in ductal and lobular carcinomas in breast cancer[21,22] and in adenocarcinoma[23,24] and non-small cell[25,26] lung cancers. Nonetheless, only a few reports have compared TAM density based on histological subtype. Although our data did not detect a significant difference related to histological subtype in lung or breast cancers, the number of each subtype in our sample population was limited. Therefore, we recommend a larger-scale study of TAM density in a variety of histological subtypes.

In this study, there were no significant differences in CD163-positive macrophage density among TNM stages in lung, breast, or thyroid cancers. In addition, cancer tissues showed higher CD163-positive macrophage densities than those in normal tissues in lung, breast, and thyroid samples. In breast cancer, there were trends toward negative correlations of TAM density with ER and PR expression, whereas there were trends toward positive correlations of TAM density with p53 and C-erbB2 expression. Previous reports indicate that TAM infiltration is inversely correlated with ER expression in breast cancer.[7,27] However, this correlation might vary with TAM location.[22] Medrek *et al*.[22] reported that a dense infiltration of CD163-positive macrophages in tumor stroma was associated with ER- and PR-negativity, but there was no such association in tumor nest. Our study results show a non-significant trend toward negative correlations between ER and PR expressions and density of CD163-positive macrophages. Due to data limitations, we could not assess such correlations according to infiltration location.

Selecting the most appropriate marker for TAM assessment can be challenging. Originally, a TAM was seen as a residual macrophage within the tumor microenvironment, and the biological characteristics of TAMs have been shown to be anti-tumorigenic, cytotoxic, or pro-tumorigenic.[1,28] Furthermore, macrophages can undergo polarization and change from an M1-macrophage (classically activated, pro-inflammatory) to an M2-macrophage (alternatively activated, anti-inflammatory or regenerative).[29] Collectively, these findings indicate the difficulty in choosing a cancer-specific TAM marker. In the beginning of this study, we performed IHC investigations using both CD68, a pan macrophage marker,[29] and CD163, a more specific marker for M2-macrophages.[30] Those investigations revealed that the CD163-positive areas were significantly positively correlated with the CD68-positive areas in lung, breast, and thyroid cancers; thus, our remaining IHC assessments were performed with CD163 data.

Previous clinical studies have shown a correlation between TAM density and cancer prognosis. Most studies have shown a significant correlation between TAM density and poor prognosis, especially among breast, thyroid, and lung cancers.[5,7,8,22]

However, several studies have reported that TAM density is associated with good prognosis. Such contradictory results might be due to differences in the number, grade, stage, or size of tumors among the studies. In addition, previous clinical studies have used various methods to assess TAM infiltration. The use of different approaches could have also contributed to the inconsistent results. Although the sample size for each cancer subtype in our study population was small, the results in this study comparing TAM density in various human cancers are significant; therefore, further studies with larger sample sizes are warranted.

In summary, we detected a trend toward an inverse correlation between CD163-positive macrophage density and five-year survival rate in 14 different types of human cancers. In particular, PTC and ATC clearly showed an inverse correlation between TAM density and prognosis. Our results suggest that TAM density is a potential biomarker of poor prognosis in human cancers.

Conflicts of Interest

No potential conflict of interest relevant to this article was reported.

Acknowledgments

This work was supported by a grant from the Next-Generation BioGreen 21 Program (No.PJ00954003), Rural Development Administration, Republic of Korea.

REFERENCES

1. Coussens LM, Werb Z. Inflammation and cancer. Nature 2002; 420: 860-7.
2. Cho SW. Interactions between immune cells and tumor cells. J Korean Thyroid Assoc 2013; 6: 96-100.
3. Zhang QW, Liu L, Gong CY, *et al*. Prognostic significance of tumor-associated macrophages in solid tumor: a meta-analysis of the literature. PLoS One 2012; 7: e50946.
4. Bingle L, Brown NJ, Lewis CE. The role of tumour-associated macrophages in tumour progression: implications for new anticancer therapies. J Pathol 2002; 196: 254-65.
5. Kim S, Cho SW, Min HS, *et al*. The expression of tumor-associated macrophages in papillary thyroid carcinoma. Endocrinol Metab (Seoul) 2013; 28: 192-8.
6. Zeni E, Mazzetti L, Miotto D, *et al*. Macrophage expression of interleukin-10 is a prognostic factor in nonsmall cell lung cancer. Eur Respir J 2007; 30: 627-32.
7. Campbell MJ, Tonlaar NY, Garwood ER, *et al*. Proliferating macrophages associated with high grade, hormone receptor negative breast cancer and poor clinical outcome. Breast Cancer Res Treat 2011; 128: 703-11.
8. Sato S, Hanibuchi M, Kuramoto T, *et al*. Macrophage stimulating protein promotes liver metastases of small cell lung cancer cells by affecting the organ microenvironment. Clin Exp Metastasis 2013; 30: 333-44.
9. Forssell J, Oberg A, Henriksson ML, Stenling R, Jung A, Palmqvist R. High macrophage infiltration along the tumor front correlates with improved survival in colon cancer. Clin Cancer Res 2007; 13: 1472-9.
10. Ohno S, Inagawa H, Dhar DK, *et al*. The degree of macrophage infiltration into the cancer cell nest is a significant predictor of survival in gastric cancer patients. Anticancer Res 2003; 23: 5015-22.
11. Welsh TJ, Green RH, Richardson D, Waller DA, O'Byrne KJ, Bradding P. Macrophage and mast-cell invasion of tumor cell islets confers a marked survival advantage in non-small-cell lung cancer. J Clin Oncol 2005; 23: 8959-67.
12. Kawai O, Ishii G, Kubota K, *et al*. Predominant infiltration of macrophages and CD8(+) T cells in cancer nests is a significant predictor of survival in stage IV nonsmall cell lung cancer. Cancer 2008; 113: 1387-95.
13. Ohno S, Ohno Y, Suzuki N, *et al*. Correlation of histological localization of tumor-associated macrophages with clinicopathological features in endometrial cancer. Anticancer Res 2004; 24: 3335-42.
14. Cho SW, Kim YA, Sun HJ, *et al*. Therapeutic potential of Dickkopf-1 in wild-type BRAF papillary thyroid cancer via regulation of beta-catenin/E-cadherin signaling. J Clin Endocrinol Metab 2014; 99: E1641-9.
15. Jung KW, Won YJ, Kong HJ, Oh CM, Lee DH, Lee JS. Cancer statistics in Korea: incidence, mortality, survival, and prevalence in 2011. Cancer Res Treat 2014; 46: 109-23.
16. Cornett WR, Sharma AK, Day TA, *et al*. Anaplastic thyroid carcinoma: an overview. Curr Oncol Rep 2007; 9: 152-8.
17. Are C, Shaha AR. Anaplastic thyroid carcinoma: biology, pathogenesis, prognostic factors, and treatment approaches. Ann Surg Oncol 2006; 13: 453-64.
18. Smallridge RC, Copland JA. Anaplastic thyroid carcinoma: pathogenesis and emerging therapies. Clin Oncol (R Coll Radiol) 2010; 22: 486-97.
19. Haymart MR, Banerjee M, Yin H, Worden F, Griggs JJ. Marginal treatment benefit in anaplastic thyroid cancer. Cancer 2013; 119: 3133-9.
20. Lin JD, Chen ST, Hsueh C, Chao TC. A 29-year retrospective review of papillary thyroid cancer in one institution. Thyroid 2007; 17: 535-41.
21. Murri AM, Hilmy M, Bell J, *et al*. The relationship between the systemic inflammatory response, tumour proliferative activity, T-lym-

phocytic and macrophage infiltration, microvessel density and survival in patients with primary operable breast cancer. Br J Cancer 2008; 99: 1013-9.
22. Medrek C, Pontén F, Jirström K, Leandersson K. The presence of tumor associated macrophages in tumor stroma as a prognostic marker for breast cancer patients. BMC Cancer 2012; 12: 306.
23. Ohtaki Y, Ishii G, Nagai K, *et al*. Stromal macrophage expressing CD204 is associated with tumor aggressiveness in lung adenocarcinoma. J Thorac Oncol 2010; 5: 1507-15.
24. Zhang BC, Gao J, Wang J, Rao ZG, Wang BC, Gao JF. Tumor-associated macrophages infiltration is associated with peritumoral lymphangiogenesis and poor prognosis in lung adenocarcinoma. Med Oncol 2011; 28: 1447-52.
25. Ma J, Liu L, Che G, Yu N, Dai F, You Z. The M1 form of tumor-associated macrophages in non-small cell lung cancer is positively associated with survival time. BMC Cancer 2010; 10: 112.
26. Al-Shibli K, Al-Saad S, Donnem T, Persson M, Bremnes RM, Busund LT. The prognostic value of intraepithelial and stromal innate immune system cells in non-small cell lung carcinoma. Histopathology 2009; 55: 301-12.
27. Steele RJ, Eremin O, Brown M, Hawkins RA. Oestrogen receptor concentration and macrophage infiltration in human breast cancer. Eur J Surg Oncol 1986; 12: 273-6.
28. Pollard JW. Tumour-educated macrophages promote tumour progression and metastasis. Nat Rev Cancer 2004; 4: 71-8.
29. Heusinkveld M, van der Burg SH. Identification and manipulation of tumor associated macrophages in human cancers. J Transl Med 2011; 9: 216.
30. Ambarus CA, Krausz S, van Eijk M, *et al*. Systematic validation of specific phenotypic markers for *in vitro* polarized human macrophages. J Immunol Methods 2012; 375: 196-206.

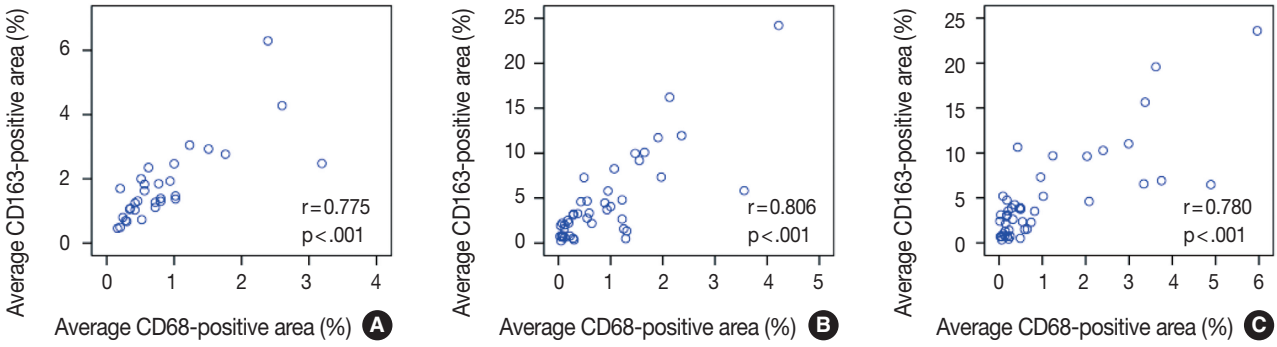

Appendix 1. The correlation between average CD163-positive area (%) and average CD68-positivie area (%). (A) Thyroid cancer. (B) Breast cancer. (C) Lung cancer.

Appendix 2. Average CD163-positive area (%) according to clinicopathologic characteristics in lung, breast, and thyroid cancer

Charaacteristic	No.	CD163 (%)	p-value[a]
Lung			
Histology			
Adenocarcinoma	19	5.8±4.4	.428
SQCC	20	5.9±4.5	
Large cell carcinoma	4	8.7±7.3	
SCC	2	1.0±0.5	
Mixed carcinoma	4	5.0±2.3	
Stage[b]			
I	16	5.7±4.4	.821
II	12	6.6±5.2	
III	10	5.5±3.8	
IV	1	2.4	
Survival			
Alive	15	3.6±3.4	.104
Death	15	5.9±3.9	
Breast			
Infiltrating ductal	45	4.0±3.4	.055
Medullary	2	9.3±3.4	
Sarcomatoid	1	1.9	
Metaplastic	1	10.1	
Stage[b]			
IIA	13	5.3±4.9	.060
IIB	10	4.2±2.4	
IIIA	12	1.8±1.4	
IIIB	10	4.5±2.3	
Alive	30	4.2±3.7	.726
Death	6	3.7±2.5	
Thyroid			
PTC	35	1.8±1.3	<.001
ATC	18	22.9±17.1	
Stage[b]			
I	3	1.4±0.6	.943
II	3	1.7±1.1	
III	21	1.8±1.2	
IV	4	1.8±0.8	
Alive	15	1.8±1.5	.241
Death	2	3.3±2.8	

SQCC, squamous cell carcinoma; SCC; small cell carcinoma, PTC; papillary thyroid carcinoma, ATC; anaplastic thyroid carcinoma.
[a]p-value by ANOVA or student t test; [b]TNM stage and survival was classified in adenocarcinoma and squamous cell carcinoma (lung), infiltrating ductal carcinoma (breast) and papillary thyroid carcinoma (thyroid).

http://dx.doi.org/10.4132/jptm.2015.06.01

Journal of Pathology and Translational Medicine 2015; 49: 325-330
http://dx.doi.org/10.4132/jptm.2015.05.20

■ CASE STUDY ■

WHO Grade IV Gliofibroma: A Grading Label Denoting Malignancy for an Otherwise Commonly Misinterpreted Neoplasm

Paola A. Escalante Abril
Miguel Fdo. Salazar
Nubia L. López García
Mónica N. Madrazo Moya
Yadir U. Zamora Guerra
Yadira Gandhi Mata Mendoza
Erick Gómez Apo
Laura G. Chávez Macías

Pathology Unit, Neuropathology Service, Mexico General Hospital, Mexico City, Mexico

Received: March 2, 2015
Revised: May 10, 2015
Accepted: May 20, 2015

Corresponding Author
Miguel Fdo. Salazar, MD
Hospital General de México "Dr. Eduardo Liceaga", Unidad de Patología, Servicio de Neuropatología, Dr. Balmis 148, Col. Doctores, Delegación Cuauhtémoc, C.P. 06726, México D.F.
Tel: +52-55-01-55-2789-2000
E-mail: k7nigricans@hotmail.com

We report a 50-year-old woman with no relevant clinical history who presented with headache and loss of memory. Magnetic resonance imaging showed a left parieto-temporal mass with annular enhancement after contrast media administration, rendering a radiological diagnosis of high-grade astrocytic neoplasm. Tumour sampling was performed but the patient ultimately died as a result of disease. Microscopically, the lesion had areas of glioblastoma mixed with a benign mesenchymal constituent; the former showed hypercellularity, endothelial proliferation, high mitotic activity and necrosis, while the latter showed fascicles of long spindle cells surrounded by collagen and reticulin fibers. With approximately 40 previously reported cases, gliofibroma is a rare neoplasm defined as either glio-desmoplastic or glial/benign mesenchymal. As shown in our case, its prognosis is apparently determined by the degree of anaplasia of the glial component.

Key Words: Gliofibroma; Bimorphic neoplasm; Desmoplastic glioma; Adult population; Tumour suppressor protein 53

Analogous to the mixed epithelial/mesenchymal tumours seen in Müllerian derivatives, some glial neoplasms can display a bimorphic appearance due to an accompanying mesodermal component. While gliosarcoma is probably the best-known paragon of this group, the existence of non-malignant mesenchymal constituents, different from the so-called Scherer's tertiary structures, is rare but feasible. Here, we describe a peculiar case of a high-grade astrocytic neoplasm (glioblastoma) blending with an innocuous spindle-cell component.

CASE REPORT

A 50-year-old female presented with headache and loss of memory over the previous six months. Magnetic resonance imaging scans showed a left parieto-temporal mass (70.82×48.56×43.97 mm) with significant perilesional oedema and post-contrast annular enhancement (Fig. 1A, B). Despite prompt tumour sampling and analysis, the patient ultimately expired one month after the surgery. Necropsy was not authorized.

Histologically, the lesion showed areas unequivocally consistent with glioblastoma due to their microvascular proliferation, palisading necrosis, hypercellularity, pleomorphism, and high mitotic activity (Fig. 1C, D). These areas intermingled with cytologically bland, long spindle-cell fascicles (Fig. 1E, F) enveloped by sturdy collagen and fine reticulin fibers (Fig. 2A–D). As expected, immunoperoxidase-coupled reactions showed strong and diffuse expression of glial fibrillary acidic protein in the glioblastoma areas (Fig. 3A), while the spindled part of the neoplasm was exclusively positive for vimentin (Fig. 3B). Ki-67 expression was variable, with positivity as high as 50% in the astroglial regions (Fig. 3C) but with immunolabeling of less than 1% in the mesenchymal portion. Likewise, expression of p53 was largely diffuse in the gliomatous parts, albeit focally in some fusiform cells (Fig. 3D, E). No reaction was detected for epidermal growth

pISSN 2383-7837
eISSN 2383-7845

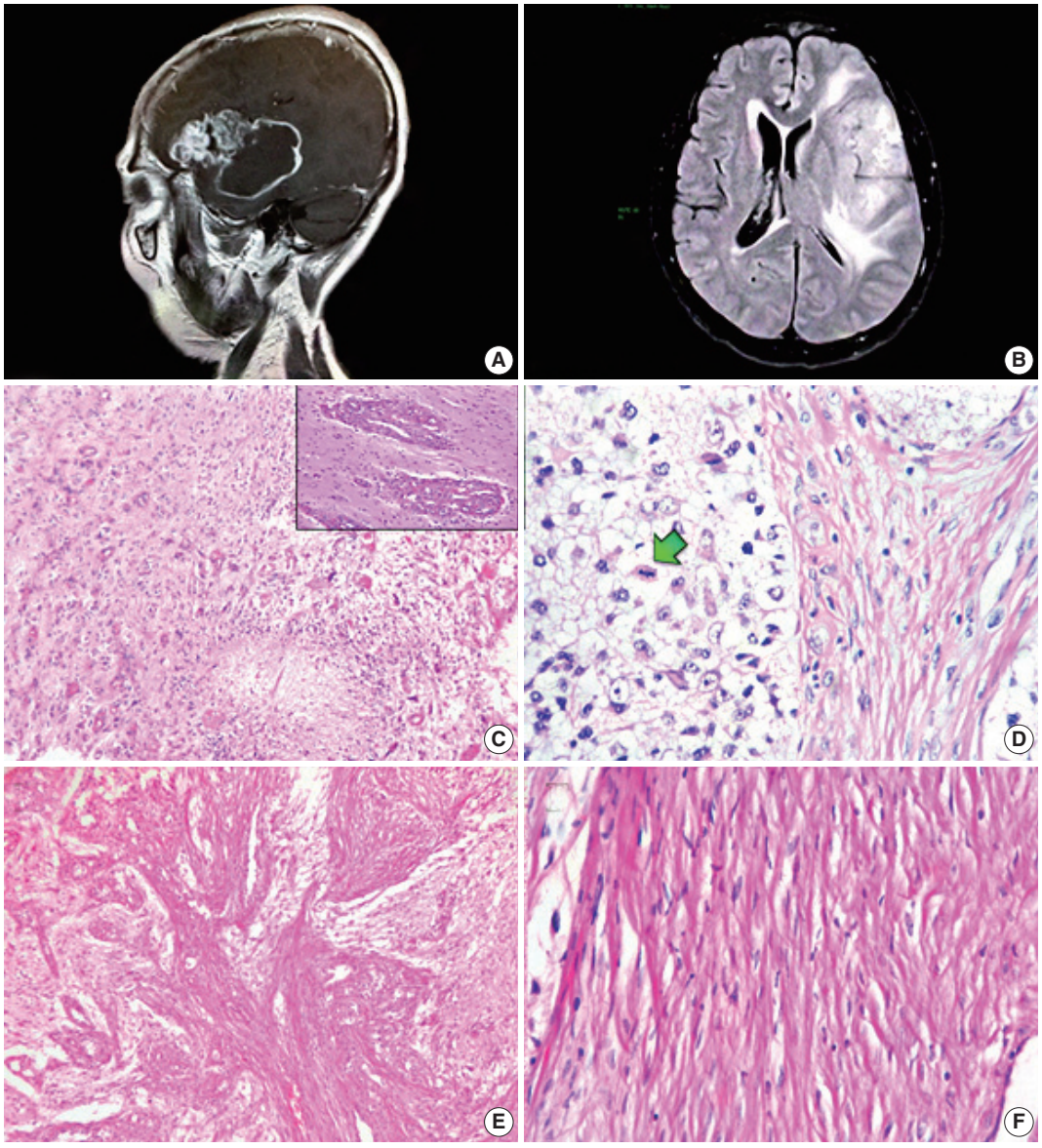

Fig. 1. Magnetic resonance imaging scans and biphasic histological features. (A) Post-contrast, T1-weighted sagittal section. A heterogeneous tumour with an enhancing peripheral rim is shown. (B) Fluid-attenuated inversion recovery sequence. Considerable outlying oedema can be seen. (C) Glioblastomatous component with palisading necrosis and microvascular proliferation (upper right inset). (D) Boundary zone with neoplastic cells of gemistocytic appearance (left) next to apparently atypical spindle cells (right). Mitoses are noticeable exclusively in neoplastic glial cells (arrow). (E) Mesenchymal component with solid fascicular tissue intermingled with loose astrocytic areas. (F) High-magnification photomicrograph of the cytologically bland mesenchymal constituent.

factor receptor in either element.

The lesion was diagnosed as gliofibroma (mixed astrocytic neoplasm with a low-grade mesenchymal constituent), with special note of its poor prognosis based on the degree of anaplasia of the glial component, suggestive of glioblastoma. This note was written prior to the patient´s demise.

All procedures performed in this study were in accordance with the ethical standards of the institutional and/or national research committee and with the 1964 Helsinki Declaration and its later amendments or comparable ethical standards. Informed consent was obtained from the patient's legal guardian, and the anonymity of the patient was preserved.

http://dx.doi.org/10.4132/jptm.2015.05.20

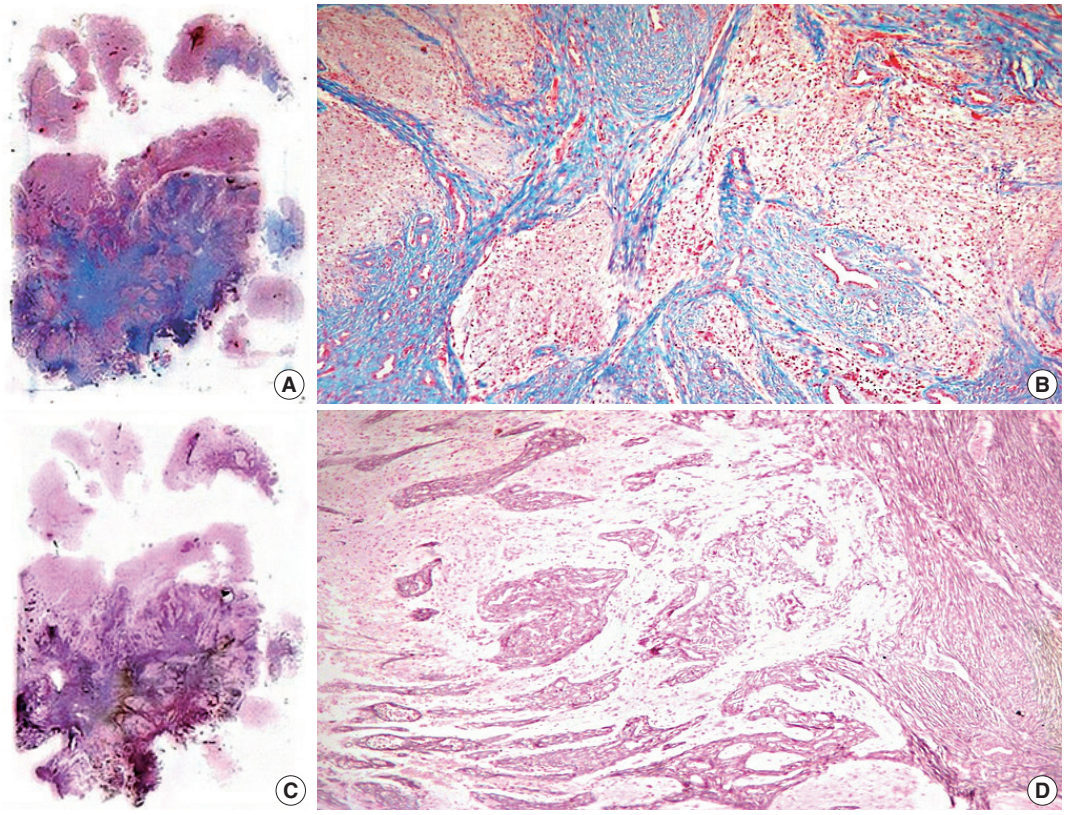

Fig. 2. Histochemical stains of whole-mount sections. (A, B) Collagen-rich tissue seen with Masson's trichrome. (C, D) Reticulin pattern showed with reticular fiber stain.

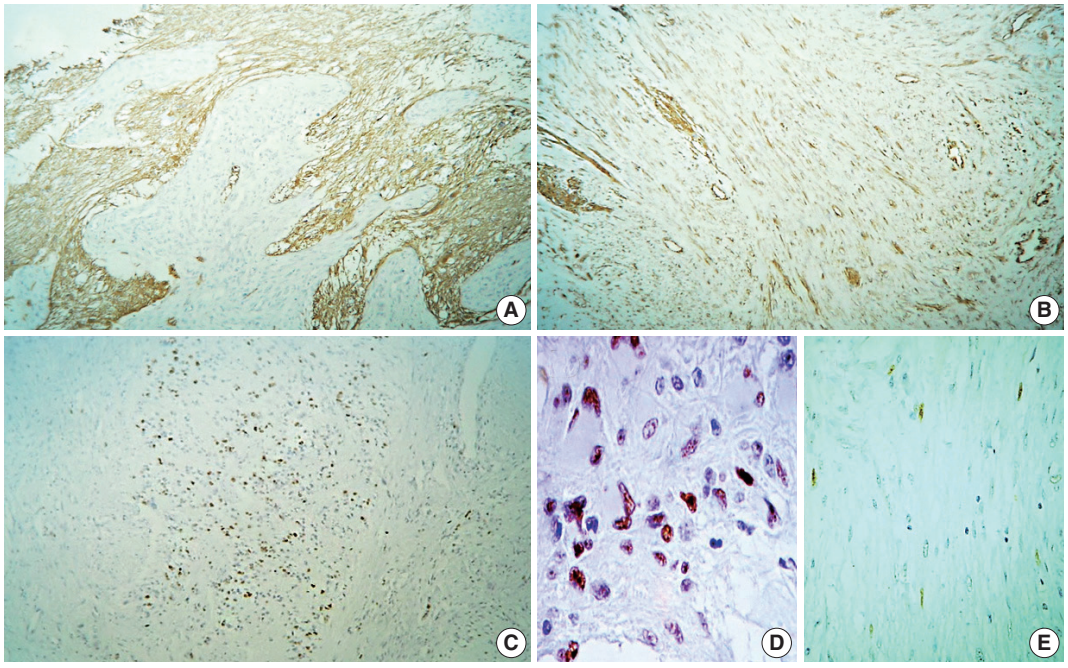

Fig. 3. Immunohistochemistry panel. (A) Glial fibrillary acidic protein. (B) Vimentin. (C) Ki-67. (D) p53 (glial portion) with diffuse immunolabeling. (E) p53 (mesenchymal portion) with very focally positive immunoreactivity.

Table 1. High-grade gliofibroma cases

Case No.	Reference	Age/ Sex	Location	Grade according to the described features of the glial component	Outcome (follow-up)
1	Friede (1978)[1]	3.9 yr/F	Lower medulla oblongata	Dedifferentiation of the glial component	Died (3 mo)
2	Snipes *et al*. (1991)[8]	2 mo/F	Right thalamus and floor of the fourth ventricle	Anaplastic astrocytoma, WHO grade III (mitoses up to 5 per 10-HPF)	Died (16 mo)
3	Vazquez *et al*. (1991)[5]	11 mo/F	Right temporal lobe	Anaplastic astrocytoma, WHO grade III (pleomorphism and numerous MFs)	Alive (2 yr)
4	Schober *et al*. (1992)[9]	18 yr/M	Right frontal lobe	Anaplastic astrocytoma, WHO grade III (foci of pleomorphism, sparse and abnormal MFs)	Alive (7 days)
5	Cerda-Nicolas and Kepes (1993)[10]	4 yr/F	Fourth ventricle, extending to the prepontine cistern and left temporal lobe	Anaplastic astrocytoma, WHO grade III	No data
6	Cerda-Nicolas and Kepes (1993)[10]	9 yr/F	Left parietal lobe	Anaplastic astrocytoma, WHO grade III (pleomorphism and ocassional MFs)	Alive (5.5 mo)
7	Caldemeyer *et al*. (1995)[11]	8 yr/M	Right temporal lobe	Anaplastic astrocytoma, WHO grade III (numerous MFs)	No data
8	Sharma *et al*. (1998)[4]	54 yr/F	Right parietal lobe	Anaplastic astrocytoma, WHO grade III (pleomorphism, MFs and 10.5% of PI)	Died (6 mo)
9	Kim *et al*. (2003)[12]	25 yr/M	Left parietal lobe	Anaplastic astrocytoma, WHO grade III (up to 35.8% of PI)	Alive (2 mo)
10	Gargano *et al*. (2014)[2]	10.7 yr/F	Left fronto-parietal lobe	Anaplastic astrocytoma, WHO grade III (mild to moderate pleomorphism with up to 10% of PI)	Alive (2 yr)
Subtotal (10 cases)				Mortality rate (cases with available data) (5/8) = 62.5%	
11	Bastos Leite *et al*. (2002)[13]	47 yr/F	Left parietal lobe	Glioblastoma, WHO grade IV (nuclear atypia, endothelial proliferation, necrosis and mitoses)	Died (1 yr)
12	Present case	50 yr/F	Left parieto-temporal lobe	Glioblastoma, WHO grade IV (microvascular proliferation, palisading necrosis and up to 50% of PI)	Died (1 mo)
Subtotal (2 cases)				Mortality rate (2/2) = 100.0%	
Total (12 cases)				Overall mortality rate (cases with available data) (7/10) = 70.0%	

F, female; WHO, World Health Organization; HPF, high-power fields; M, male; MFs, mitotic figures; PI, proliferation index (MIB-1, Ki-67).

DISCUSSION

The term gliofibroma was first introduced by Friede in 1978[1] to describe an unusual neoplasm featuring astroglial cells within collagen bundles. Since then, nearly 40 cases of gliofibroma have been reported in the worldwide literature, the vast majority occurring in the paediatric population.[2] Only 11 cases have been recorded in adults, with age ranging from 19 to 54 years.[3,4] More importantly, some cases described in both, children and adults, bear morphological traits indicative of biologically aggressive lesions (Table 1). The prognostic value of these features in gliofibromas has been widely debated, as some non-lethal tumours have a high-grade glial component while other are recurrent lesions despite their low-grade glial associate.[5,6] Moreover, as accurately demonstrated by Suarez *et al*.,[7] the overall mortality for these lesions is approximately 23%. However, when considering the lethality of the high-grade-only subset, this value increases to 70% or even 100% in cases with an accompanying glioblastoma component (Table 1).[8-13]

In their work, Schober *et al*.[9] were the first to tentatively assign a World Health Organization (WHO) grade to their diagnosis, while Cerda-Nicolas and Kepes[10] preferred to add a descriptive modifier (anaplastic). In a similar way, Sharma *et al*.[4] proposed to dichotomize these lesions into low-grade (benign) or high-grade (malignant/anaplastic) based on the Ki-67 proliferation index. In spite of these grading attempts, Snipes *et al*.[8] seminally pointed out that prognosis seems to be more related to location rather than to any morphological or immunohistochemical feature, though the degree of anaplasia and the mitotic index might be worthy of consideration. On the other hand, the case documented by Altamirano *et al*.[14] highlights the issue of whether atypia can exist in the fibroma portion of the neoplasm. This is exceedingly difficult to assert, as the boundaries of either a gliosarcoma or sarcoglioma are unavoidably blurred. In the aforementioned case, increased immunolabeling for Ki-67 was noted in the nuclei of the mesenchymal part, though it was rated

http://dx.doi.org/10.4132/jptm.2015.05.20

in less than 5% of the overall tumour. The authors interpreted the mass as a proliferative activity of uncertain relevance. Though our case displays focal nuclear enlargement and vacuolization (Fig. 1D), we did not observe an increment in mesenchymal Ki-67 expression and did not find any areas suggestive of a true sarcomatous component. Nonetheless, this presumed "atypia" might not reliably worsen the prognosis, as in our case it was based on histology (glioblastoma) while in Altamirano's group was determined by location (thalamus/mesencephalon). p53 immunostaining in our case was also of conjectural significance, indicating not only a possible secondary glioblastoma, but also a common origin of both the glial and mesenchymal elements, similar to the demonstration of Biernat regarding gliosarcomas,[15] and thus possibly representing a true benign mesodermal differentiation as formerly hypothesised by Snipes *et al*.[8] Furthermore, p53 immunolabeling has been previously tested in nine gliofibroma cases with no positive result.[2,4,6,12,16-18] Interestingly, Goyal *et al*.[19] also applied this immunohistochemical marker in three other cases but never mentioned the final outcome. This lack of p53 expression is shared by the so-called desmoplastic infantile astrocytoma and may hint, at least in these aforementioned cases, at a different developmental pathway from that of diffuse or anaplastic astrocytomas and glioblastomas.

Three more issues briefly deserve our attention. (1) As previously mentioned, the first report of gliofibroma clearly detailed a desmoplastic astrocytoma (Friede-type gliofibroma);[1] nonetheless, this designation was subsequently applied to similar lesions consisting of both glial and mesenchymal derivatives (authentic glioma/fibroma),[10] as in the present case. It is worth mentioning that the glial constituent can range from innocuous to evidently malignant, while the latter is a consistently benign fusocellular component. (2) In the bimorphic subset, it has not been fully corroborated whether the two populations are distinct cell lineages or if the fusiform cells are glia capable of differentiating into fibroblasts, myofibroblasts, Schwann cells or histiocytes.[2,20] (3) Recently, some desmoplastic lesions displaying a non-astrocytic glial phenotype with immunohistochemical properties more akin to ependymoma (as in the case described by Gargano *et al*.[2]) have also been diagnosed as gliofibromas. Thus, as pointed out by Suárez *et al*.,[7] a controversial dilemma of "splitting versus lumping" currently prevails in the conceptual and classification schemes regarding these kinds of tumours. Nevertheless, it seems to be more of an academic and histopathological predicament rather than one of clinical concern or prognostic relevance.

As shown in our case and previously advised by other authors, gliofibroma prognosis is greatly influenced by the degree of anaplasia of the glial component. Hence, we suggest adding a grade (WHO I–IV) or descriptive (low-grade, high-grade, anaplastic, malignant/glioblastomatoid) modifier to the diagnosis of gliofibroma.

It had been previously claimed that necrosis and prominent vascular proliferation are not usual features of gliofibromas.[16] Thus, we document the second case of gliofibroma with a glioblastomatous component[13] (though this is the first case involving a mixture of glioma and fibroma) as well as the third case occurring in Latin American population.[2,14]

Conflicts of Interest

No potential conflict of interest relevant to this article was reported.

REFERENCES

1. Friede RL. Gliofibroma: a peculiar neoplasia of collagen forming glia-like cells. J Neuropathol Exp Neurol 1978; 37: 300-13.
2. Gargano P, Zuccaro G, Lubieniecki F. Intracranial gliofibroma: a case report and review of the literature. Case Rep Pathol 2014; 2014: 165025.
3. Prayson RA. Disseminated spinal cord astrocytoma with features of gliofibroma: a review of the literature. Clin Neuropathol 2013; 32: 298-302.
4. Sharma MC, Gaikwad S, Mehta VS, Dhar J, Sarkar C. Gliofibroma: mixed glial and mesenchymal tumour: report of three cases. Clin Neurol Neurosurg 1998; 100: 153-9.
5. Vazquez M, Miller DC, Epstein F, Allen JC, Budzilovich GN. Glioneurofibroma: renaming the pediatric "gliofibroma": a neoplasm composed of Schwann cells and astrocytes. Mod Pathol 1991; 4: 519-23.
6. Deb P, Sarkar C, Garg A, Singh VP, Kale SS, Sharma MC. Intracranial gliofibroma mimicking a meningioma: a case report and review of literature. Clin Neurol Neurosurg 2006; 108: 178-86.
7. Suarez CR, Raj AB, Bertolone SJ, Coventry S. Carboplatinum and vincristine chemotherapy for central nervous system gliofibroma: case report and review of the literature. J Pediatr Hematol Oncol 2004; 26: 756-60.
8. Snipes GJ, Steinberg GK, Lane B, Horoupian DS. Gliofibroma: case report. J Neurosurg 1991; 75: 642-6.
9. Schober R, Bayindir C, Canbolat A, Urich H, Wechsler W. Gliofibroma: immunohistochemical analysis. Acta Neuropathol 1992; 83: 207-10.
10. Cerda-Nicolas M, Kepes JJ. Gliofibromas (including malignant forms), and gliosarcomas: a comparative study and review of the

literature. Acta Neuropathol 1993; 85: 349-61.
11. Caldemeyer KS, Zimmerman RA, Azzarelli B, Smith RR, Moran CC. Gliofibroma: CT and MRI. Neuroradiology 1995; 37: 481-5.
12. Kim Y, Suh YL, Sung C, Hong SC. Gliofibroma: a case report and review of the literature. J Korean Med Sci 2003; 18: 625-9.
13. Bastos Leite AJ, Palmeira de Sousa C, Honavar M. Malignant gliofibroma (desmoplastic glioblastoma) in an adult: case report. J Neuroradiol 2002; 29: 215-8.
14. Altamirano E, Jones MC, Drut R. Gliofibroma. Comunicación de un caso pediátrico y revisión de la bibliografía. Patol Rev Latinoam 2011; 49: 221-5.
15. Biernat W, Aguzzi A, Sure U, Grant JW, Kleihues P, Hegi ME. Identical mutations of the p53 tumor suppressor gene in the gliomatous and the sarcomatous components of gliosarcomas suggest a common origin from glial cells. J Neuropathol Exp Neurol 1995; 54: 651-6.
16. Prayson RA. Gliofibroma: a distinct entity or a subtype of desmoplastic astrocytoma? Hum Pathol 1996; 27: 610-3.
17. Kim NR, Suh YL, Shin HJ, Park IS. Gliofibroma with extensive calcified deposits. Clin Neuropathol 2003; 22: 14-22.
18. Matsumura A, Takano S, Nagata M, Anno I, Nose T. Cervical intramedullary gliofibroma in a child: a case report and review of the literature. Pediatr Neurosurg 2002; 36: 105-10.
19. Goyal S, Puri T, Gunabushanam G, *et al*. Gliofibroma: a report of three cases and review of literature. Acta Oncol 2007; 46: 1202-4.
20. Erguvan-Onal R, Ateş O, Onal C, Aydin NE, Koçak A. Gliofibroma: an incompletely characterized tumor. Tumori 2004; 90: 157-60.

 http://dx.doi.org/10.4132/jptm.2015.05.20

Journal of Pathology and Translational Medicine 2015; 49: 331-334
http://dx.doi.org/10.4132/jptm.2015.04.16

■ CASE STUDY ■

A Rare Case of Primary Tubular Adenocarcinoma of the Thymus, Enteric Immunophenotype: A Case Study and Review of the Literature

Hae Yoen Jung · Hyundeuk Cho
Jin-Haeng Chung[1] · Sang Byoung Bae[2]
Ji-Hye Lee · Hyun Ju Lee
Si-Hyong Jang · Mee-Hye Oh

Department of Pathology, Soonchunhyang University Cheonan Hospital, Cheonan; [1]Department of Pathology and Respiratory Center, Seoul National University Bundang Hospital, Seongnam; [2]Division of Hematology and Oncology, Department of Internal Medicine, Soonchunhyang University Cheonan Hospital, Cheonan, Korea

Received: March 10, 2015
Revised: April 8, 2015
Accepted: April 16, 2015

Corresponding Author
Mee-Hye Oh, MD, PhD
Department of Pathology, Soonchunhyang University Cheonan Hospital, 31 Suncheonhyang 6-gil, Dongnam-gu, Cheonan 330-930, Korea
Tel: +82-41-570-3580
Fax: +82-41-570-3580
E-mail: mhoh0212@schmc.ac.kr

Thymic carcinomas are uncommon malignant tumors, and thymic adenocarcinomas are extremely rare. Here, we describe a case of primary thymic adenocarcinoma in a 59-year-old woman. Histological examination of the tumor revealed tubular morphology with expression of cytokeratin 20 and caudal-type homeobox 2 according to immunohistochemistry, suggesting enteric features. Extensive clinical and radiological studies excluded the possibility of an extrathymic primary tumor. A review of the literature revealed only two global cases of primary tubular adenocarcinomas of the thymus with enteric immunophenotype.

Key Words: Thymus gland; Adenocarcinoma; Keratin-20; Caudal type homeobox 2

Thymic carcinomas are uncommon malignant tumors. According to the World Health Organization (WHO), thymic carcinomas are mostly squamous cell, lymphoepithelioma-like, or basaloid carcinomas.[1] Thymic adenocarcinomas are extraordinarily rare. We herein report a case of primary thymic adenocarcinoma with tubular morphology and enteric immunophenotype as determined by expression of cytokeratin (CK) 20 and caudal type homeobox 2 (CDX2). The immunophenotype suggests metastasis from the gastrointestinal tract; however, extensive clinical evaluation revealed no extrathymic primary tumor. In addition, we review the literature to facilitate a discussion of the clinicopathologic characteristics of thymic adenocarcinoma.

CASE REPORT

A previously healthy 59-year-old woman presented with abdominal pain in the lower left quadrant that had persisted for 3 months. Endoscopic studies failed to reveal specific changes in the whole gastrointestinal tract mucosa. Imaging studies revealed an anterior mediastinal mass (Fig. 1A) and multiple lung nodules. Additionally, a whole-body positron emission tomography scan showed abnormal hyperuptake lesions in the left 10th rib and 10th vertebral body, suggesting metastasis (Fig. 1B). Laboratory tests indicated elevated levels of several serum tumor markers (carbohydrate antigen [CA] 19-9, 252.2 U/mL; CA125, 62.9 IU/mL; and carcinoembryonic antigen, 8.73 ng/mL).

The surgeon prioritized surgery for this patient not only because of her aggravated symptoms, but also because the tumor had invaded the left brachiocephalic vein. Approached through a median sternotomy, an extended thymectomy and combined resection of the pericardium were performed. Incomplete resection was inevitable because of tumor invasion into the pericar-

pISSN 2383-7837
eISSN 2383-7845

dium, phrenic nerve, innominate vein, and aorta.

Gross examination identified a solid mass measuring 6.8×4.7×3.9 cm. The tumor was unencapsulated and invaded the pericardium. The mass was firm and rubbery with a homogeneous gray-whitish cut surface. There was no internal fibrous septation (Fig. 2A). Microscopic examination revealed that the tumor was surrounded by normal thymic tissue and was composed of various-sized glandular structures (Fig. 2B). The tumor cells were columnar and oval, forming cystic, tubular, and cribriform structures containing necrotic material. Immunohistochemical staining showed focally positive CK7 staining and diffusely strong positive staining for CK20 and CDX2 (Fig. 2C–G) but negative staining for thyroid transcription factor 1 (TTF-1) and Napsin A. CD5 staining was positive for both tumor cells and T lymphocytes in the normal thymus parenchyma and stroma between tumor cell nests (Fig. 2H).

Clinically, the possibility of metastatic adenocarcinoma from the lung was raised; however, the multiple small lung nodules measured less than 1 cm, and the tumor cells were negative for TTF-1 and Napsin A. Furthermore, the pathologic features suggested metastatic adenocarcinoma of enteric origin; however, physical and radiologic examinations did not reveal primary tumors elsewhere, including in the gastrointestinal tract. These observations collectively led to a pathologic diagnosis of primary thymic adenocarcinoma of enteric immunophenotype with tubular morphology. Adjunctively, extensive sampling revealed no mucin pools or papillary structures and no other histologic components such as thymic cysts, thymomas, or teratomas.

After the operation, palliative chemoradiotherapy and radiotherapy were administered. The patient is alive with aggravated bone and lung metastasis after 11 months of follow-up.

DISCUSSION

Primary thymic adenocarcinoma is very rare. It was first reported in 1989 by Moriyama *et al.*[2] but was not accepted as a valid histologic subtype until 1997.[3] The current WHO classification system subtypes thymic adenocarcinomas as either papillary or nonpapillary. Nonpapillary adenocarcinomas include a heterogeneous group of tumors, such as mucinous adenocarcinoma, adenocarcinoma with glandular differentiation, adenocarcinoma with adenoid cystic carcinoma features, and hepatoid carcinoma.[1] This heterogeneity, coupled with the rarity of the carcinoma, has led to a paucity of information on the specific clinicopathologic features of thymic adenocarcinoma.

According to a series of case reports in which descriptive classifications are commonly used, thymic adenocarcinomas comprise papillary,[4-6] mucinous,[3,7-9] glandular (or tubular),[10-12] and papillotubular[2,13,14] adenocarcinomas. In 2003, Maghbool *et al.*[3] reviewed 26 previous cases of reported thymic adenocarcinomas and demonstrated that the mucinous type shows a significantly worse prognosis than the papillary type. Moser *et al.*[12] recently reported two cases of primary thymic adenocarcinoma with CK20 and CDX2 expression, which reflects enteric differentiation, and suggested this is a novel subtype along with 11 reported thymic adenocarcinomas with enteric immunophenotype.

For this study, we also reviewed English literature of thymic adenocarcinomas, except for thymic carcinomas with adenoid cystic carcinoma features. In analysis of clinicopathologic features, including the current case, there are currently 39 reports of primary thymic adenocarcinomas, consisting of 16 mucinous adenocarcinomas (41.0%), 13 papillary adenocarcinomas (33.3%), seven tubular adenocarcinomas (17.9%), and three papillotubu-

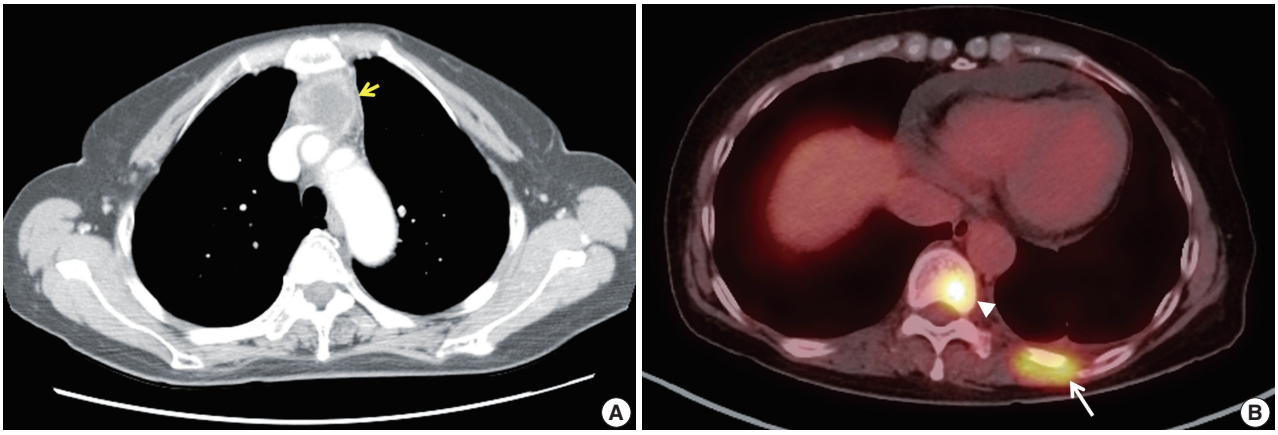

Fig. 1. Radiologic examination of the anterior mediastinum. (A) An irregularly enhancing mass (arrow) in the anterior mediastinum on a chest computed tomography scan. (B) Abnormal hyperuptake in lesions at the 10th vertebra (arrowhead) and the left 10th rib (arrow) on a whole-body positron emission tomography scan.

http://dx.doi.org/10.4132/jptm.2015.04.16

lar adenocarcinomas (7.7%). Among these cases, information on CK20 and/or CDX2 expression was available for 20 cases, revealing that 15 were enteric type and five were not.

The morphology of these enteric-type adenocarcinomas was mucinous in 11 cases, tubular in three cases, and papillotubular in one case. Furthermore, the enteric-type adenocarcinomas and mucinous/tubular adenocarcinomas have similar clinicopathologic features. A total of seven of the 14 cases of mucinous/tubular adenocarcinomas were accompanied by thymic cysts. Moreover, mucinous/tubular adenocarcinomas showed CD5 expression

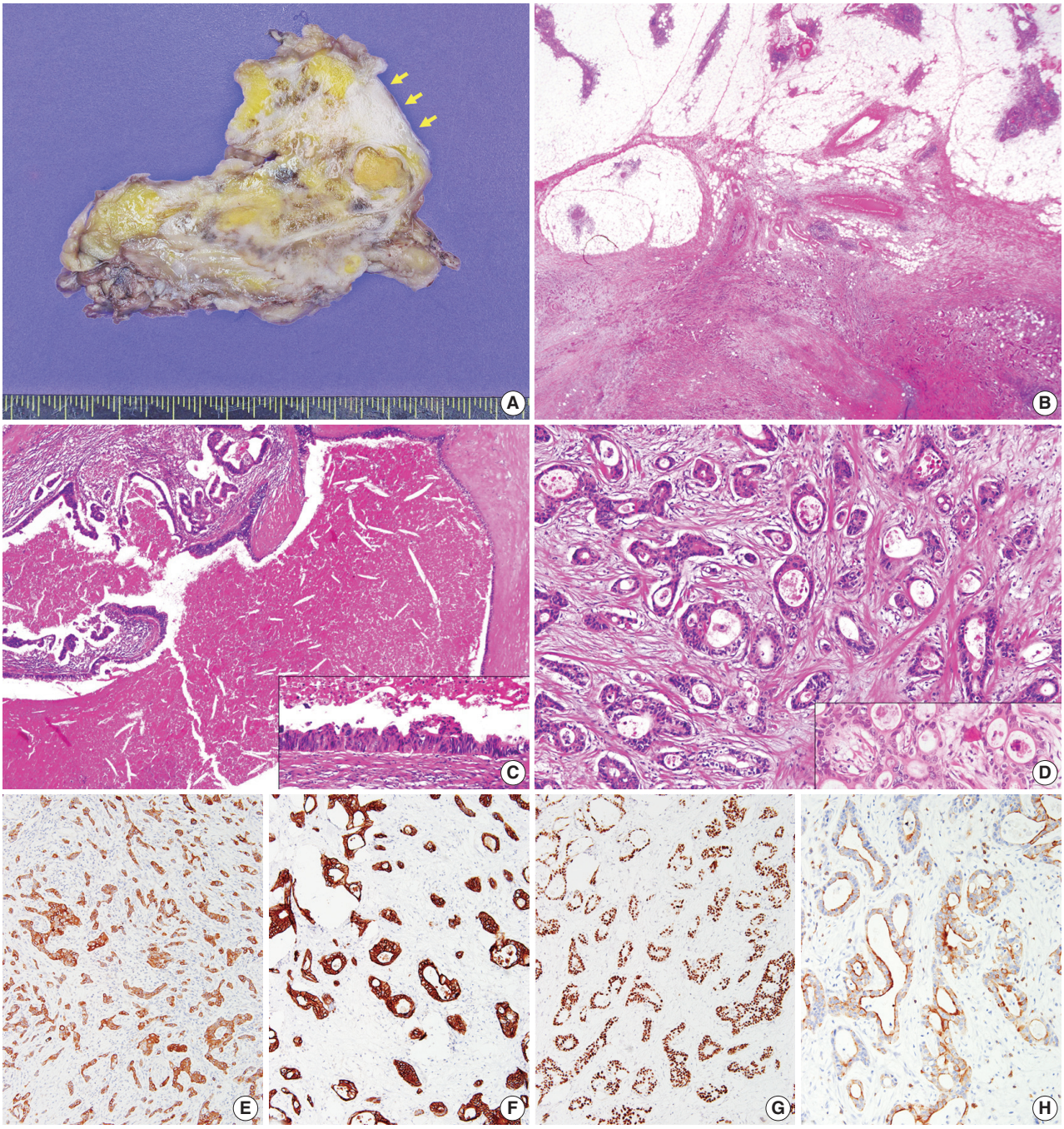

Fig. 2. Pathologic examination. (A) Gross examination of the tumor reveals an ill-defined mass with pericardial invasion (arrows, pericardium). (B) Microscopically, the tumor is surrounded by normal thymic tissues. At higher magnification, the tumor is composed of glandular or tubular structures with large glands lined by tall columnar cells (C) and oval cells forming small glands (D). The tumor cells show positive staining for CK7 (E), CK20 (F), CDX2 (G), and CD5 (H). CK, cytokeratin; CDX2, caudal type homeobox 2.

more frequently (76.4%) than papillary adenocarcinomas (33.3%). Similarly, 12 of 15 enteric-type adenocarcinomas (80%) showed CD5 expression, and eight (53.3%) were accompanied by thymic cysts.

In general, low-grade histology (well-differentiated squamous cell carcinoma, mucoepidermoid carcinoma, and basaloid carcinoma),[15] low Masaoka stage, and complete resection are factors known to be associated with better survival from thymic carcinoma.[16,17] Kaplan-Meier analysis of thymic adenocarcinomas revealed that modified Masaoka stage I or II disease had better disease-free survival than stage III or IV disease ($p = .040$). Additionally, we found that mucinous/tubular subtype showed a trend toward poorer overall survival than papillary or papillotubular subtype, in line with previous findings;[3] however, this result failed to reach statistical significance in Kaplan-Meier analysis ($p = .610$). Interestingly, the nonenteric type seemed to have worse prognosis than the enteric type (mean survival time, nonenteric vs enteric type, 22.1 ± 7.4 months vs 85.6 ± 23.1 months), especially for those with mucinous morphology (mean survival time, nonenteric vs enteric type, 7.3 ± 4.2 months vs 91.9 ± 24.4 months); however, the number of cases was too small to analyze for statistical significance. Other factors of sex, tumor size, associated thymic cyst or thymomas, serum tumor marker elevation, or c-kit or CD5 immunoexpression were not related to prognosis.

In summary, we report a rare case of primary tubular adenocarcinoma of the thymus with enteric immunophenotype. To the best of our knowledge, there have been only two such cases worldwide. The tumor presented at an advanced stage and demonstrated aggressive behavior. We believe that identification of more cases is essential in order to investigate the clinicopathologic characteristics of primary thymic adenocarcinomas.

Conflicts of Interest

No potential conflict of interest relevant to this article was reported.

REFERENCES

1. Müller-Hermelink HK, Marx A, Kuo TT, Kurrer M, Chen G, Shimosato Y. Non-papillary adenocarcinomas. In: Travis WD, Brambilla E, Müller-Hermelink HK, Harris CC, eds. World Health Organization classification of tumours: pathology and genetics of tumours of the lung, pleura, thymus and heart. 3rd ed. Lyon: IARC Press, 2004; 184.
2. Moriyama S, Shimizu N, Kurita A, Teramoto S, Taguchi K. A case of adenocarcinoma of the thymus. Nihon Kyobu Geka Gakkai Zasshi 1989; 37: 717-22.
3. Maghbool M, Ramzi M, Nagel I, *et al.* Primary adenocarcinoma of the thymus: an immunohistochemical and molecular study with review of the literature. BMC Clin Pathol 2013; 13: 17.
4. Matsuno Y, Morozumi N, Hirohashi S, Shimosato Y, Rosai J. Papillary carcinoma of the thymus: report of four cases of a new microscopic type of thymic carcinoma. Am J Surg Pathol 1998; 22: 873-80.
5. Yoshino M, Hiroshima K, Motohashi S, *et al.* Papillary carcinoma of the thymus gland. Ann Thorac Surg 2005; 80: 741-2.
6. Furtado A, Nogueira R, Ferreira D, Tente D, Eisele R, Parente B. Papillary adenocarcinoma of the thymus: case report and review of the literature. Int J Surg Pathol 2010; 18: 530-3.
7. Choi WW, Lui YH, Lau WH, Crowley P, Khan A, Chan JK. Adenocarcinoma of the thymus: report of two cases, including a previously undescribed mucinous subtype. Am J Surg Pathol 2003; 27: 124-30.
8. Ra SH, Fishbein MC, Baruch-Oren T, *et al.* Mucinous adenocarcinomas of the thymus: report of 2 cases and review of the literature. Am J Surg Pathol 2007; 31: 1330-6.
9. Abdul-Ghafar J, Yong SJ, Kwon W, Park IH, Jung SH. Primary thymic mucinous adenocarcinoma: a case report. Korean J Pathol 2012; 46: 377-81.
10. Sawai T, Inoue Y, Doi S, *et al.* Tubular adenocarcinoma of the thymus: case report and review of the literature. Int J Surg Pathol 2006; 14: 243-6.
11. Misao T, Yamamoto Y, Nakano H, Toyooka S, Yamane M, Satoh K. Primary thymic adenocarcinoma with production of carbohydrate antigen 19-9 and carcinoembryonic antigen. Jpn J Thorac Cardiovasc Surg 2004; 52: 30-2.
12. Moser B, Schiefer AI, Janik S, *et al.* Adenocarcinoma of the thymus, enteric type: report of 2 cases, and proposal for a novel subtype of thymic carcinoma. Am J Surg Pathol 2015; 39: 541-8.
13. Ishiwata T, Sekiya M, Suzuki T, Matsuoka T, Kumasaka T, Takahashi K. Thymic adenocarcinoma with sarcomatoid features characterized by intracaval tumor growth: report of a case. Surg Today 2010; 40: 1068-72.
14. Teramoto K, Kawaguchi Y, Hori T, *et al.* Thymic papillo-tubular adenocarcinoma containing a cyst: report of a case. Surg Today 2012; 42: 988-91.
15. Suster S, Rosai J. Thymic carcinoma: a clinicopathologic study of 60 cases. Cancer 1991; 67: 1025-32.
16. Wang S, Wang Z, Liu X, Wang D, Liu F. Prognostic factors of patients with thymic carcinoma after surgery: a retrospective analysis of 58 cases. World J Surg 2014; 38: 2032-8.
17. Filosso PL, Guerrera F, Rendina AE, *et al.* Outcome of surgically resected thymic carcinoma: a multicenter experience. Lung Cancer 2014; 83: 205-10.

http://dx.doi.org/10.4132/jptm.2015.04.16

Journal of Pathology and Translational Medicine 2015; 49: 335-338
http://dx.doi.org/10.4132/jptm.2015.04.22

■ BRIEF CASE REPORT ■

Sclerosing Extramedullary Hematopoietic Tumor Mimicking Intra-abdominal Sarcoma

Serap Karaarslan · Nalan Nese[1] · Guray Oncel[2] · Nazan Ozsan[3] · Taner Akalin[3]
Hasan Kaplan[4] · Filiz Buyukkececi[5] · Mine Hekimgil[3]

Department of Pathology, Sifa University Faculty of Medicine, Izmir; [1]Department of Pathology, Celal Bayar University Faculty of Medicine, Izmir; [2]Department of Radiology, Sifa University Faculty of Medicine, Izmir; [3]Department of Pathology, Ege University Faculty of Medicine, Izmir; [4]Department of General Surgery, Sifa University Faculty of Medicine, Izmir; [5]Department of Hematology, Kent Hospital, Izmir, Turkey

Sclerosing extramedullary hematopoietic tumor (SEMHT) is a rare tumor that occurs in patients with chronic myeloproliferative disorders (CMPDs). The tumor is classified in the chronic idiopathic myelofibrosis (MF) subgroup, and cases have been reported at various localizations since 1980.[1-4] Such tumors are usually seen in the abdominal organs, retroperitoneum, and mesenteric region.[3] The clinical, radiological, and morphological features may complicate differentiation from sarcoma, carcinoma, and lymphoma. It is sometimes also difficult to differentiate between a SEMHT and extramedullary hematopoiesis (EMH). These two lesions have similar clinical features, but EMH is morphologically more cellular. To aid in the differentiation, SEMHT has a more solid mass appearance with dense fibrosis and atypical megakaryocytes.[3]

EMH is the presence of hematopoietic tissue in locations other than the bone marrow. The basic mechanism is bone marrow dysfunction and decreased production of hematopoietic cells, followed by production of bone marrow cells in other organs and tissues. EMH is seen in many disorders such as sickle cell anemia, hemoglobinopathies, thalassemia, hereditary spherocytosis, and MF.[5] EMH is most commonly observed in the liver and spleen and is rarely found in the peritoneum, lymph nodes, kidneys, thymus, central nervous system, retroperitoneum, myocardium, uterus, pleura, paraspinal region, or intestines.[6-9]

Corresponding Author
Serap Karaarslan, MD
Department of Pathology, Sifa University Faculty of Medicine, Sanayi Caddesi No. 7, Bornova, Izmir 35100, Turkey
Tel: +90-232-343-4445, Fax: +90-232-343-5656
E-mail: serapkaraarslan@gmail.com

Received: January 19, 2015 **Revised:** April 20, 2015
Accepted: April 22, 2015

CASE REPORT

A 57-year-old female patient was examined for the chief complaint of fatigue. She was diagnosed with severe anemia, and a palpable intra-abdominal mass was identified on physical examination. Radiological examinations revealed hepatosplenomegaly and hypodense soft tissue lesions measuring 15×6 cm in size along the medial liver contour at the liver portal hilus level and 9.8×6 cm in size along the right iliac vascular structures in the right lower quadrant (Fig. 1), as well as several enlarged lymph nodes in the paraaortic and paracaval regions (the largest measured 5 cm and was located in the right paracaval region). Intra-abdominal free fluid deposition was noted. Radiologically, the soft tissue masses observed along the medial liver contour (15×6 cm) invaded the portal vein, and the characteristics of those along the right iliac vascular structures in the right lower quadrant (~9.8×6 cm) were reported to be consistent with infiltrative sarcomatous lesion or lymphoma (diffuse infiltrative type), and pathologic evaluation was recommended. Whole blood analysis revealed a mildly increased neutrophil count (14,500/μL). Other blood analysis results were as follows: platelets 299×10^3/μL, erythrocytes 3.91×10^6/μL, hemoglobin 10.6 g/dL (reference range, 10.80 to 14.90 g/dL), and hematocrit 34.4% (reference range, 35.60% to 45.40%).

The patient was referred for general surgery, and the right lower quadrant mass was removed with a preliminary diagnosis of intra-abdominal malignant tumor. Macroscopically, the soft tissue mass was solid, off-white in color, and 9.5×7×3 cm in size.

pISSN 2383-7837
eISSN 2383-7845

Microscopically, there were thick fibrotic bands, areas with more prominent collagen bands, mixed inflammatory cell infiltration including eosinophils, and occasional foci with individual or grouped enlarged cells with large cytoplasm and pleomorphic nucleoli in the background. Lymphoid follicles with prominent germinal centers were observed mostly in the periphery of the mass, and some contained the large cells described above (Fig. 2A, B). No mitosis or necrosis was found. Increased collagen was seen in the background on Masson's trichrome stain (Fig. 2C). Immunohistochemistry revealed suspicious large cells that were negative for CD34, DKA, S-100, CD31, desmin, vimentin, CD117, CD10, CD68, CD30, mast cell tryptase, CD1a, CD45, CD30, CD15, CD3, CD20, CD21, CD23, anaplastic lymphoma kinase (ALK), pancytokeratin, and epithelial membrane antigen. The Ki-67 proliferation index was very low at about 2%. The background lymphoid follicle structures became more evident with CD3 and CD20 staining. Additional stains were then applied, and the large cells were positive for CD61 (Fig. 3A), indicating dysplastic megakaryocytes. Some myeloperoxidase-positive cells with mononuclear or polynuclear morphology were seen, indicating granulocytic series. Glycophorin staining revealed some precursor cells belonging to the erythroid series (Fig. 3B). We concluded that all these characteristics were re-

Fig. 1. A soft tissue lesion approximately 9.8×6 cm in size with a lobulated contour along the right iliac vascular structures of the right lower quadrant.

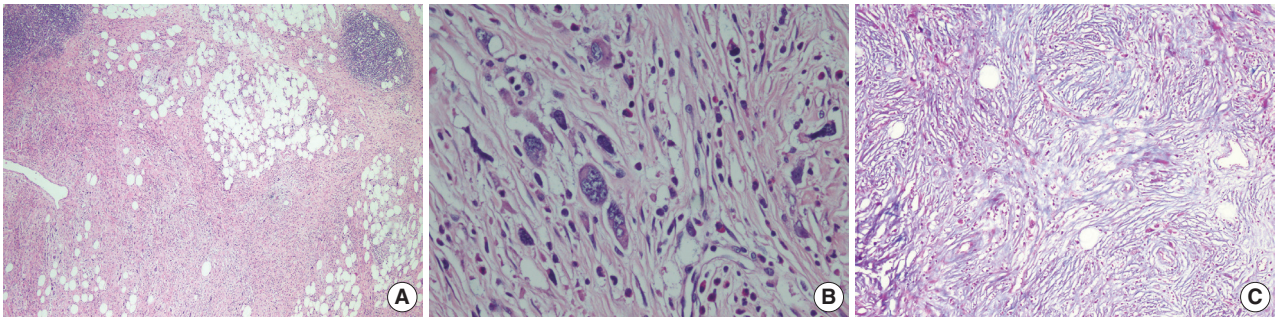

Fig. 2. (A) Thick fibrotic bands and increased collagen tissue with occasional mixed inflammatory cell infiltration including eosinophils and foci of individual or grouped cells showing pleomorphic nuclei and large cytoplasm. (B) Features of the large cells are seen more clearly at larger magnification. (C) Increased collagen is seen in the background (Masson's trichrome).

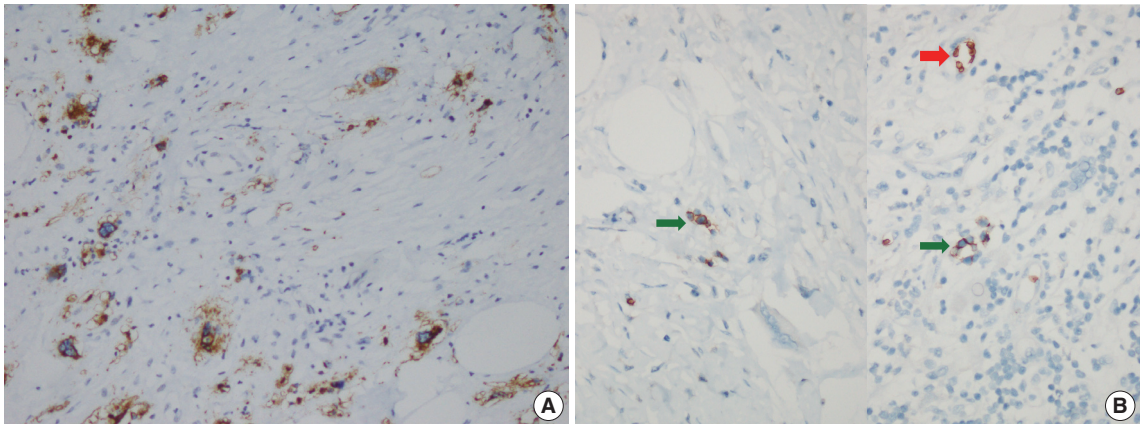

Fig. 3. (A) Large cells are CD61-positive on immunohistochemical stain, indicating that they are megakaryocytes. (B) Glycophorin positivity in precursor cells (green arrows) belonging to the erythroid lineage and surrounding erythrocytes (red arrow).

http://dx.doi.org/10.4132/jptm.2015.04.22

lated to SEMHT.

Detailed investigation of the patient history revealed that she had been diagnosed with MF after a bone marrow biopsy 14 years prior. A liver biopsy had been performed at that time, and EMH was reported. The previous bone marrow biopsy evaluation found hypercellular bone marrow (90%) with a prominent increase in occasional clustering of megakaryocytes. The bone marrow showed thick reticulin fibers with reticulin staining and collagen formation according to Masson's trichrome staining. The diagnosis of MF was made, and the patient had been followed for 14 years without treatment.

We diagnosed the retroperitoneal soft tissue mass that was highly suspicious for malignancy as SEMHT given the morphological and immunophenotypical results and the medical history. The patient was started on Hydrea (DEVA, Istanbul, Turkey) (500 g tablet, twice daily) and Urikoliz (SANDOZ, Istanbul, Turkey) (300 mg, half tablet, three times daily) to suppress the features related to SEMHT. Hydrea treatment was terminated six months later due to development of leukopenia and anemia. No other problems have developed during follow-up thus far.

DISCUSSION

SEMHT is a rare tumor more commonly seen with chronic idiopathic MF rather than CMPDs.[1] It is usually located in the abdomen, retroperitoneum, and mesenteric region.[3] Our patient had multiple masses located in the abdomen. EMH generally indicates the presence of bone marrow elements in an area other than the bone marrow. It can develop as a result of bone marrow failure due to various causes in a wide range of disorders including MF. EMH is most commonly observed in the spleen and liver and is rarely seen in the peritoneum, lymph nodes, kidneys, thymus, central nervous system, intestines, retroperitoneum, myocardium, uterus, pleura, or paraspinal region.[2-6] Differentiation of SEMHT from EMH is made based on several characteristics such as cellularity, tendency to form a mass, and presence of fibrosis and atypical megakaryocytes. Marked cellularity indicates EMH, while the presence of fibrosis and atypical megakaryocytes and a tendency to form a mass favors a diagnosis of SEMHT.[3] This case had background fibrosis, atypical megakaryocytes, and mass formation and was therefore diagnosed as SEMHT.

The differential diagnosis of large intra-abdominal or retroperitoneal soft tissue masses varies from case to case, and a clinicopathological correlation is important. A detailed immunohistochemical (IHC) panel is used together with morphological indicators of the degree of differentiation, number of mitoses, and the presence/absence of necrosis in the pathologic evaluation of soft tissue tumors. In this case, there was no necrosis in the background and no mitosis in the large cells, which did not invade the surrounding tissues, vessels, or nerves. We performed IHC stains for all entities that should be considered in the differential diagnosis of a retroperitoneal mass such as liposarcoma, malignant peripheral nerve sheath tumor, leiomyosarcoma, gastrointestinal stromal tumor, solitary fibrous tumor, inflammatory myofibroblastic tumor, and fibrosarcoma. All were negative (large cells were negative for CD34, DKA, S-100, CD31, desmin, vimentin, CD117, CD10, ALK), and the diagnosis of SEMHT was made with the help of a detailed medical history and the positivity for CD61 and glycophorin. It is difficult to differentiate some sarcomas (especially sclerosing liposarcoma) from SEMHT without using IHC markers.

Differentiating benign proliferations of bone marrow cells from those that are malignant is important. Myeloid sarcoma, which should also be considered in the differential diagnosis, is a tumor that consists of myeloid blastic cells and can develop in various anatomical sites such as the skin, lymph nodes, small intestine, and mediastinum.[10] IHC analysis is usually used for the differential diagnosis with hematological malignancies (large cells are negative for CD34 and CD117). We also eliminated other lymphomas including Hodgkin lymphoma (lymphocyte-poor type, appearance similar to Reed-Steinberg cells in some of the large cells) and histiocytic lymphoma through IHC investigation (large cells were negative for CD68, CD30, mast cell tryptase, CD1a, CD45, CD30, CD15, CD3, CD20, CD21, CD23, ALK, and S100).

We were able to make a correct diagnosis with detailed clinicopathological correlation although the initial histopathological and radiological findings supported a possible sarcomatous neoplasm. We emphasize the importance of a thorough history and highlight the fact that radiologic and pathologic data may be difficult to interpret when the medical history is inadequate. We presented this case to remind physicians to consider this pathology in the differential diagnosis of soft tissue masses, especially when hematological disorder is also present.

Conflicts of Interest

No potential conflict of interest relevant to this article was reported.

REFERENCES

1. Remstein ED, Kurtin PJ, Nascimento AG. Sclerosing extramedul-

lary hematopoietic tumor in chronic myeloproliferative disorders. Am J Surg Pathol 2000; 24: 51-5.
2. Sukov WR, Remstein ED, Nascimento AG, Sethi S, Lewin M. Sclerosing extramedullary hematopoietic tumor: emphasis on diagnosis by renal biopsy. Ann Diagn Pathol 2009; 13: 127-31.
3. Kwon Y, Yu E, Huh J, Lee SK, Ro JY. Sclerosing extramedullary hematopoietic tumor involving lesser omentum and ligamentum-teres in liver explant. Ann Diagn Pathol 2004; 8: 227-32.
4. Yuen HK, Mahesh L, Tse RK, Yau KC, Chan N, Lam DS. Orbital sclerosing extramedullary hematopoietic tumor. Arch Ophthalmol 2005; 123: 689-91.
5. Koch CA, Li CY, Mesa RA, Tefferi A. Nonhepatosplenic extramedullary hematopoiesis: associated diseases, pathology, clinical course, and treatment. Mayo Clin Proc 2003; 78: 1223-33.
6. Hanamornroongruang S, Neungton C, Warnnissorn M. Extramedullary hematopoiesis in the uterine cervix associated with tissue repair. Case Rep Obstet Gynecol 2013; 2013: 626130.
7. Luo Y, Zhang Y, Lou SF. Bilateral pleural effusion in a patient with an extensive extramedullary hematopoietic mass. Case Rep Hematol 2013; 2013: 857610.
8. Cui X, Peker D, Greer HO, Conner MG, Novak L. Extramedullary hematopoiesis in uterine leiomyoma associated with numerous intravascular thrombi. Case Rep Pathol 2014; 2014: 957395.
9. Ahmad K, Ansari S, Koirala R, Agarwal M, Chaudhary S. Paraspinal and presacral extramedullary hematopoiesis: a rare manifestation of polycythemia vera. Iran J Radiol 2013; 10: 164-8.
10. O'Malley DP. Benign extramedullary myeloid proliferations. Mod Pathol 2007; 20: 405-15.

 http://dx.doi.org/10.4132/jptm.2015.04.22

Journal of Pathology and Translational Medicine 2015; 49: 339-342
http://dx.doi.org/10.4132/jptm.2015.04.28

■ BRIEF CASE REPORT ■

Ureteral Marginal Zone Lymphoma of Mucosa-Associated Lymphoid Tissue, Chronic Inflammation, and Renal Artery Atherosclerosis

Hojung Lee · Jong Eun Joo · Young Ok Hong · Won Mi Lee
Eun Kyung Kim · Jeong Joo Woo[1] · Soo Jung Gong[2] · Jooryung Huh[3]

Departments of Pathology, [1]Radiology, and [2]Internal Medicine, Eulji General Hospital, Eulji University College of Medicine, Seoul;
[3]Department of Pathology, Asan Medical Center, University of Ulsan College of Medicine, Seoul, Korea

Malignant lymphoma of the upper urinary tract including the renal pelvis and ureter is extremely rare. Less than ten cases have been reported in the literature, of which extranodal marginal zone lymphoma of mucosa-associated lymphoid tissue (MALT lymphoma) is the most frequent histologic type.[1] MALT lymphoma arising in the stomach, skin, thyroid, and salivary gland is associated with chronic inflammation caused by pathogenic microorganisms or autoimmune disorder;[2] however, the pathogenesis of MALT lymphoma in the upper urinary tract is unknown. Herein, we report a case of upper ureteral MALT lymphoma with extensive peri-ureteropelvic inflammation and atherosclerosis of the renal artery, and discuss the possible correlation between these lesions.

CASE REPORT

A 73-year-old male patient was admitted to the emergency room with a chief complaint of right flank pain for one week. Laboratory tests showed an elevated white blood cell count of $13.21 \times 10^3/\mu L$ (neutrophilic leukocytes, 85%; lymphocytes, 5%) and high C-reactive protein (CRP) level of 23.71 mg/dL. Urine analysis was unremarkable, and no microbial growth was observed in blood or urine cultures. Abdominal computed tomography (CT) showed diffuse thickening of the right ureteropelvic wall with hydroureteronephrosis (Fig. 1A). Urine cytology and washing cytology of the right ureter revealed no atypical cells. Right nephroureterectomy was performed for histologic diagnosis, and the intraoperative diagnosis of lymphoid malignancy was made. Positron emission tomography/CT revealed multiple hypermetabolic lesions throughout the neck, chest, and abdomen, suggesting lymphoma seeding (Fig. 1B). The resected specimen showed an elongated, concentric, whitish yellow solid lesion along the walls of the renal pelvis and proximal ureter (Fig. 2). This lesion also surrounded the atherosclerotic renal artery (Fig. 2, upper inset).

Histologic examination revealed peri-ureteropelvic nodular lymphoid infiltrates encroaching upon the ureter wall (Fig. 3A). The perimuscular layer of the ureter was heavily infiltrated with tumor cells. There were centrocyte-like cells with slightly irregular nuclear contours and clear cytoplasm, occasional larger activated cells, monocytoid cells, and plasma cells forming numerous lymphoid follicles. Immunohistochemically, the neoplastic cells were positive for CD20 (Fig. 3B) but negative for CD3, CD5, CD10, Bcl-2, Bcl-6, and cyclin D1. Tumor-infiltrating T cells were mostly CD4+ cells (Fig. 3C). Monotypic expression of λ light chain was demonstrated in the plasma cells. This case was diagnosed as a MALT lymphoma. Adjacent peripelvic adipose tissue showed a dense inflammatory infiltrate composed of lymphoplasma cells, eosinophils, and histiocytes with fibroblastic proliferation (Fig. 3D). Infiltrating lymphocytes were mainly CD4+ T cells, and CD20+ B cells were rare. Neither IgG4-positive plasma cells nor anaplastic lymphoma kinase–stained cells were noted, excluding the possibility of IgG4-associated disease or an inflammatory myofibroblastic tumor.

Corresponding Author
Jooryung Huh, MD, PhD
Department of Pathology, Asan Medical Center, University of Ulsan College of Medicine, 88 Olympic-ro 43-gil, Songpa-gu, Seoul 138-736, Korea
Tel: +82-2-3010-4553, Fax: +82-2-472-7898, E-mail: jrhuh@amc.seoul.kr

Received: March 24, 2015 **Revised:** April 24, 2015
Accepted: April 27, 2015

pISSN 2383-7837
eISSN 2383-7845

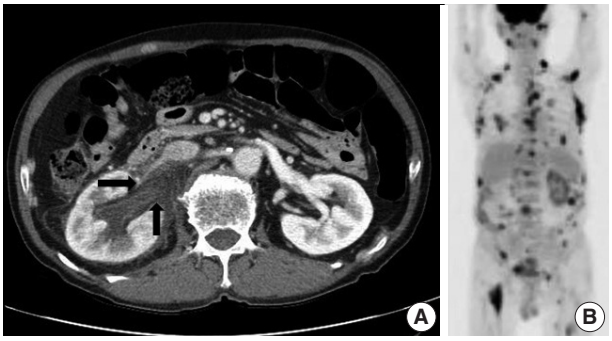

Fig. 1. (A) Contrast-enhanced axial computed tomography scan of the abdomen shows thickening with enhancement of the right renal pelvis wall with perinephric soft tissue infiltration (arrows) and hydroureteronephrosis. (B) Positron emission tomography computed tomography reveals hypermetabolic lesions in multiple neck, axillary, mediastinal, and pelvic lymph nodes as well as the chest, abdominal wall, left parotid gland, and right thigh.

The patient received rituximab-cyclophosphamide, doxorubicin, vincristine, and prednisone (R-CHOP) chemoimmunotherapy. Complete remission was achieved with no recurrence at the 14-month follow-up.

DISCUSSION

Lymphomas constitute approximately 5% of non-urothelial tumors of the urinary tract, affecting urinary bladder in more than 90% of cases.[3] In contrast, lymphoma of the upper urinary tract is extremely rare. Of the reported cases, MALT lymphoma is the most frequent, with eight case reports;[1,4-7] seven in the renal pelvis and one in the upper ureter. While MALT lymphoma of the urinary bladder is frequently associated with chronic cystitis and female predominance,[3,8] MALT lymphoma of the upper urinary tract typically affects middle-aged or elderly males with unknown preceding conditions.[1] MALT lymphoma of the urinary tract presents with incidental mass or thickening on radiographs, although some may complain of pain.[1,4-7] It usually presents at a localized stage and has excellent prognosis, although dissemination can occur, as in the present case.[1,9] Despite its widespread extent, the primary origin in the urinary system of this case was supported by the growth pattern within the renal pelvis and ureter walls. However, the possibility of secondary ureteral involvement of MALT lymphoma in other organs still remains since histologic confirmation at other sites was not performed. Unlike its gastric or even bladder counterpart, ureteropelvic MALT lymphoma rarely shows subepithelial lymphoid infiltrates or lymphoepithelial lesions, mainly involving periureteral fat.[1,4-8] Thus, ureteral MALT lymphoma is probably not associated with 'mucosa' or luminal insults but rather with periureteral inflammation. Therefore, in the case of lymphoma accompanied by inflammatory lesion, it may be better to be called 'inflammation-associated lymphoid tissue lymphoma' rather than MALT lymphoma, if MALT is not present, as in this case.

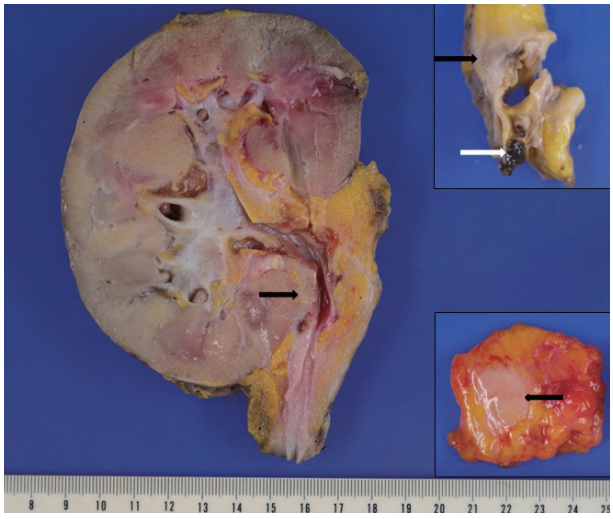

Fig. 2. Grossly, the specimen shows whitish yellow solid lesions along the renal pelvis and the ureter (black arrow), forming a concentric mass (black arrow, lower inset) compressing the ureter lumen. Renal artery surrounded by white solid lesions (black arrow, upper inset) shows atheromatous plaques and a thrombus (white arrow, upper inset).

In MALT lymphoma, a chronic inflammatory microenvironment is important for the development of the tumor.[2] The intratumoral T-cell component is a crucial factor, and CD4+T cells activate B cells in a CD40-dependent manner in combination with Th2 cytokines (interleukin [IL] 4 and/or IL-10).[2] Thus, the chronic inflammatory infiltrates seen in the peripelvic area in the present case may have provided the appropriate conditions for growth of a malignant clone.

On the other hand, atherosclerosis is defined as a chronic inflammatory response of the arterial wall to endothelial injury triggered by a variety of insults including lipid accumulation.[10] Many inflammatory cells, mostly monocytes and CD4+T cells, are recruited into the arterial intima, forming atheromatous plaques and accompanied by high blood levels of acute phase reactants such as CRP, as in the present case.[10] Renal artery atherosclerosis in our patient may be a coincidental lesion considering his old age. However, the patient's laboratory and pathologic findings indicated that the inflammatory process was concurrently ongoing within the renal artery and peripelvic adipose tissue. Therefore, in the present case, the final outcome may

http://dx.doi.org/10.4132/jptm.2015.04.28

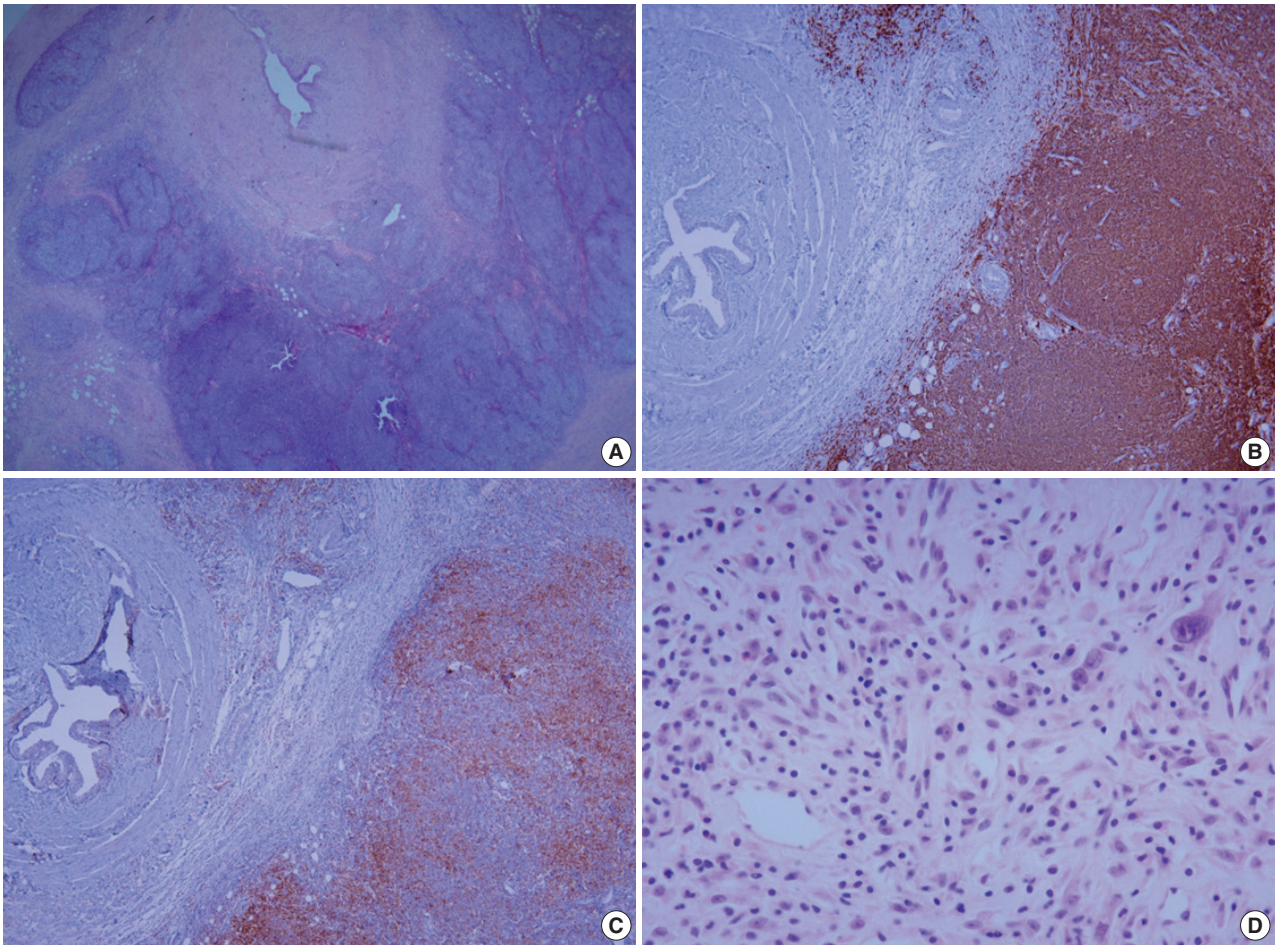

Fig. 3. Microscopic features of mucosa-associated lymphoid tissue lymphoma and adjacent chronic inflammation. (A) Tumor cells infiltrating the perimuscular layer of the ureter form lymphoid follicles with follicular colonization. Immunohistochemically, tumor cells are diffusely positive for CD20 (B) and accompanying T cells are mostly CD4 positive (C). (D) Peripelvic adipose tissue shows a mixed infiltrate of lymphoplasma cells, eosinophils, and histiocytes with fibroblastic proliferation.

manifest as ureteral MALT lymphoma and renal artery atherosclerosis.

Conflicts of Interest

No potential conflict of interest relevant to this article was reported.

REFERENCES

1. Otsuki H, Ito K, Sato K, *et al*. Malignant lymphoma of mucosa-associated lymphoid tissue involving the renal pelvis and the entire ureter: a case report. Oncol Lett 2013; 5: 1625-8.
2. Thieblemont C, Bertoni F, Copie-Bergman C, Ferreri AJ, Ponzoni M. Chronic inflammation and extra-nodal marginal-zone lymphomas of MALT-type. Semin Cancer Biol 2014; 24: 33-42.
3. Eble JN, Sauter G, Epstein JI, Sesterhenn IA. World Health Organization classification of tumours: pathology and genetics tumors of the urinary system and male genital organs. Lyon: IARC Press, 2004.
4. Araki K, Kubota Y, Iijima Y, *et al*. Indolent behaviour of low-grade B-cell lymphoma of mucosa-associated lymphoid tissue involved in salivary glands, renal sinus and prostate. Scand J Urol Nephrol 1998; 32: 234-6.
5. Qiu L, Unger PD, Dillon RW, Strauchen JA. Low-grade mucosa-associated lymphoid tissue lymphoma involving the kidney: report of 3 cases and review of the literature. Arch Pathol Lab Med 2006; 130: 86-9.
6. Mita K, Ohnishi Y, Edahiro T, Fujii T, Yamasaki A, Shimamoto F. Primary mucosa-associated lymphoid tissue lymphoma in the renal pelvis. Urol Int 2002; 69: 241-3.
7. Hara M, Satake M, Ogino H, *et al*. Primary ureteral mucosa-associated lymphoid tissue (MALT) lymphoma: pathological and radio-

logical findings. Radiat Med 2002; 20: 41-4.
8. Matsuda I, Zozumi M, Tsuchida YA, *et al*. Primary extranodal marginal zone lymphoma of mucosa-associated lymphoid tissue type with malakoplakia in the urinary bladder: a case report. Int J Clin Exp Pathol 2014; 7: 5280-4.
9. Thieblemont C, Berger F, Dumontet C, *et al*. Mucosa-associated lymphoid tissue lymphoma is a disseminated disease in one third of 158 patients analyzed. Blood 2000; 95: 802-6.
10. Hansson GK, Robertson AK, Söderberg-Nauclér C. Inflammation and atherosclerosis. Annu Rev Pathol 2006; 1: 297-329.

http://dx.doi.org/10.4132/jptm.2015.04.28

Journal of Pathology and Translational Medicine 2015; 49: 343-345
http://dx.doi.org/10.4132/jptm.2015.04.27

■ BRIEF CASE REPORT ■

Late Bone Metastasis of Histologically Bland Struma Ovarii: The Unpredictability of Its Biologic Behavior

Sun-Ju Oh · Minjung Jung · Young-Ok Kim

Department of Pathology, Kosin University Gospel Hospital, Busan, Korea

Struma ovarii (SO) is a subtype of ovarian teratoma that contains mostly thyroid tissue comprising more than 50% of the tumor volume.[1] It is the most common type of monodermal teratoma of the ovary, accounting for approximately 2.7% of all teratomas.[1] Most cases of typical SO are benign with exceptional cases showing malignant features of papillary carcinoma, vascular invasion, or invasion into surrounding tissue. However, there are rare cases of histologically benign SO with malignant biological behavior, variously designated as peritoneal strumosis, malignant SO, metastatic SO, or highly differentiated follicular carinomas.[2,3] Here, we report on a patient who developed a vertebral metastasis ten years after oophorectomy for SO that finally proved to be malignant.

CASE REPORT

A 60-year-old woman presented with back pain. Magnetic resonance imaging revealed a destructive bone mass at the thoracic 12 level of the spine (Fig. 1A). Overall image analysis suggested a metastasis, but the origin could not be detected on a positron emission tomography–computed tomography (PET-CT) scan. Needle biopsy was performed on the spinal lesion, and microscopically it revealed thyroid follicles with colloids resembling normal thyroid tissue (Fig. 1B, C). Immunohistochemically, these cells were diffusely positive for thyroid transcription factor-1 and thyroglobulin (Fig. 1D), suggesting thyroid as origin of the tumor. Any evidence of nuclear atypia suspicious for papillary carcinoma was not detected throughout the lesion, which was consequently diagnosed as metastatic follicular carcinoma of thyroid.

Subsequent clinical evaluation revealed a high serum thyroglobulin level of 1,277 ng/mL (normal range, 1.4 to 78.0 ng/mL). However, ultrasonogram and computed tomography showed no distinct mass in the thyroid gland. The patient's past medical history revealed that she underwent total hysterectomy and bilateral salpingo-oophorectomy for a left ovarian cyst 12 years ago that was initially diagnosed as SO. Follow-up of the patient included periodic ultrasonograms and measurement of serum cancer antigen 125 levels, all of which had been normal since the surgery. A suspicion for metastasis originating from the ovarian tumor was raised, and the initial slides were reevaluated.

Upon review of the pathology report and slides, the ovarian cyst was a 12-cm-sized multilocular mass with a smooth outer surface. Microscopic examination showed benign looking thyroid tissue characterized by round follicles, most of which were dilated, but some follicles were small and others were medium sized. Many follicles contained intraluminal colloids, and they were lined by cuboidal epithelial cells with moderate amounts of cytoplasm (Fig. 2A). However, a complete examination revealed a focus of 0.5-cm-sized closely packed microfollicles with nuclear irregularity, overlapping, and vague clearing (Fig. 2B, C). These features resembled a follicular variant of papillary carcinoma (FVPC), but were insufficient to establish a definite diagnosis of FVPC. Other characteristics suspicious for malignancy such as vascular or ovarian capsular invasion were not noted. No other teratomatous components were identified. A possibility of unusual metastasis from SO was suggested for the spinal lesion.

Subsequent total thyroidectomy and spondylectomy for the spinal lesion were conducted. The resected thyroid gland showed no evidence of neoplasm, as expected, and the spinal lesion ex-

Corresponding Author
Young-Ok Kim, MD
Department of Pathology, Kosin University Gospel Hospital, 262 Gamcheon-ro, Seo-gu, Busan 602-702, Korea
Tel: +82-51-990-6744, Fax: +82-51-990-3080,
E-mail: 10highpowerfield@gmail.com

Received: April 1, 2015 **Revised:** April 22, 2015
Accepted: April 27, 2015

pISSN 2383-7837
eISSN 2383-7845

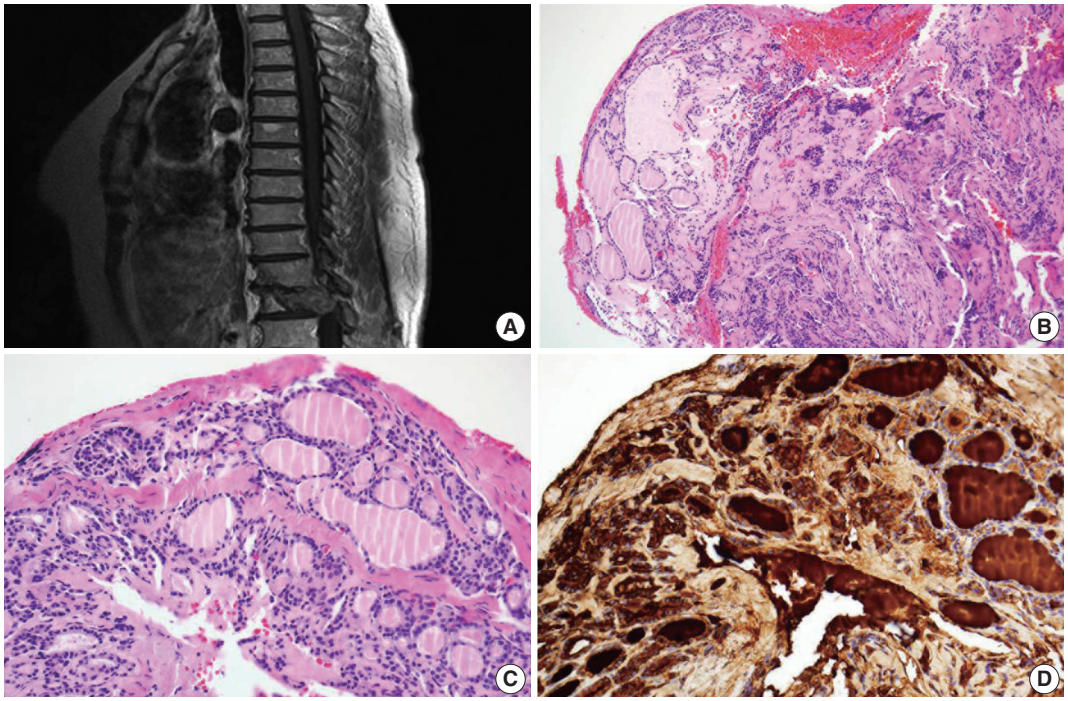

Fig. 1. (A) Sagittal magnetic resonance imaging showing an ill-defined lytic mass involving the thoracic 12 level. The mass destructs the vertebral body and spinal canal extending to the pedicle. (B, C) Needle biopsy of the spinal lesion reveals benign-looking thyroid follicles. (D) These cells are positive for thyroglobulin on immunohistochemical stain, supporting thyroid origin.

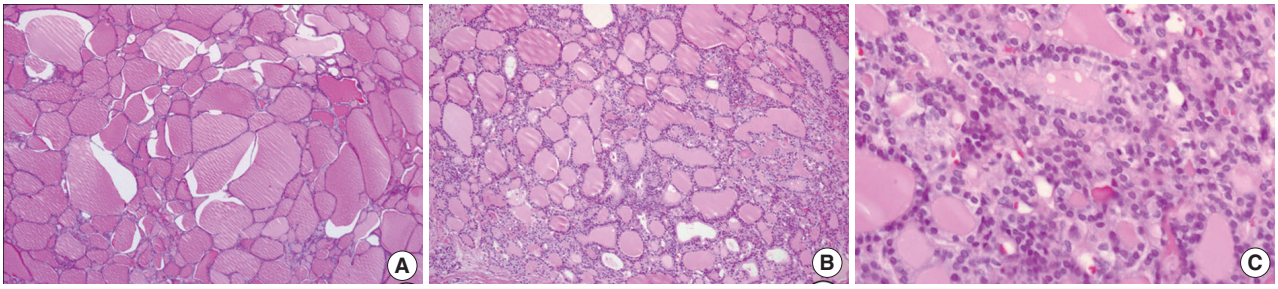

Fig. 2. Histological features of struma ovarii. Most of the tumor consist of dilated follicles reminiscent of nodular goiter (A) while a small part of the tumor shows densely packed microfollicles (B) with mild nuclear irregularity, overlapping, and vague clearing (C).

hibited the same histological features as the needle biopsy. The patient subsequently received radioactive iodine (RAI) treatment, but her PET-CT scan on the last follow-up showed multiple bone metastases in the scapula, rib, sternum, and pelvic bones.

DISCUSSION

The most common thyroid-type carcinomas originating in SO are papillary and follicular carcinomas. The diagnostic criteria for cases of papillary carcinoma are similar to those described for the cervical thyroid gland and are based primarily on nuclear and architectural features.[4] These features are almost invariable and of no clinical importance. With respect to follicular carcinoma, invasion into the surrounding ovarian tissue, vascular invasion, or metastasis is evidence of malignancy.[5]

However, SO can show a wide spectrum of histological features that should not prompt a diagnosis of malignancy. These include the presence of areas resembling follicular adenoma, foci with papillary architecture, and nuclear clearing. SO with these features have a benign clinical course and these tumors are designated "proliferative SO." These types of tumors generally do not behave in a malignant fashion.[4] However, this claim was denied later when adenomatous proliferative SO also can show the propensity for recurrence or metastasis.[6]

It is difficult to predict the metastatic potential of SO at initial diagnosis. Even SO that histologically resembles non-neo-

http://dx.doi.org/10.4132/jptm.2015.04.27

plastic thyroid tissue is sometimes associated with recurrence or extra-ovarian metastasis, which have previously been designated as peritoneal strumosis, malignant SO, metastatic SO, or related terms.[3] Roth and Karseladze[2] described three cases of SO with extra-ovarian dissemination having an innocuous appearance resembling that of a colloid or nodular goiter. They designated this entity as "highly differentiated follicular carcinoma of ovarian origin (HDFCO)." The diagnosis of HDFCO characteristically cannot be made until extra-ovarian dissemination is detected because of its non-neoplastic appearance. They also compared cases of HDFCO with those of typical thyroid-type carcinomas of ovarian origin with peritoneal involvement. They found that biological behavior is not different in the point that the prognosis seems to be favorable.

In a study of 27 cases of biologically malignant SO with extra-ovarian dissemination or metastasis, Shaco-Levy *et al*.[6] found that histologically malignant, adenomatous, or even normal primary tumors can show biologically malignant behavior. The authors found no independent factor to predict its biological behavior. However, severe fibrous adhesions, larger amounts of peritoneal fluid (≥1 L), and larger size of the stromal component (≥12 cm) have some predictive value. In the following year, the authors analyzed in more detail the natural history of biologically aggressive tumors in a study of patients with more rapid disease progression.[7] Factors predictive of a potentially more aggressive clinical course are large tumor size (>10 cm), more than 80% stromal tissue, extensive papillary carcinoma histology, more than five mitoses per 10 high-power field, and marked cytological atypia. Our case showed no adverse histological or clinical factors other than the tumor size of 12 cm according to their criteria. However, others have contradicted that the size of the stromal component is not relevant to the metastatic or recurrence potential and no histologic features seem to correlate with a propensity for an adverse clinical outcome.[8]

When no independent factor predicts biologically malignant potential of SO, controversy regarding the extent of pelvic resection and the management of the thyroid gland can arise with respect to the treatment plan. Marti *et al*.[9] suggested that pelvic surgery alone may be sufficient initial therapy for thyroid-type carcinoma confined to the ovary, whereas prophylactic total thyroidectomy with RAI may be reserved for patients with extra-ovarian spread or distant metastasis. However, there are no present series and data from the literature allowing the determination of risk stratification for patients with SO confined to the ovary at presentation. Because recurrence may occur after more than a decade following diagnosis, as in the present case, long-term follow-up is indicated with regular thyroglobulin measurements to detect metastasis.

In summary, we report a patient with a vertebral metastasis 10 years after diagnosis of histologically benign SO. On the basis of our experience with this patient and others in the literature, no determinants can predict its biologically malignant potential. Pathologists are advised to report in detail on tumor size, cytologic atypia, mitosis, and other histological factors affecting the adverse outcome when encountering large SO consisting solely of thyroid tissue as in our case. Long-term follow-up with regular thyroglobulin measurements should be warranted for any evidence of metastasis or recurrence.

Conflicts of Interest

No potential conflict of interest relevant to this article was reported.

REFERENCES

1. Kurman RJ, Carcangiu ML, Herrington CS, Young RH. WHO classification of tumours of female reproductive organs. 4th ed. Lyon: IARC Press, 2014.
2. Roth LM, Karseladze AI. Highly differentiated follicular carcinoma arising from struma ovarii: a report of 3 cases, a review of the literature, and a reassessment of so-called peritoneal strumosis. Int J Gynecol Pathol 2008; 27: 213-22.
3. Karseladze AI, Kulinitch SI. Peritoneal strumosis. Pathol Res Pract 1994; 190: 1082-5.
4. Devaney K, Snyder R, Norris HJ, Tavassoli FA. Proliferative and histologically malignant struma ovarii: a clinicopathologic study of 54 cases. Int J Gynecol Pathol 1993; 12: 333-43.
5. Rosenblum NG, LiVolsi VA, Edmonds PR, Mikuta JJ. Malignant struma ovarii. Gynecol Oncol 1989; 32: 224-7.
6. Shaco-Levy R, Bean SM, Bentley RC, Robboy SJ. Natural history of biologically malignant struma ovarii: analysis of 27 cases with extraovarian spread. Int J Gynecol Pathol 2010; 29: 212-27.
7. Robboy SJ, Shaco-Levy R, Peng RY, *et al*. Malignant struma ovarii: an analysis of 88 cases, including 27 with extraovarian spread. Int J Gynecol Pathol 2009; 28: 405-22.
8. Garg K, Soslow RA, Rivera M, Tuttle MR, Ghossein RA. Histologically bland "extremely well differentiated" thyroid carcinomas arising in struma ovarii can recur and metastasize. Int J Gynecol Pathol 2009; 28: 222-30.
9. Marti JL, Clark VE, Harper H, Chhieng DC, Sosa JA, Roman SA. Optimal surgical management of well-differentiated thyroid cancer arising in struma ovarii: a series of 4 patients and a review of 53 reported cases. Thyroid 2012; 22: 400-6.

Journal of Pathology and Translational Medicine 2015; 49: 346-350
http://dx.doi.org/10.4132/jptm.2015.04.17

■ BRIEF CASE REPORT ■

Necrotizing Sarcoid Granulomatosis: Possibly Veiled Disease in Endemic Area of Mycobacterial Infection

Yosep Chong · Eun Jung Lee · Chang Suk Kang · Tae-Jung Kim · Jung Sup Song[1] · Hyosup Shim[2]

Departments of Hospital Pathology and [1]Internal Medicine, College of Medicine, The Catholic University of Korea, Seoul;
[2]Department of Pathology, Yonsei University College of Medicine, Seoul, Korea

Necrotizing sarcoid granulomatosis (NSG) is a rare granulomatous disease that primarily affects the lung and presents as nodular masses of confluent sarcoid-like granulomas with extensive necrosis and vasculitis.[1] Proper diagnosis and treatment are challenging for clinicians, radiologists, and pathologists because of the rarity and diagnostic difficulty of this disease.[2-4] Since it was first described by Liebow,[1] only 135 cases have been reported.[2,4,5]

In addition to its rarity, the similarity of the clinical, radiological, and pathological features of NSG to other granulomatous diseases, such as granulomatous infection, nodular sarcoidosis, and Wegener's granulomatosis (WG), is the largest obstacle in its proper diagnosis. The initial symptoms are non-specific or frequently do not present at all.[2-4] Radiologically, NSG can present as cavitary lesions, ill-defined pneumonic consolidations, or even as a solitary nodule or a mass.[6,7] Pathologically, NSG shares features of sarcoidosis and WG.[1,4]

Thus, it is not surprising that NSG is often easily mistaken for granulomatous infections, such as tuberculosis, especially in endemic areas. Although the general level of hygiene in Korea has dramatically improved, the reported incidence of pulmonary tuberculosis remains the highest among the Organization for Economic Cooperation and Development member countries.[8,9] Identification of causal microorganisms is essential for proper treatment of tuberculosis; however, empirical treatment with anti-tuberculosis medication is often performed in endemic countries like Korea, in spite of tests failing to show any causative microorganisms.[9]

Here, we report the first two cases of NSG in Korean patients, one of whom showed a dramatic response to immediate application of systemic corticosteroids, and the other of whom showed no response to empirical treatment with anti-tuberculosis medication.

Corresponding Author
Tae-Jung Kim, MD, PhD
Department of Hospital Pathology, Yeouido St. Mary's Hospital, 10 63-ro, Yeongdeungpo-gu, Seoul 150-713, Korea
Tel: +82-2-3779-2157, Fax: +82-2-783-6648, E-mail: kimecho@catholic.ac.kr

Received: February 2, 2015 **Revised:** April 2, 2015
Accepted: April 16, 2015

CASE REPORT

The publication of the case information and materials was approved by the institutional review board of The Catholic University of Korea, College of Medicine (SC11ZISE0221).

Case 1

A 70-year-old man with a history of smoking presented with a three-week history of cough, fever, and chill. He reported no change in body weight, no cyanosis, and no clubbing. Vital signs were stable, and inflammatory markers were slightly increased (erythrocyte sedimentation rate, 90 mm/hr; C-reactive protein [CRP], 3.52 mg/L).

Radiological examination revealed multifocal ill-defined, nodular consolidations in both lungs, with moderate enlargement of paratracheal and hilar lymph nodes, suggesting granulomatous infection (Fig. 1A, B).

On microscopic examination of the wedge-resected tissue, confluent small granulomas with necrosis of variable sizes were seen in the lung parenchyma. The granulomas were accompanied by central necrosis that was suppurative rather than caseous, palisaded by Langerhans-type giant cells and mononuclear

pISSN 2383-7837
eISSN 2383-7845

lymphohistiocytes. At first glance, granulomatous vasculitis did not seem evident, but on closer observation, mild transmural vasculitis with fibrosis distant from the necrotic area was clearly noted in a significant portion of the lesion (Fig. 2A–D). The differential diagnosis based on pathologic findings included granulomatous diseases of various causes. Special stains for fungus and acid-fast bacilli on the resected tissue and sputum were negative. Tuberculosis–polymerase chain reaction and culture on bronchial washing fluid and peripheral blood were both negative. Serum cryptococcal antigen and IgG for parasites were all negative.

An extensive battery of autoimmune markers was all negative (antineutrophil cytoplasmic antibody, antinuclear, anti-ds-DNA, anti-sm, anti-SS-A/Ro, anti-Scl72, anti-Jo1, etc.). Serum angiotensin-converting enzyme was unremarkable. With these results, a diagnosis of NSG was highly suspected and treated with oral prednisolone.

After one month of therapy, the patient showed a dramatic improvement of symptoms and chest radiography (Fig. 1C). He has had no symptoms through two years of follow-up.

Case 2

A 41-year-old non-smoking woman presented with a two-week history of cough and sputum. Laboratory findings showed only a mild increase in acute inflammatory marker (CRP, 37.4 mg/L).

Radiologically, multiple nodules with ill-defined margins scattered mainly in the left lower lobe were found with minimal pleural effusion, suggesting hematogenous spread of metastatic cancer, pulmonary lymphoma, or septic pneumonia (Fig. 1D). Hilar lymph nodes were unremarkable.

Histological examination of resected tissue revealed variably-

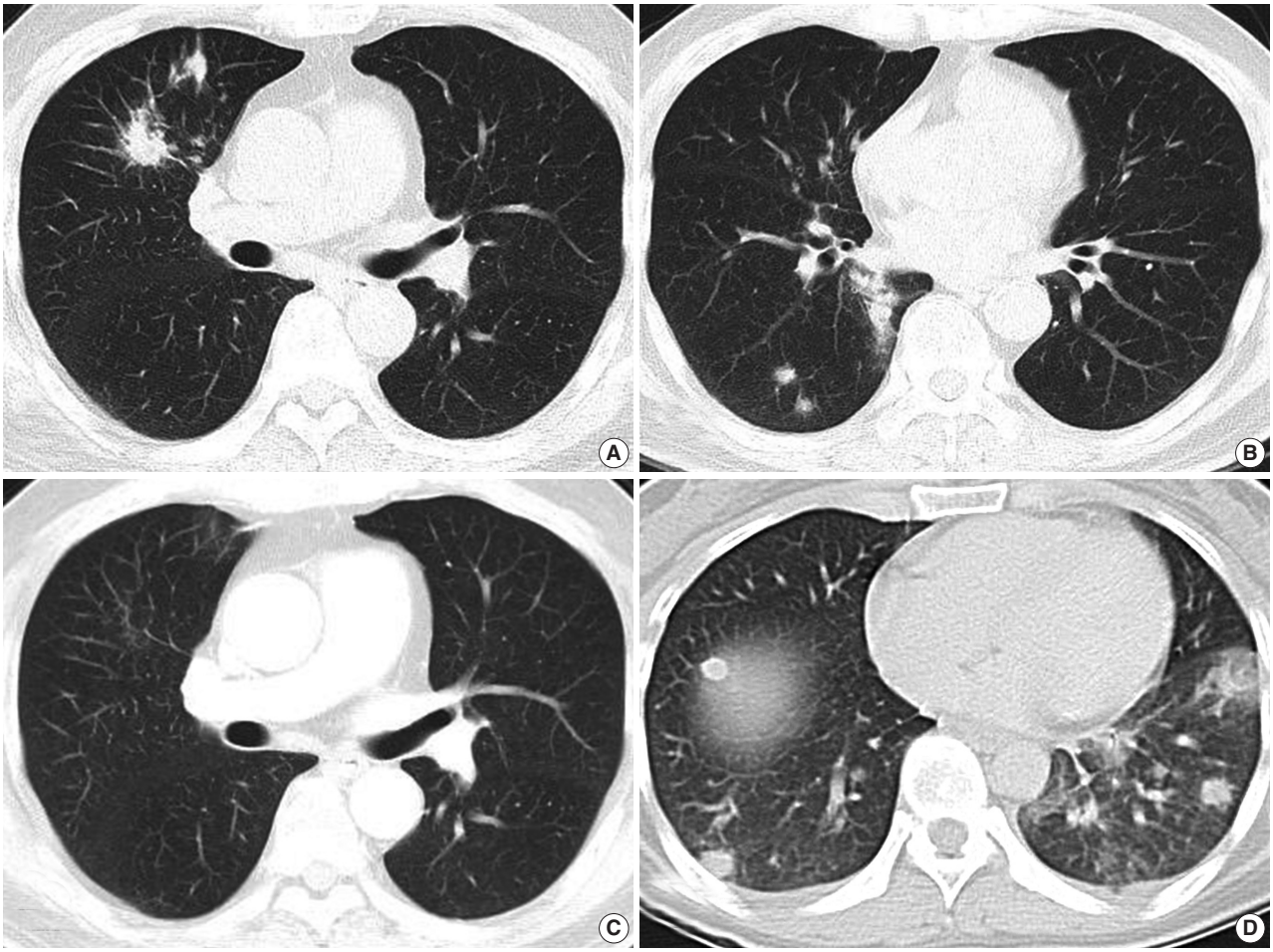

Fig. 1. Radiologic findings. (A, B) Computed tomography (CT) of case 1 shows multiple variably-sized nodular lesions with hilar node enlargement. (C) Follow-up CT after one month of corticosteroid therapy reveals dramatic resolution. (D) CT of case 2 also reveals multiple ill-defined nodules.

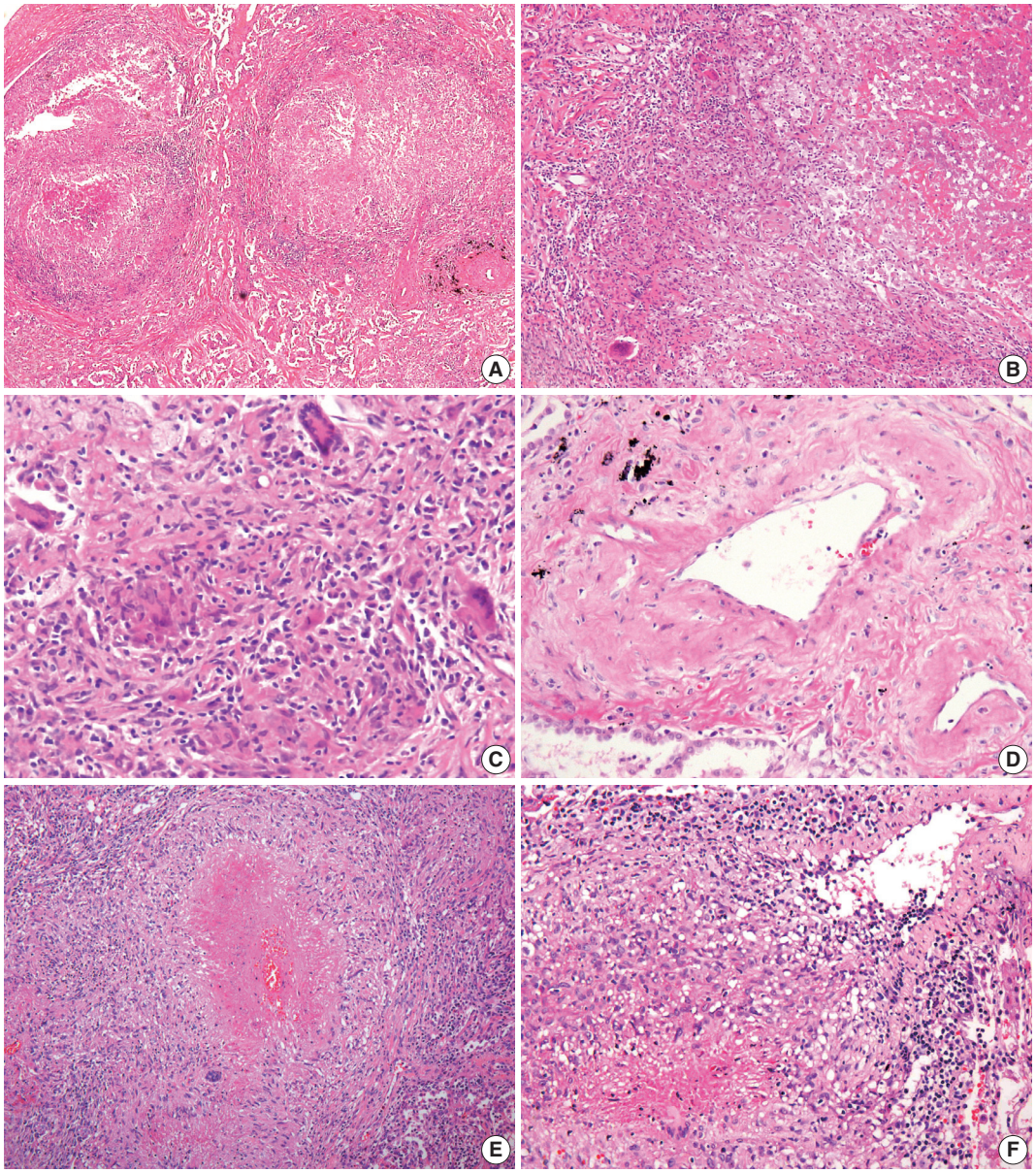

Fig. 2. Microscopic findings. (A–C) Multifocal nodular granulomatous inflammation with extensive central necrosis is replacing normal architecture (case 1). (D) Mild transmural vasculitis distant from necrotic area, i.e., cicatricial-type vasculitis, is observed. (E, F) Multiple confluent granulomas with central caseous necrosis and granulomatous vasculitis are found (case 2).

sized granulomas with varying amounts of suppurative necrosis and frequent granulomatous vasculitis, raising suspicion for sarcoidosis or other kinds of granulomatous vasculitis (Fig. 2E, F). However, autoimmune markers were all negative, and no causative microorganisms were found on various tests.

An anti-tuberculosis treatment regimen was started based on the clinicoradiographic findings in order to exclude the possibility of potential pulmonary tuberculosis. During the first three weeks of anti-tuberculosis treatment, the patient reported no improvement in symptoms. She was treated for another month and slowly improved, irrespective of treatment, and even after its cessation. Bacterial cultures of sputum, blood, and bronchial washing remained negative.

DISCUSSION

In 1973, Liebow[1] described three chief features of NSG that differentiate it from sarcoidosis, WG, and other granulomatous infections. First, histologically, NSG appears as sarcoid-like granuloma with vasculitis and necrosis. Second, radiological

http://dx.doi.org/10.4132/jptm.2015.04.17

findings include multiple lung nodules without hilar lymphadenopathy. Third, it has a very benign clinical course. However, subsequent reports have since shown that NSG can present with more variable radiologic findings and is commonly accompanied by lymphadenopathy and pleural effusion.[3,4]

Because the symptoms of NSG are often non-specific and the radiologic findings vary widely, the pathological findings are important for accurate diagnosis. If one finds a mixture of pathologic features of pulmonary sarcoidosis and mild to moderate granulomatous vasculitis, combined with negative tests for causative microorganisms, the possibility of NSG can be raised. However, conclusive diagnosis cannot be made on histologic features alone, and the final pathologic diagnosis of NSG should be made after thorough exclusion of the other possible diseases with similar features. Nodular sarcoidosis is excluded by the presence of necrotizing vasculitis and diffuse parenchymal necrosis.[4] WG is excluded by the presence of sarcoid-like granulomas and granulomatous vasculitis distant from necrotic areas.[4] Most importantly, granulomatous infections should be carefully excluded because they can also produce variable vasculitis, extensive necrosis, and sarcoid-like granulomas.[3,4] Such distinction can be very challenging because most microbiological studies, including those that use the latest technologies such as polymerase chain reaction, can produce false-negative results.

In describing the characteristic pathologic findings of NSG, Katzenstein[4] has mentioned that transmural vasculitis with fibrosis distant from necrotic area, as seen in the first case of this report, is an important defining finding of NSG. It is important to remember that these findings can be easily overlooked and considered as usual nodular sarcoidosis if pathologists do not pay enough attention to the lung biopsy samples of similar conditions. For this reason, Rosen[5] suggests in his recent review that NSG is a specific form of sarcoidosis and should be referred to with the diagnostic term sarcoidosis with necrotizing sarcoid granulomatosis pattern. However, since this specific form of sarcoidosis mimics granulomatous infections such as tuberculosis and results in inadequate anti-tuberculosis treatment, the distinction from usual pulmonary sarcoidosis should continue to be emphasized.

According to the guidelines on treatment of tuberculosis by the Centers for Disease Control and Prevention, a four-drug anti-tuberculosis regimen is recommended for the first two months of treatment for patients who are highly suspected as having an active tuberculosis infection based on clinicoradiographical findings, even without isolation of mycobacterium.[10] The Korean Guidelines for Tuberculosis also recommend empirical chemoprevention in sputum-negative patients while waiting for the results of culture studies.[9] Thus, it is inevitable that patients with NSG in Korea will undergo the risks and inconvenience of anti-tuberculosis treatment considering the socioeconomic burden of tuberculosis. However, it should be noted that there may be more unrecognized patients with NSG in Korea, and that they might be overlooked in the endemic setting of tuberculosis, considering that NSG has been reported quite commonly in Japan, the most similar Asian country to Korea.[11]

Collectively, for the accurate recognition of NSG, the following diagnostic steps should be performed. If pathologically suspicious features for NSG are found in the absence of identification of any causative microorganisms and the radiologic findings demonstrate multiple nodules with hilar lymphadenopathy, the possibility of NSG should be considered. If NSG is clinically suspected, the initial two to three weeks of anti-tuberculosis treatment can be used to monitor the disease response. If there is no change in symptoms or radiological findings, then systemic steroid treatment can be applied.

To our knowledge, this is the first case report of NSG in Korean patients, one of whom showed a dramatic response to corticosteroid therapy. A case of NSG was reported in 1997 by Kim *et al*.,[12] but the evidence for NSG in their report is insufficient because polymerase chain reaction was not used to exclude tuberculosis, the patient was not appropriately treated, and there was no radiographic improvement.

In conclusion, the diagnosis of NSG should be made very carefully in suspected cases based on consistent radiologic and histologic findings and thorough exclusion of possible causative microorganisms.

Conflicts of Interest

No potential conflict of interest relevant to this article was reported.

REFERENCES

1. Liebow AA. The J. Burns Amberson lecture: pulmonary angiitis and granulomatosis. Am Rev Respir Dis 1973; 108: 1-18.
2. Corrin B, Nicholson AG. Pathology of the lungs. 3rd ed. New York: Churchill Livingstone/Elsevier, 2011.
3. Leslie KO, Wick MR. Practical pulmonary pathology: a diagnostic approach. 2nd ed. Philadelphia: Saunders, 2011.
4. Katzenstein AL. Katzenstein and Askin's surgical pathology of non-neoplastic lung disease. 4th ed. Philadelphia: Saunders Elsevier, 2006.

5. Rosen Y. Four decades of necrotizing sarcoid granulomatosis: what do we know now? Arch Pathol Lab Med 2015; 139: 252-62.
6. Chittock DR, Joseph MG, Paterson NA, McFadden RG. Necrotizing sarcoid granulomatosis with pleural involvement: clinical and radiographic features. Chest 1994; 106: 672-6.
7. Sahin H, Ceylan N, Bayraktaroglu S, Tasbakan S, Veral A, Savas R. Necrotizing sarcoid granulomatosis mimicking lung malignancy: MDCT, PET-CT and pathologic findings. Iran J Radiol 2012; 9: 37-41.
8. Kim HJ. Current status of tuberculosis in Korea. Korean J Med 2012; 82: 257-62.
9. Joint Committee for the Development of Korean Guidelines for Tuberculosis, Korea Centers for Disease Control and Prevention. Korean guidelines for tuberculosis. Seoul: Korea Centers for Disease Control and Prevention, 2011; 220.
10. American Thoracic Society; CDC; Infectious Diseases Society of America. Treatment of tuberculosis. MMWR Recomm Rep 2003; 52: 1-77.
11. Harada T, Amano T, Takahashi A, *et al*. Necrotizing sarcoid granulomatosis presenting with elevated serum soluble interleukin-2 receptor levels. Respiration 2002; 69: 468-70.
12. Kim GS, Lee SJ, Lee JC, *et al*. A case of necrotizing sarcoid granulomatosis. Korean J Med 1997; 53: 574-9.

 http://dx.doi.org/10.4132/jptm.2015.04.17

Journal of Pathology and Translational Medicine 2015; 49: 351-353
http://dx.doi.org/10.4132/jptm.2015.05.06

■ BRIEF CASE REPORT ■

Salivary Gland Hyalinizing Clear Cell Carcinoma

Jung-Chia Lin[1] · Jia-Bin Liao[1,2] · Hsiao-Ting Fu[1] · Ting-Shou Chang[2,3,4] · Jyh-Seng Wang[1,2,5]

[1]Department of Pathology and Lab Medicine, Kaohsiung Veterans General Hospital, Kaohsiung; [2]National Defense Medical Center, Taipei;
[3]Department of Otolaryngology, Kaohsiung Veterans General Hospital, Kaohsiung; [4]Institute of Public Health, College of Medicine, National Cheng Kung University, Tainan;
[5]Department of Medicine, National Yang-Ming University School of Medicine, Taipei, Taiwan.

Hyalinizing clear cell carcinoma (HCCC) is a rare malignant salivary gland tumor that was characterized as a distinct entity by Milchgrub *et al*. in 1994.[1] It has a slight female predominance with ages ranging from 25 to 87 years (mean, 59.4 years).[2] Most cases occur in the oral cavity, mainly the palate and tongue.[2] Histologically, HCCC is characterized by the predominance of clear cells embedded in a characteristic dual hyaline and fibrocellular stroma.[3] In 2011, Antonescu *et al*.[2] identified *EWSR1* rearrangements in this tumor, which have been subsequently observed in 82% of cases. This genetic change allows the distinction of HCCC from other salivary gland neoplasms with a clear cell phenotype. Here, we present a typical case of HCCC, which we believe is the first case report from Taiwan.

CASE REPORT

A 37-year-old female patient visited our clinic complaining of painless swelling on the ventral tongue that had been present for months. Intraoral examination revealed a 1 × 1 cm nodule on the left ventral tongue and an excisional biopsy was done. Light microscopy showed an infiltrative tumor composed mostly of clear cells with spindle cell stroma. The tumor cells were immunoreactive for cytokeratin AE1/3 (CKAE1/3) and p63, and the spindle cell stroma for smooth muscle actin (SMA). The original pathology report was myoepithelial carcinoma (MC) due to misinterpretation of the p63 immunoreactivity as myoepithelial differentiation. The diagnosis was soon revised to HCCC after recognizing this new entity.

The tumor comprised of cords and nests of tumor cells with skeletal muscle infiltration and perineural invasion (Fig. 1A). The tumor cells had clear and pale eosinophilic cytoplasm (Fig. 1B), fine nuclear chromatin with occasional small nucleoli, and no mitotic figure. The tumor cells were embedded in a characteristic dual hyaline and fibrocellular stroma (Fig. 1C). No ductal formation was seen. On immunohistochemical stains, the tumor cells were positive for CKAE1/3 and p63 (Fig. 1D), but negative for myoepithelial cell markers, such as SMA, CD10, S100, myosin, calponin, glial fibrillary acidic protein (GFAP), muscle specific actin (MSA), and desmin. The spindle cells in the fibrocellular stroma were positive for SMA and CD10 (Fig. 1E) but negative for CKAE1/3, p63, myosin, calponin, GFAP, MSA, S100, and desmin. The clear cells contained abundant glycogen highlighted by a diastase sensitive periodic acid-Schiff positive reaction (Fig. 1F, G). The result of the mucicarmine stain for mucin was negative. Fluorescence *in situ* hybridization for *EWSR1* showed a break-apart signal pattern in 25% of the tumor cells (Fig. 1H), confirming the presence of *EWSR1* gene rearrangement. Since the margin was focally involved by the tumor, the patient received further excision with safe resection margin, which showed no residual tumor.

DISCUSSION

HCCC was first described by Milchgrub *et al*. in 1994[1] as a rare salivary gland carcinoma made up of clear cells forming cords and nests in a hyalinized stroma. This tumor was often

Corresponding Author
Jyh-Seng Wang, MD, PhD
Department of Pathology and Lab Medicine, Kaohsiung Veterans General Hospital,
386 Ta-Chung 1st Rd., Kaohsiung 813, Taiwan
Tel: +886-7-3422121 (ext 6318), Fax: +886-3422288,
E-mail: jswang@vghks.gov.tw

Received: March 27, 2015 **Revised:** April 20, 2015
Accepted: May 6, 2015

pISSN 2383-7837
eISSN 2383-7845

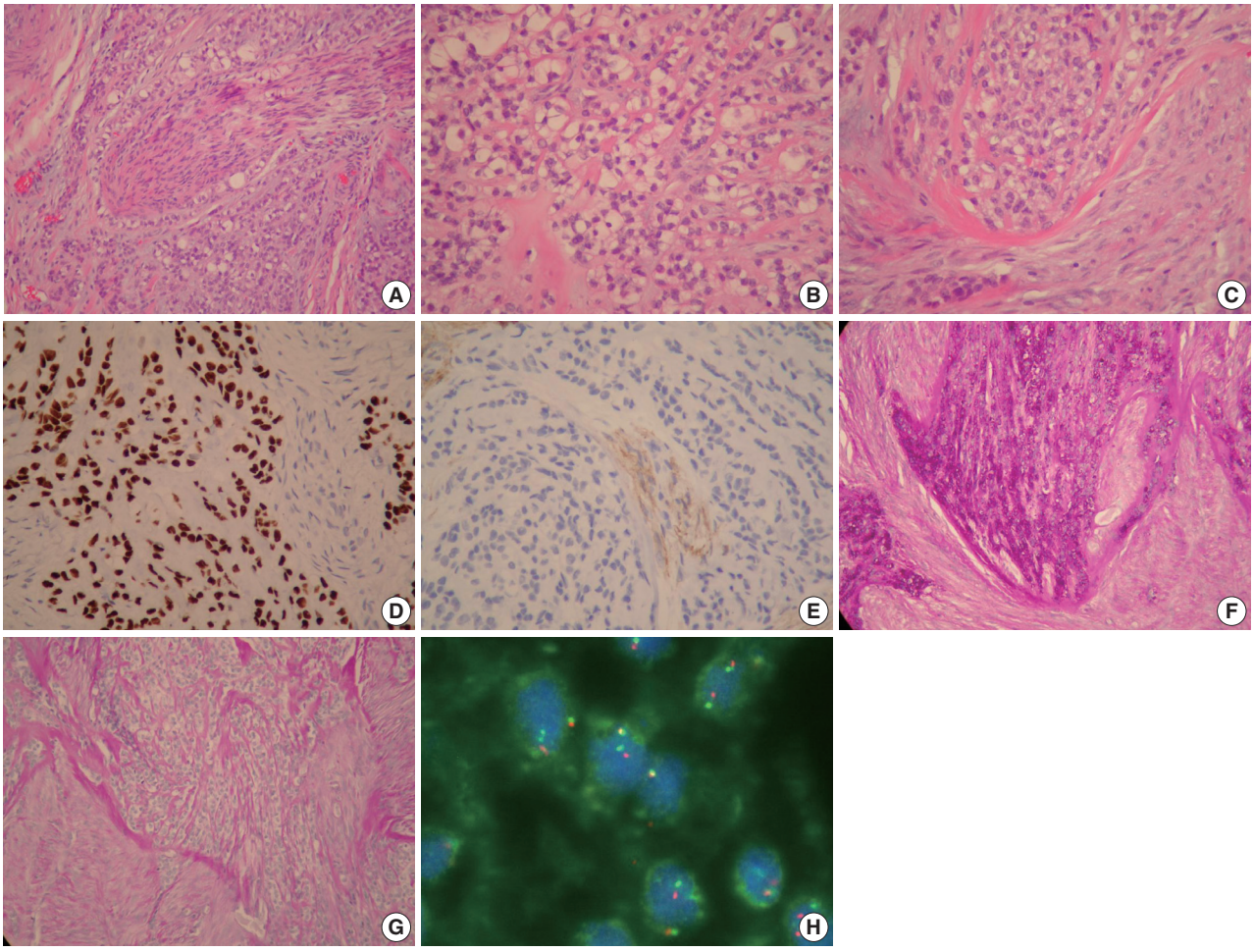

Fig. 1. (A) Hyalinizing clear cell carcinoma (HCCC) showing cords and nests of tumor cells with perineural invasion. The tumor cells have a clear cytoplasm (B) and are embedded in a characteristic dual hyaline and fibrocellular stroma (C). (D) Almost all clear cells are positive for p63. (E) The tumor cells are negative for CD10 while the myofibroblastic spindle cells in the stroma are positive for CD10. (F, G) Tumor cells with clear cytoplasm contain abundant glycogen which is positive for periodic acid–Schiff and sensitive to diastase digestion. (H) Fluorescence *in situ* hybridization shows a break-apart signal pattern in 25% of the tumor cells confirming the presence of *EWSR1* rearrangement.

confused with other clear cell mimics, such as epithelial-myoepithelial carcinoma (EMC), mucin-depleted mucoepidermoid carcinoma (MEC) and MC. It was separated from these entities because of its lack of apparent squamous, mucinous, and myoepithelial differentiation.[1] HCCC is currently classified by the World Health Organization (WHO) as a diagnosis of exclusion: "clear cell carcinoma, not otherwise specified."[4] Many small case series and case reports have been described,[5-7] but none added new insights into HCCC until Antonescu *et al*.[2] recently identified a consistent *EWSR1-ATF1* fusion in HCCC.

In the differential diagnosis, EMC has a prominent ductal structure of tumor cells and does not show characteristic dual hyalinizing and fibrocellular stroma of HCCC. HCCC can be distinguished from MC by lack of myoepithelial cell markers such as S100, calponin, and SMA. Neither EMC nor MC has the *EWSR1* gene rearrangement as seen in HCCC. Mucous cells may be absent in mucin-depleted MEC and is very difficult to differentiate from HCCC. However, mucin-depleted MEC lacks the characteristic dual stroma and *EWSR1* rearrangement of HCCC.[3] It should be noted that clear cell odontogenic carcinoma also has *EWSR1* rearrangement as well as dual hyalinizing and fibrocellular stroma, and cannot be separated reliably from HCCC by the morphology or molecular marker, except by its location in the jaw bone.[3,8]

Treatment usually involves primary resection with negative margins. Cases of HCCC with recurrence or metastasis have been reported and proven by molecular analysis; however, the vast majority of HCCC have had good outcomes.[3,4]

In summary, we present a typical case of HCCC with characteristic dual stroma, lack of myoepithelial differentiation and

http://dx.doi.org/10.4132/jptm.2015.05.06

presence of *EWSR1* rearrangement. This is the first case report from Taiwan. Molecular genetic methods have become an integral part of modern oral pathology and play an important role in helping to categorize cases that defy traditional morphologic analysis. In the molecular era, "NOS" is no longer fitting for HCCC. The term "NOS" is at odds with the presence of the specific *EWSR1-ATF1* fusion that clearly sets HCCC apart from other salivary neoplasia. Adding "hyalinizing" is also recommended, even though this feature is not present in all cases. The benefit of its inclusion is the mental association with a salivary clear cell malignancy.[9]

Conflicts of Interest

No potential conflict of interest relevant to this article was reported.

REFERENCES

1. Milchgrub S, Gnepp DR, Vuitch F, Delgado R, Albores-Saavedra J. Hyalinizing clear cell carcinoma of salivary gland. Am J Surg Pathol 1994; 18: 74-82.
2. Antonescu CR, Katabi N, Zhang L, *et al*. *EWSR1-ATF1* fusion is a novel and consistent finding in hyalinizing clear-cell carcinoma of salivary gland. Genes Chromosomes Cancer 2011; 50: 559-70.
3. Weinreb I. Hyalinizing clear cell carcinoma of salivary gland: a review and update. Head Neck Pathol 2013; 7 Suppl 1: S20-9.
4. Ellis G. Clear cell carcinoma, not otherwise specified. In: Barnes L, Eveson JW, Reichart P, Sidransky D, eds. World Health Organization classification of tumours: pathology and genetics of head and neck tumors. Lyon: IARC Press, 2005; 227-8.
5. O'Sullivan-Mejia ED, Massey HD, Faquin WC, Powers CN. Hyalinizing clear cell carcinoma: report of eight cases and a review of literature. Head Neck Pathol 2009; 3: 179-85.
6. Solar AA, Schmidt BL, Jordan RC. Hyalinizing clear cell carcinoma: case series and comprehensive review of the literature. Cancer 2009; 115: 75-83.
7. Yang S, Zhang J, Chen X, Wang L, Xie F. Clear cell carcinoma, not otherwise specified, of salivary glands: a clinicopathologic study of 4 cases and review of the literature. Oral Surg Oral Med Oral Pathol Oral Radiol Endod 2008; 106: 712-20.
8. Bilodeau EA, Weinreb I, Antonescu CR, *et al*. Clear cell odontogenic carcinomas show *EWSR1* rearrangements: a novel finding and a biologic link to salivary clear cell carcinomas. Am J Surg Pathol 2013; 37: 1001-5.
9. Brandwein-Gensler M, Wei S. Envisioning the next WHO head and neck classification. Head Neck Pathol 2014; 8: 1-15.